

Sudhir Man Shrestha

Physical modeling of pressurized flushing operation with lightweight material

Master's thesis in Hydropower Development

Supervisor: Nils Ruther

August 2019

Sudhir Man Shrestha

Physical modeling of pressurized flushing operation with lightweight material

Master's thesis in Hydropower Development
Supervisor: Nils Ruther
August 2019

Norwegian University of Science and Technology
Faculty of Engineering
Department of Civil and Environmental Engineering

 **NTNU**
Norwegian University of
Science and Technology

M.SC. THESIS IN HYDRAULIC ENGINEERING

Candidate: Mr. Sudhir Man Shrestha

Title: Physical modelling of pressurized flushing operation with light weight material

1. Background

The idea of using lightweight (low-density) materials, having density lower than natural sand but higher than that of water, as sediment in physical hydraulic models has been around since decades and has been practiced by different hydraulic laboratories around the world. Those laboratories have their own scaling criteria and study methodologies based largely on their own experiences with such models. There is still a lack of common scaling criteria for designing a lightweight model and for quantitative interpretation of results from such models. In this study, pressurized flushing of non-cohesive reservoir sediment through a bottom orifice was simulated in steady flow conditions. Two sets of laboratory experiments were carried out in identical setups, one with a lightweight (low-density) material at Hydraulic Laboratory of NTNU, Norway and another with natural sand at Hydraulic Laboratory of Hydro Lab, Nepal. Each set of experiment were carried out by varying flushing discharge, reservoir water level, thickness of sediment deposit layer and opening height of bottom orifice. To make the results from both sets of experiments comparable, the sizing of the sediments were chosen in such a way that they could be scaled up to represent a common arbitrary prototype.

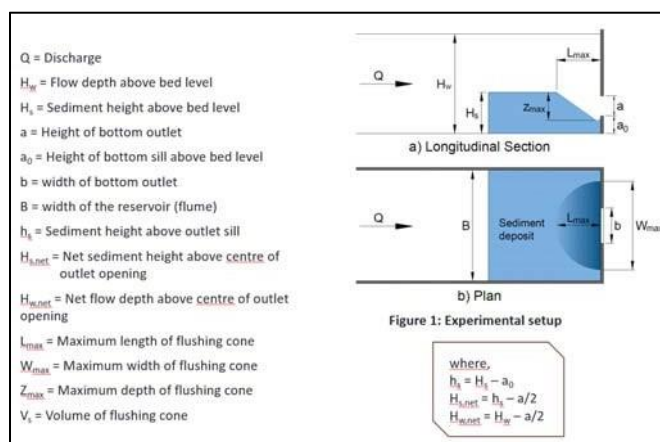


Figure 1: Parameter definition of the experimental setup

2. Work description

The thesis shall cover, though not necessarily be limited to the main tasks listed below. Based on the available documentation the following shall be carried out:

- 1 Literature review on scale model for pressurized flushing.
- 2 Visit HydroLAB Nepal for a knowledge exchange with Co-supervisor Sanat Karmacharya
- 3 Building experimental setup at Hydraulic Laboratory at NTNU, Trondheim
- 4 Running the necessary experimental program and post processing the data.

- 5 Presentation of the results
- 6 Discussion of the results
- 7 Conclusions
- 8 Proposals for future work
- 9 Presentation

The literature review should outline the previous contributions in a condensed manner and result in the motivation for the current study.

The candidate will stay approximately two weeks at HydroLab Nepal for a knowledge exchange. HydroLab will provide help to conduct his study and will support him with a working place. The period of stay in Nepal is planned by the candidate and should not be longer than three weeks, preferably two, and the candidate should be back to Norway latest at the end of February 2019. The cost for the travel will be covered by the department, via the project SediPASS.

3. Supervision

Associate Prof. Nils R  ther will be the main supervisor and Associate Prof. Elena Pummer will be the co-supervisor. The supervisors shall assist the candidate and make relevant information, documents and data available.

Discussion with and input from other research or engineering staff at NTNU or other institutions are recommended. Significant inputs from others shall be referenced in a convenient manner. The research and engineering work carried out by the candidate in connection with this thesis shall remain within an educational context. The candidate and the supervisors are free to introduce assumptions and limitations, which may be considered unrealistic or inappropriate in a contract research or a professional/commercial context.

4. Report format and submission

The report should be written with a text editing software. Figures, tables and photos shall be of high quality. The report format shall be in the style of scientific reports and must contain a summary, a table of content, and a list of references.

The report shall be submitted electronically in B5-format .pdf-file in Blackboard, and three paper copies should be handed in to the institute. Supplementary working files such as spreadsheets, numerical models, program scripts, figures and pictures shall be uploaded to Blackboard. The summary shall not exceed 450 words. The Master's thesis should be submitted within 15th of June 2019.

The candidate shall present the work at a MSc. seminar towards the end of the master period. The presentation shall be given with the use of power-point or similar presentation tools. The date and format for the MSc. seminar will be announced during the semester.

Trondheim, 14. January 2019



Nils R  ther Associate Professor

Department of Civil and Environmental Engineering NTNU

Acknowledgement

I would first like to acknowledge my supervisors Prof. **Nils Ruther** Department of Civil and Environmental Engineering, Norwegian Institute of Science and Technology (NTNU) and **Sanath Karmacharya** (PhD candidate of NTNU) for their valuable supervision, guidance, and their constant support without whom this research work would not have been possible. Their suggestion, patience, and immense knowledge always have motivated me to achieve my desired goal and provided me extensive personal and professional guidance and taught me a great deal about research work and the right approach to move forward.

I would also like to express my gratitude to the Faculty of Civil and Environmental Engineering of NTNU, Trondheim for providing such a platform to conduct research on such scale and improve my knowledge and myself.

I am very much grateful to the Hydrolab, Nepal and Hydraulic Laboratory of NTNU for allowing me to share their facilities without which this research work would not have been possible. My gratitude also goes to all the staff members of both the laboratories mentioned above, with whom I had a pleasure to work together during my research work.

Along with my adviser and my faculty, my heartfelt grace goes to my family and friends who always inspire me throughout the process of researching and writing this research paper. Furthermore, I must also oblige their valuable suggestions and comments during my quest.

Ultimately, I would like to thank all those people who were directly or indirectly involved in my research work.

Abstract

Sedimentation in reservoirs and its removal is one of the serious and biggest challenges in reservoirs which has serious consequences for water management, flood control and production of energy. Several methods like catchment's management, flushing, sluicing, density current venting, and dredging have been proposed to control the significant problem of sediment deposit on water storage facilities. Among them, pressure flushing is considered to be one of the methods with a few local effects. During pressure flushing a scour cone will be developed in the vicinity of the bottom outlet. To study the formation and characteristics of funnel-shaped crater laboratory experiments were carried out of different hydraulic parameters such as discharge, depth of sediment, flow depth and bottom outlets. In this study, 16 experiments were carried out for two sediment height of 140 and 120 mm of two different lightweight material and one sand samples at different discharges and different water depth with four different bottom outlets. The result revealed that the volume and dimension of flushing cone were affected by the outlet discharge, sediment depth, flow depth, and bottom outlets. Also, by comparing the outcomes between lightweight material and corresponding sand it notified that there exists a strong correlation between one another. This study unfolded that, with the use of proper scaling relation among prototype, lightweight material could be conveniently used for quantitative studies of the process involving sediment transport. Finally, MatLab and Eureka program was employed to ease the calculation of flushed volume during experiments and to carry out the regression analysis and proposed an empirical dimensionless relationship for estimating the volume of flushing cone.

Keywords: - Pressure Flushing, Flushing Cone, Outlet Discharge, Sediment Depth, Flow Depth, Bottom Outlets.

List of abbreviation

h_s	-	Sediment height above outlet sill
A_r	-	Scale ratio of Area
D_*	-	Dimensionless Grain Size
Fr_*	-	Shield's number (Densimetric Froude number)
Fr_{*c}	-	Critical Shield's number
$H_{s\ net}$	-	Net sediment height above center of outlet opening
H_s	-	Sediment height above bed level
$H_{w\ net}$	-	Net flow depth above center of outlet opening
H_w	-	Flow depth above bed level
L_{max}	-	Maximum length of flushing cone
L_r	-	Scale ratio of Length
Re_*	-	Grain Reynolds number
S_s	-	Relative density
V_r	-	Scale ratio of Velocity
V_s	-	Volume of flushing cone
V_w	-	Fall velocity
W_{max}	-	Maximum width of flushing cone
Z_{max}	-	Maximum depth of flushing cone
a_0	-	Height of bottom sill above bed level
d_{50}	-	Median sediment grain size
q_{*sr}	-	Unit sediment discharge ratio
q_s	-	Unit sediment
u_*	-	Shear velocity
κ_s	-	Bottom roughness
ρ_s	-	Sediment density
τ_b	-	Bottom shear stress
A	-	Area
a	-	Acceleration
a	-	Height of bottom Outlet
B	-	Width of bottom outlet
B	-	Width of flume
BLWM	-	Blue Lightweight Material
c	-	Speed of sound in fluid
cm	-	Centimeter
d	-	sediment diameter
D/s	-	Downstream
E	-	Bulk modulus of elasticity
f	-	Darcy Weisbach friction factor
Fr	-	Froude number
g	-	Gravitational Acceleration
G-1	-	Submergence specific gravity
h	-	Water depth
L	-	Characteristics length
l/s	-	Liter per second
m	-	Meter

m/s	-	Meter per second
m^3	-	Cubic meter
m^3/s	-	Meter cubic per second
MHz	-	Megahertz
mm	-	Millimeter
Q	-	Discharge
q	-	Unit discharge
S	-	Slope
SSPM	-	Small scale physical model
u, v	-	Velocity
U/s	-	Upstream
YLWM	-	Yellow Lightweight Material
ν, ϑ	-	Kinematic Viscosity
ω	-	Oscillating frequency
KE	-	Kinetic Energy
P	-	Pressure Force
PE	-	Potential energy
Re	-	Reynolds number
k	-	Bulk Modulus
l	-	Length
n	-	Manning's number
δ	-	Distortion
μ	-	Viscosity
ρ	-	Density of water

Contents

1	Introduction	1
1.1	General Background	1
1.2	Aim and Objectives of the study	2
1.3	Methodology of the study.....	3
1.4	Structure of the Report	4
2	Background in Reservoir Sedimentation.	5
2.1	Effects of Sedimentation on Hydropower	7
2.1.1	Impact on Generation	7
2.1.2	Impact on Stability	7
2.1.3	Impact on Discharge capability.....	8
2.1.4	Impact on Equipment	8
2.1.5	Impact on Environment	8
2.2	Reservoir Sediment Management Strategies	9
2.2.1	Dredging.....	9
2.2.2	Venting Turbid Density Current	10
2.2.3	Sediment Bypassing	11
2.2.4	Flushing	12
2.2.5	Limitations.....	12
2.3	Types of Flushing.....	12
2.3.1	Empty or Free flow flushing.....	12
2.3.2	Pressure Flushing	12
2.4	Importance of Flushing Strategy	13
2.5	Flushing Procedures.	15
2.6	Flushing Period	16
2.6.1	Flushing During Flood Season	16
2.6.2	Flushing During Nonflood Season.....	16
2.7	Erosion Process During Flushing	16
2.7.1	Slope Failure.....	16
2.7.2	Retrogressive Erosion	17
2.7.3	Progressive Erosion.....	17
3	Physical Modeling	18
3.1	Introduction.....	18
3.2	Advantages and Disadvantages of Physical Modelling	19
3.2.1	Advantages.....	19

3.2.2	Disadvantages	19
3.3	Why Physical Modelling?	19
3.4	Some Definitions	20
3.4.1	Prototype	20
3.4.2	Scale	20
3.4.3	Similitude(or Scaling) Criteria	20
3.4.4	Similarity	20
3.4.5	Scale Effects	20
3.4.6	Laboratory Effects.....	20
3.5	Basic Aspect of Physical Modeling	20
3.6	Previous Studies of Physical modeling of pressure flushing.....	21
3.6.1	Experimental Investigation of Local Half-Cone Scouring Against Dam.	21
4	Theory	24
4.1	Dimensional Analysis.....	24
4.2	Hydraulic Similitude	25
4.2.1	Froude Criterion.....	26
4.2.2	Reynolds Criterion.....	26
5	Scaling	28
5.1	Fixed Bed Models	28
5.2	Movable-Bed Models	29
5.2.1	Movable–Bed scaling Requirements	29
5.2.2	Sediment Transport Similitude Requirements	30
5.2.3	Dimensionless Unit Sediment Discharge	34
5.3	Bedload Model Scale Requirements	34
5.4	Best Model Requirements.....	35
5.5	Lightweight Model Requirements (LWM).....	35
5.6	Lightweight Model Scale Effects	36
5.7	Densimetric Froude Model	36
5.8	Sand Model Requirements.....	36
5.9	Selected similarity conditions:	36
5.10	Summary for scale ratios.	37
6	Method	38
6.1	Experimental Setup	38
6.2	Experimental procedure.....	39
6.2.1	Types and size distribution of the sediments.	39

6.2.2	Experimental Setup.....	40
6.2.3	Number of Experiments and it's constraints.	40
6.2.4	Measuring of flushing cone volume.	41
7	Results and Discussion	43
7.1	Comparison with empirical relations	44
7.2	The variation of flushing cone volume versus $H_{w\ net}$ for different water depth and the bottom outlet.	44
7.3	The variation of flushing cone width versus outflow discharge	46
7.4	The variation of Outflow discharge versus volume of flushing cone and sediment height.....	47
7.5	Comparison between Blue lightweight material and sand.....	49
7.6	Statistical analysis for estimating ratio flushing cone volume and $H_{w\ net}$ ($VsH_{w\ net}^3$).....	49
7.7	Comparison between Yellow lightweight material and sand	51
8	Conclusion.....	52
9	Future Work.....	54
10	References:	55
11	Appendix A Basic Formulas & Calculations.....	58
12	Appendix B. Measured volume of sediment flushed	63
13	Appendix C Calculation and comparison of Parameter $VsH_{w\ net}^3$ with M. E. Meshkati (2010) equation & new empirical relation.	67

LIST OF FIGURES

Figure 1.1 Longitudinal and Plan view of the pressure flushing(3).	2
Figure 1.2 Flow Chart for Methodology of Study.	3
Figure 2.1 Reservoir Sediment Profile(10).....	5
Figure 2.2 Comparison of Hydroelectric Potential and Sediment Production(1, 12).....	6
Figure 2.3 World Storage Volume and Storage loss(13).....	7
Figure 2.4 Sediment erosion in turbines from various Power Plant.	8
Figure 2.5 Sediment Management Strategies(17).....	9
Figure 2.6 Basic concept of Dredging (Source: USEPA 2005, Adapted by Battelle, NAVFAC Contact No, N62473-07-D4013); cited from(18)	10
Figure 2.7 Venting Turbidity Density Current(19).	10
Figure 2.8 Sediment Bypassing(20).....	11
Figure 2.9 Longitudinal and Plan View of the pressure flushing(22).....	13
Figure 2.10 Effect of sediment flushing on the storage capacity of the reservoir.	14
Figure 2.11 Hydraulic and sediment characteristics during flushing events at constant discharge(21).	15
Figure 2.12 Slope failure in consolidated sediments(21).	16
Figure 2.13 Slope failure in unconsolidated silt and clay(21).....	16
Figure 2.14 Process of Retrogressive erosion(21).	17
Figure 3.1 Example of Physical Modelling a & b.....	18
Figure 3.2 Experimental setup schematic plan view.	21
Figure 3.3 Variation of flushing cone volume and width of flushing cone versus outflow discharge for the bottom outlet of 2.54cm diameter.	22
Figure 3.4 Variation of flushing cone volume and width of flushing cone versus outflow discharge for the bottom outlet of 3.81cm diameter.	22
Figure 3.5 Variation of flushing cone volume and width of flushing cone versus outflow discharge for the bottom outlet of 36 cm diameter.	22
Figure 3.6 Variation of flushing cone volume and width of flushing cone versus outflow discharge for the bottom outlet of 66 cm diameter.	23
Figure 3.7 Variation of flushing cone volume and width of flushing cone versus outflow discharge for the bottom outlet of 96 cm diameter.....	23

Figure 3.8 Observed and Dimensionless flushing cone volume using regressive model.	23
Figure 5.1 Shields Diagram for Unidirectional Flow (Vanoni,1975)(50).	31
Figure 6.1 Plan and Longitudinal view of the model and its details.	38
Figure 6.2 Details of the flushing gate.	38
Figure 6.3 Initial bed for different sediment material during experiments.	39
Figure 6.4 Arrangement of Multiple Transducers.	41
Figure 6.5 Data acquisition software.	41
Figure 6.6 3-Dimensional view of the flushing cone after the experiment with 1.30 l/s outflow discharge, 140 mm sediment thickness, 267mm water depth and 20 mm X 50mm bottom outlet of yellow lightweight material.	42
Figure 6.7 The bed topographic view of the flushing cone after the experiment with 1.30 l/s outflow discharge, 140 mm sediment thickness, 267mm water depth and 20 mm X 50mm bottom outlet of yellow lightweight material.	42
Figure 7.1 Flushing cone at the vicinity of bottom outlet with Blue & Yellow Lightweight Material.	43
Figure 7.2 Flushing cone at the vicinity of the bottom outlet with Sand.	43
Figure 7.3 Sand Hs 140 mm (left) and 120 mm (right)	45
Figure 7.4 Blue Lightweight Material Hs 140 mm (left) and 120 mm (right).....	45
Figure 7.5 Yellow Plastic Material Hs 140 mm (left) and 120 mm (right)	45
Figure 7.6 Flushing cone width versus outflow discharge for Blue Lightweight material (a), sand (b) & Yellow Lightweight material(c).....	46
Figure 7.7 The variation of flushing cone volume versus outflow discharge for different depth of sediment and different outlet openings.	48
Figure 7.8 Comparison between Blue lightweight material and sand for (a) 140 mm& (b) 120 mm sediment thickness.	49
Figure 7.9 Comparison of $V_s / H^3_{w\ net}$ of Blue Material, Sand and Yellow Material of sediment thickness 140 & 120 mm.	50
Figure 7.10 Comparison between Yellow lightweight material and sand for 140 mm (a) & 120 mm (b) sediment thickness.....	51
Figure 8.1 Comparison of $V_s H w_{net}^3$ ratio between sand and lightweight material.	53

LIST OF TABLES

Table 2-1 Distribution of storage volume and sedimentation loss(13).....	7
Table 3-1 Range of Dimensionless parameters	21
Table 4-1 Froude Law versus Reynolds Law	27
Table 5-1 Classification of Models (Kamphuis 1985).....	34
Table 6-1 Types of sediments used for experiments.....	39
Table 6-2 Different test constraints.....	40
Table 7-1 Result summary	44
Table 7-2 Statistical verification for presented equation	51
Table 11-1 Test parameters and scaling ratios for blue lightweight material and sand	61
Table 11-2 Test parameters and scaling ratios for yellow lightweight material and sand.	62
Table 12-1 Measured volume of BLWM flushed. ($H_s = 140\text{mm}$)	64
Table 12-2 Measured volume of BLWM flushed. ($H_s = 120\text{ mm}$)	64
Table 12-3 Measured volume of sand flushed. ($H_s = 140\text{ mm}$).....	65
Table 12-4 Measured volume of sand flushed. ($H_s = 120\text{ mm}$).....	65
Table 12-5 Measured volume of YLWM flushed. ($H_s = 140\text{ mm}$).....	66
Table 12-6 Measured volume of YLWM flushed. ($H_s = 120\text{ mm}$).....	66
Table 13-1 Comparison and computation of BLWM ($H_s = 140\text{ mm}$).....	68
Table 13-2 Comparison and computation of BLWM ($H_s = 120\text{ mm}$).....	69
Table 13-3 Comparison and computation of Sand ($H_s = 140\text{ mm}$).	70
Table 13-4 Comparison and computation of Sand ($H_s = 120\text{ mm}$).	71
Table 13-5 Comparison and computation of YLWM ($H_s = 140\text{mm}$)	72
Table 13-6 Comparison and computation of YLWM ($H_s = 120\text{mm}$)	73

1 Introduction

1.1 General Background

The increase in renewable energy demand has increased in the frequency of reservoir constructions during the past few decades. There are still many big reservoirs which are either in planning or in the construction stage. Installation of such artificial infrastructures impacts the rate of natural sediment flow and its transport rate in a river, trapping behind all those natural flow sediments instead of flowing them downstream. As the dams are built, still water will furthermore deposit all those transported sediments which are even more and unfavorable during monsoon and floods. This deposition phenomenon makes reservoir capacity smaller which ultimately affects a plant's output capacity and operating life, a very common problem of most of the reservoir around the world. In addition, it further reduces the flood handling capacity of a dam with loss of storage making power production more expensive with shorter power generation cycle and higher maintenance costs.

Lots of reservoir around the world are facing significant amounts of sediment deposition, affecting the effective operation of reservoir and power production. According to researchers (G Schellenberg, C.R Donnelly, C Holder and R Ashan) about 0.5% to 1% of the total volume of 6,800km³ of water stored in reservoirs around the world is lost annually as a result of sedimentation(Schellenberg et al., 2017). The Sediment rate is estimated to be higher in Asia with river merging from high slopes as compared to rivers in Europe. Therefore, reservoir sedimentation problem and consequence of this problem (loss of reservoir storage and efficient operation of the reservoir) raise a much serious problem in regions with high sediment yield.

Stickling environmental rules and regulations, impacts and issues with existing aquatic life, lack of suitable sites and higher construction costs do not make new reservoir a very good alternative to the sediment deposition issue. Therefore, it is very important to sustain and maintain the reservoir free of sediment.

Numerous approaches like watershed management, flushing, sluicing, sediment by-pass, density current venting, and dredging have been adopted to control the process of sedimentation. Among them, watershed management is one of the best alternatives to reduce concentrations of deposited sediments but could be expensive. While flushing, on the other hand, maybe the most economical method to extract all the accumulated sediments and restore the lost storage of the reservoir without any mechanical means.

Hydraulic flushing is one of the oldest techniques used in hydraulic engineering being practiced in the 16th century in Spain as credited by D' Rohan(Brown, 1944). When bottom outlets are opened suddenly, rapid outflow with excess shear force makes the deposited sediments in motion and washed out from the system with the flow. If flushing is operated under pressurized condition and water is maintained at the approximately same level above the bottom outlet, this flushing is called pressure flushing and has limited effect only around the outlet. Under such flushing conditions scour cone will be developed near the outlet opening. **Error! Reference source not found.** below shows the plan and sectional view of the pressure flushing near the vicinity of the bottom outlets.

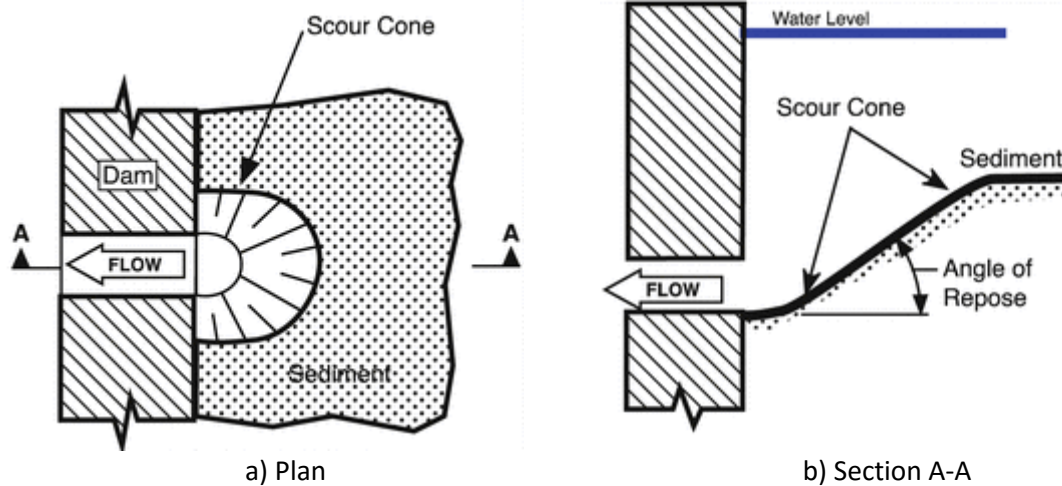


Figure 1.1 Longitudinal and Plan view of the pressure flushing (Morris, 2014).

There has been lots of research going with the physical model on the pressurized flushing from the past few decades. Using the physical model Emamgholizadeh (2006) found out that the volume of flushed sediment increased with the decrease of water depth and with increasing of discharge from the outlet (Emamgholizadeh et al., 2006). Similarly, he also found out that under similar conditions the volume of flushed sediments increased when the sediment size changes from coarse to fine sediment. Meshkati (2010) (Shahmirzadi et al.) found out that the volume of flushing cone was strongly affected by the diameter of the bottom outlet. Emamgholizadeh (2014) (Emamgholizadeh and Fathi-Moghdam, 2014) again experimented and discovered that the volume of flushed sediment increases with the increase of discharge, and decreases with the increase of sediment bulk density and the water level above the sediment. Furthermore, he also found out that water depth over the sediments is the most significant parameter in the collapse of sediments above the intake and the initial development of cone.

Similarly, B.T. Mohammad in 2018 also conducted some experiments with a physical model to study the hydraulic performance of pressure flushing in a straight-wall reservoir and concluded that the flushed sediment volume increased with the increase in outlet discharge, sediment depth and internal offset length of the outlet. He also revealed that the optimal ratio of water to sediment depth that introduced maximum volumes of flushed sediments was 2.08 and 2.26 (Mohammad et al., 2018). S. A. Kamble (Kamble et al., 2018) also conducted experiments to estimate scour cone development during pressure flushing of the reservoir and concluded that length and depth of scour cone increases with an increase in discharge, sediment deposit, area of outlet and decreases with water flow depth.

There has been an extensive study on investigation of pressure flushing technique at reservoir outlets in very wide ranges. However, studies related to physical modeling or pressurized flushing operation with lightweight materials are not common and limited. Research with lightweight materials with different hydraulic parameters such as outlet discharge, depth of sediment, flow depth and bottom outlets could be beneficial to estimate the volume of very small sand particles that will behave as a cohesive material in the laboratory.

1.2 Aim and Objectives of the study

The purpose of this study is to find how pressurized flushing operates on deposited sediments. The main objective of this work is to find the relation between the volume of sediments flushed with different hydraulic parameters like outlet discharge, depth of sediment, flow depth and bottom outlet. Furthermore, the objective of this study is to develop scaling relations among parameters of prototype

and lightweight model so that such models can be conveniently used for quantitative studies of processes involving sediment transport. The study was carried out for varying discharge, water depth, the thickness of upstream sediment layer and height of gate opening, and the results were compared to previous studies on the development of flushing cone under pressurized flushing condition. The results of this study can be useful in developing a scaling relation for quantitative interpretation of model study results to prototype values and vice versa.

1.3 Methodology of the study

For the study of the physical modeling of pressurized flushing operation with lightweight material, with literature review on scale model for pressurized flushing experimental setup was formed at Hydro Lab Nepal and Hydraulic Laboratory at NTNU. Two different light-weight (Blue and Yellow) materials and corresponding scaled natural sand of BLWM were used to conduct two sets of laboratory experiments with an identical setup. To make the result comparable from both sets of the experiment, the sizing of the sediments was chosen in such a way that they could be scaled up to represent a common arbitrary prototype. Each experiment was carried out by varying discharge, water level, sediment deposit thickness and different opening of the bottom outlet. The volume of sediments flushed with different outlet opening was compared with each other and with the empirical equations proposed by different researchers and the conclusion of the outcome is drawn.

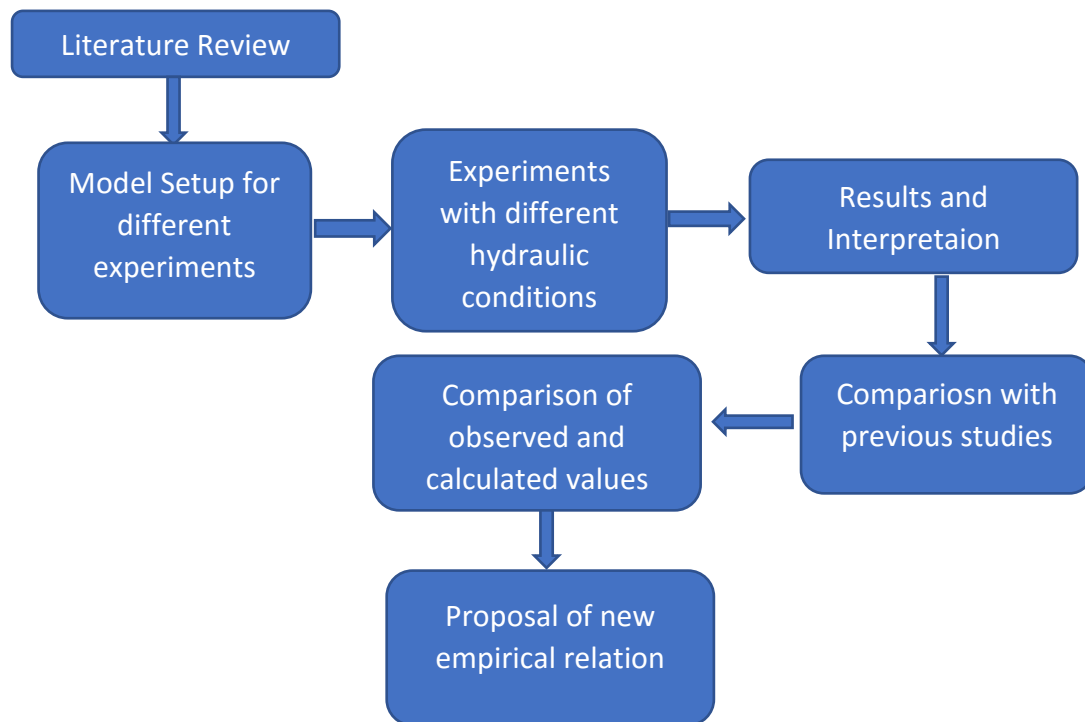


Figure 1.2 Flow Chart for Methodology of Study.

1.4 Structure of the Report

The present study addresses two different approaches, a literature review related to the scaling criteria of the sediments and the experimental values observed during different experiments for the sediments. Each chapter of the thesis is structured as follows:

- Chapter 2: Background in Reservoir Sedimentation

This chapter mentions some general background in reservoir sedimentation and the impacts of sedimentation on hydropower. Along with general background and impact of sedimentation it describes the management strategies to counteract or remove the sedimentation problem keeping focus of flushing schemes.

- Chapter 3: Physical Modelling

Chapter 3 deals with a general idea of physical modeling. This chapter emphasizes the importance of physical modeling with studies and research that have been done about the physical modeling of pressure flushing.

- Chapter 4 Theory

The fourth chapter provides a general approach to dimensional analysis and the concept and principles of similitude and similarity.

- Chapter 5 Scaling

This chapter addresses an explicit description of the scale factors and scaling laws used for physical modeling. Furthermore, this chapter encloses all derivational scaling formulas that would be required for scaling prototype material for this thesis work. Moreover, scale requirements for the different models are reviewed under this chapter.

- Chapter 6 Method

Experimental setup, the procedure of experiments, types of sediment used and its different constraints to experiment are discussed in this chapter. In general, this chapter explains the procedure that was followed for conducting experiments and the outcomes from the experiments.

- Chapter 7 Results and Discussion

All the findings with detail calculations from the experiments are arranged, compared and analyzed with the previous studies conducted by different researchers is included and discussed under this topic.

- Chapter 8 Conclusion

This chapter comprises the conclusion of the findings of the results.

- Chapter 9 Future work

Recommendations and future works are presented in this chapter

2 Background in Reservoir Sedimentation.

Reservoir sedimentation is a gradual process of filling the reservoir with sediments that are eroded, transported and deposited from the watershed. The nature of the material and ground cover and the slope in the catchment area are the main factors contributing to reservoir sedimentation. In natural or uncontrolled rivers, sediment processes are relatively balanced. When artificial structures (dams or weirs) are constructed for power generation or other water diversion purposes, causes decreases in natural velocities of river flow, initiating or accelerating sedimentation, resulting in progressively finer materials being trapped upstream of the reservoirs. Furthermore, decrement of natural sediment flows further downstream can cause dramatic changes to flood plains and the formation of deltas.

Figure 2.1 illustrates the typical deposition of sedimentation with progressive deposition of finer materials as the flow advances the dam. This accumulation is a serious problem in many parts of the world and has severe consequences for water management, flood control, and production of energy. The life of the reservoir can be divided into three stages(Garcia, 2008); cited from(Schellenberg et al., 2017). The first stage is the continuous sediment trapping stage where sediments are accumulated rapidly. Currently, most reservoirs around the world are in the first stage or continuous sediment trapping. The second stage of the sedimentation process is partial sediment balance. During this stage, there will be a mixture of sediment deposition and removal in reservoirs. Fine sediments outflow towards downstream reaching the sediment balance whereas, coarse sediment continues to get accumulated at the bottom.

The third and final stage is full sediment balance, which occurs when sediment inflow and outflow are equal. Sediment balance can only be achieved either if incoming sediment load can be moved or transferred towards downstream or removed from the reservoir.

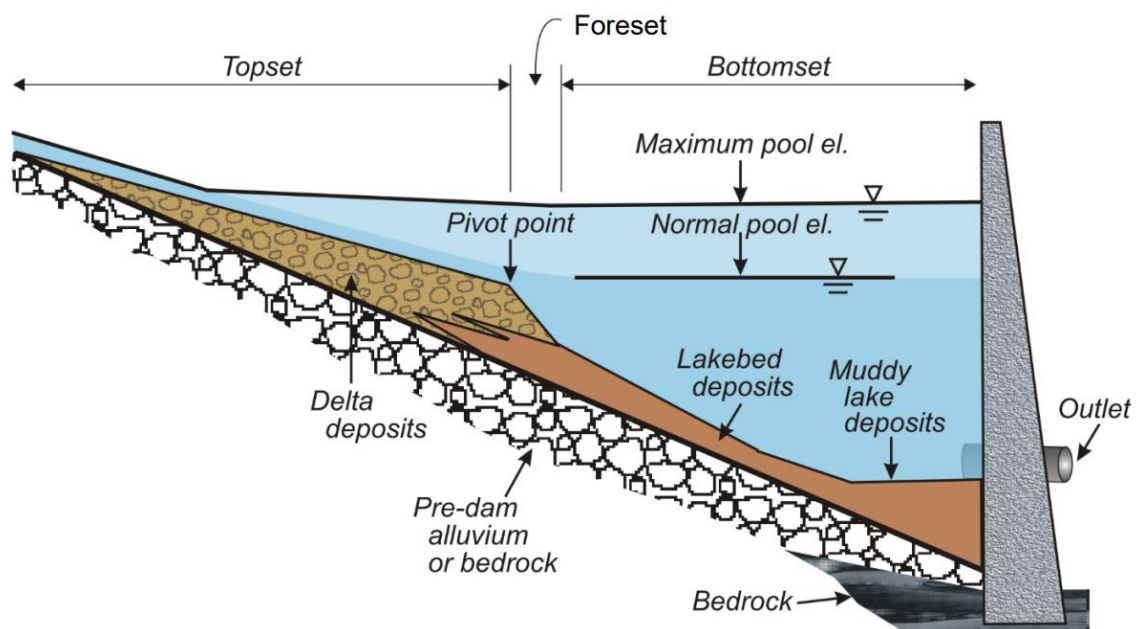


Figure 2.1 Reservoir Sediment Profile(Randle et al., 2017).

As discussed earlier most of the world's reservoirs are in the continuous accumulation stage. Many reservoirs were designed by estimating sedimentation rates to provide a pool with enough volume to achieve a specified design life. However, this design life is typically far less than what is achievable. Therefore, managing reservoirs to achieve a full sediment balance is essential to maximize their lives. According to Grummer (2009) developing regions of the world that stand to benefit most from hydroelectricity are often those with the highest sediment yields (Gummer, 2009); cited from (Schellenberg et al., 2017). Figure 2.2 below shows the world's hydropower potential with sediment production. Areas with higher sediment yields and significant hydropower potential will need to consider sediment management techniques before developing hydropower schemes.

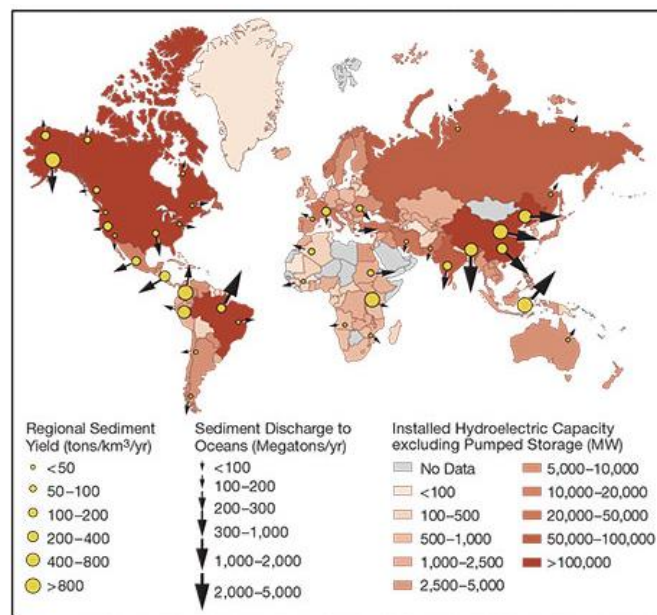


Figure 2.2 Comparison of Hydroelectric Potential and Sediment Production (Milliman and Meade, 1983, Schellenberg et al., 2017).

Figure 2.3 and Table 2-1 gives a general idea about the loss of storage volume due to sedimentation.

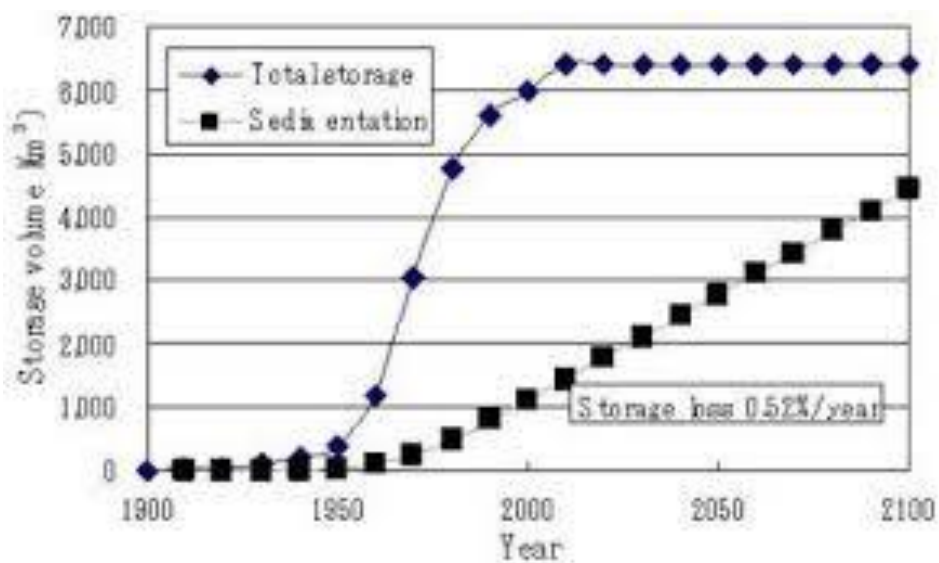


Figure 2.3 World Storage Volume and Storage loss(Sumi et al., 2009).

Table 2-1 Distribution of storage volume and sedimentation loss(Sumi et al., 2009).

Region	Total capacity [km ³]	Annual sedimentaion [km ³]	Sedimentaion Loss (%)	Total Capacity Loss [km ³]
North America	1845	3.69	7.9	112
South America	973	1.04	2.5	17
Northern Europe	822	1.88	6.8	48
Southern Europe	135	0.25	5.6	6
Sub-saharan Africa	574	1.32	7.8	32
Northern Africa	188	0.15	2.4	3
China	526	14.93	45.8	230
Southern Asia	233	1.66	13.1	31
Central Asia	132	1.48	26.9	29
South East Asia	117	0.35	8	6
Pacific Rim	232	0.75	7.6	15
Middle East	199	3.36	27.7	38
Global Totla	5976	30.86	11.8	567

2.1 Effects of Sedimentation on Hydropower

2.1.1 Impact on Generation

One of the main impacts of reservoir sedimentation on waterpower generation is the loss of storage. Globally, the total volume of water stored in reservoirs used for hydropower and other purposes around the world currently exceeds 6,800 km³ and about 0.5 to 1% of this global reservoir volume is lost every year as a result of sediment deposition (Garcia, 2008); cited from (Schellenberg et al., 2017). If these rates continue unabated half of the world's reservoir storage would be lost within the next 50 to 100 years. Without the ability to store water, waterpower facilities operate entirely as run-of-river plants with generation entirely dependent on seasonal flows eliminating one of the key benefits of water storage during the time of the dry season.

2.1.2 Impact on Stability

Sediment loads are commonly idealized as static soil pressure. But the literature studies advice different sediments that could accumulate in front of the dam have that wide range of internal friction angles. The sediments sourcing from lower step slope stream (loose silt or clayey sediments) likely to have a much lower internal friction angle and therefore higher-pressure coefficient. Whereas, sediments on a steep slope stream that will have a larger bed material (sand and boulders) as sediments have a higher internal frictional angle.

Sediments could be both useful or harmful. Fine silt or clay sediments are expected to reduce seepage pressure at the bottom of the dam whereas, completely suspended particles would transfer high pressure at the bottom of the reservoir.

Adopted Seismic loads vary with the individuals but the basic assumption for fully liquidize reservoirs sedimentation is that it loses all shear strength and exerts a full hydrostatic load based on the buoyant

weight of the sediment on the upstream face of the dam or concrete structure. Furthermore, the behavior of reservoir sediments during the earthquake and their effect on the water-retaining structure is poorly understood. Therefore, to ensure the impacts of sediment during the earthquake, an investigation with a multidisciplinary approach between geotechnical and sediment structural engineer is necessary.

2.1.3 Impact on Discharge capability

Many dams are facilitated with low-level outlets located at the base level of the dam to lower the water level of reservoirs in the event of a dam safety incident. Continuous tapping of sediments will fill up the dead storage of reservoirs and block the flow. Fine sediments could travel further down to headrace tunnels and clog the conduits as well as penstocks not allowing to use its full capacity for power generation.

Sedimentation could also cause loss of spillway capacity as a result of the loss of approach depth when the sediment front reaches the dam. Many hydro projects have encountered such a problem. Loss of flood routing effects in another additional impact that infilled reservoir could confront.

2.1.4 Impact on Equipment

The presence of sediments that operate the mechanical equipment for hydropower generation leads to a significant amount of damages leading to a drop in turbine efficiency, generation loss due to the extended shutdown of maintenance and replacement eventually leading to a huge loss of revenue. These problems to mechanical equipment get worse in the monsoon season when sediment concentration is very high.

Mechanical erosion can be prevented either by selecting appropriate erosive resistance metal or by reducing the sediment concentration reaching the mechanical equipment. An alternative method of protecting mechanical equipment from such extensive damage could be done also by the use of hard surface coating or by using hard alloys. Selection of proper alternative to protect the mechanical equipment depends upon the costs.



a. Francis turbine at Kaligandaki Power Plant, Nepal(Chhettry et al., 2014) b. Francis turbine at Nathapa Jhakri Power Plant, India(Sharma and dams, 2010) c. Francis turbine at Chawai Power Plant, Peru(Neopane, 2010)

Figure 2.4 Sediment erosion in turbines from various Power Plant.

2.1.5 Impact on Environment

All reservoirs will disturb the natural flow movements of sediments. Interruption of natural flow due to constructions of water impound storage may alter the concentration of suspended sedimentation in the water column, resulting in potential ecological impacts downstream. In addition, an increase in

sediment concentration can decrease the natural habitat for plant productivity which could have various negative impacts on the food cycle of living aquatic, fish as well as bird species.

The environmental impacts of sedimentation include followings

- Loss of important aquatic habitat
- Change in the migration pattern of fish
- Loss of wetlands
- Change in the food cycle of aquatic life
- Los of submerged vegetation

2.2 Reservoir Sediment Management Strategies

Reservoir sediment management strategies both prolong and benefit downstream reaches by mitigating the sediment starvation that results from sediment trapping. Two basic strategies that may reduce the sediment yield entering the reservoirs from upstream are:

1. Control the soil and channel erosion from the source.
2. Trap the eroded sediment upstream of the reservoir.

These strategies are summarized below.

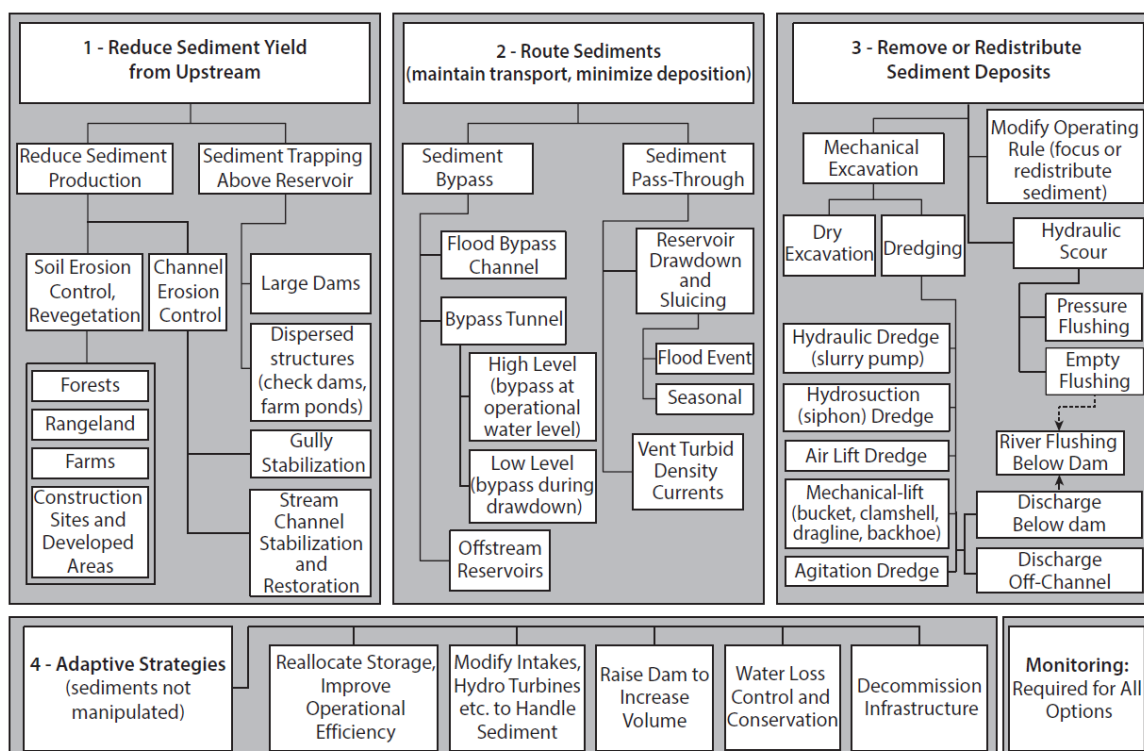


Figure 2.5 Sediment Management Strategies (Annandale et al., 2016).

2.2.1 Dredging

Dredging is the process of removing deposited sediment from the reservoir. Dredging could be done by hydraulic operation or by dry excavation. The selection of the excavation method will depend upon sediment volume, grain size, and geometry of the deposit, disposal and reuse options, water levels, and environmental criteria. This method is costly mainly because of the large volume of materials being

involved to excavate out, availability of suitable sites for deposition of excavated materials within the vicinity.

In large hydropower reservoirs, dredging is done for cleaning or extracting accumulated materials especially from intakes and deposit to another location. Whereas, in small impounding structures dredging focuses on the removal of silts and organic sediments. Size and the frequency-dependent upon the number of sediments collected in the reservoir. Types of dredges can be classified as

- Hydraulic Suction Dredges
- Siphon Dredge
- Jet Pump
- Cable-Suspended Dredge Pumps
- Mechanical Dredges

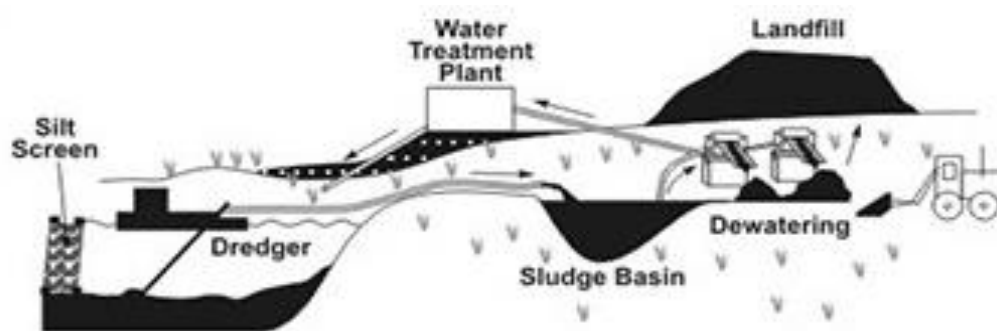


Figure 2.6 Basic concept of Dredging (Source: USEPA 2005, Adapted by Battelle, NAVFAC Contact No, N62473-07-D4013); cited from(Center)

2.2.2 Venting Turbid Density Current

Sediment-laden water enters and plunges under the clear water surface of the reservoir due to their higher density called turbidity current. Turbidity current can travel a long distance of the dam, depending upon the size of the reservoir, sediment size, and its concentration and temperature difference. During the movement, if the dam bottom outlets are opened it can reduce deposition of sediments by turbidity current venting.

Since the operation of venting requires very low outlet discharge it could be beneficial for the downstream environment along with reducing the amount of the sediments in the reservoir. However, this method requires information on the turbidity currents and their monitoring which could be costly.

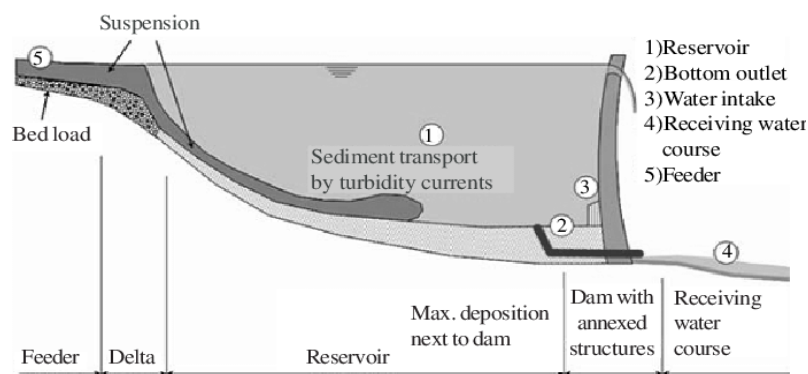


Figure 2.7 Venting Turbidity Density Current(Pari et al., 2010).

2.2.3 Sediment Bypassing

Sediment bypassing is a process of transporting sediments from upstream of the reservoir to downstream with a conveyor system. On-stream sediment bypassing diverts part of the sediment-laden water around the reservoir, typically using a weir that operates during high flows when sediment concentrations are high. Highly concentrated sediment-water is diverted using a channel or tunnel before joining the river downstream side of the dam.

An off-stream reservoir can be used such that only the clear water is diverted over a bypass weir. An off-stream reservoir typically has limited capacity and can only exclude sediments carried by higher streamflows. However, it does reduce the amount of suspended sediment and bedload reaching the reservoir. Other advantages include the fact that the reservoir and dam are located away from the main river channel, allowing for minimal disruption to aquatic species and habitat and reducing the need for large on-stream spillways. On the other hand, off-stream reservoirs typically do not permit maximization of generation capacity, especially in areas that depend on high stream flows occurring over a short period.

Sediment bypassing works best in areas of high relief where the sediment-laden flows are carried efficiently through the diversion tunnel or channel. Bypassing is most cost-effective at dams that are on the bend of a river, as this allows for a relatively short diversion between the weir and the downstream side of the dam. In Figure 2.8 below (a) conventional reservoir trapping sediments, contrasted to alternative configurations for bypass of sediment-laden flood flows around the reservoir, (b) bypass off-stream storage, diversion dam diverts water to the off-channel reservoir during times of clear flow but does not divert when suspended sediment concentrations are high, (c) sediment bypass channel or tunnel, diverts flow from the river upstream or the reservoir passing it around the reservoir and into downstream channel.

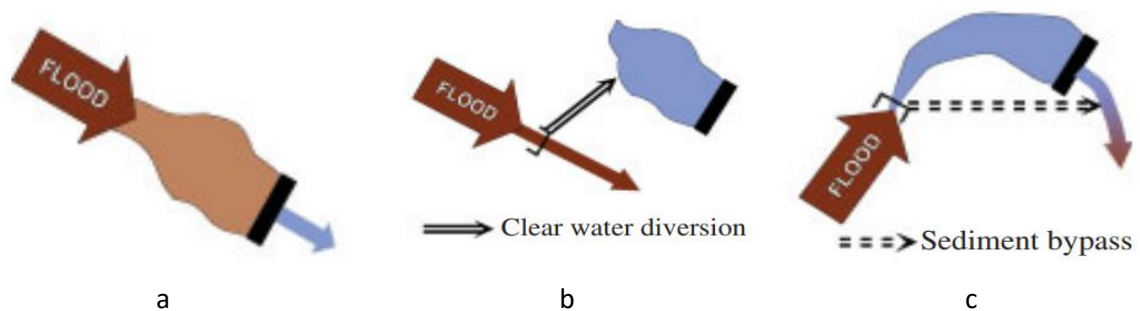


Figure 2.8 Sediment Bypassing(Kondolf et al., 2014).

2.2.4 Flushing

In simple words flushing refers to the process of hydraulically removing of deposited sediments from a reservoir or passing incoming sediments through the reservoir to preserve and maintain reservoir storage capacity. Hydraulic flushing involves reservoir drawdown and emptying by opening a low-level outlet to temporarily establish riverine flow along the impounded reach, eroding a channel through the deposits and flushing the eroded sediment through the outlet. Flushing uses drawdown and emptying to scour and release sediment after it has been deposited. However, sediment entering the reservoir during flushing periods will also be routed through the impoundment and released (Morris and Fan, 1998).

Flushing actions involves two key features

1. Removal of sediments that have been already deposited.
2. Release of sediment downstream varies significantly from sediment inflow.

Repeated flushing usually per annual interval is required to maintain and scour through the deposited sediments. In the case of large reservoirs, only narrow channels of deposits are flushed forming a flood plain-type geometry. In such cases, auxiliary or secondary channels in addition to main flushing channels may be used to flush the floodplain sediments.

2.2.5 Limitations

There are two main limitations of flushing

- Necessary to draw down or empty the reservoir, which limits power production during flushing periods.
- Flushing will end up discharging high concentrated sediments from the reservoir at a more advanced rate than a natural flow.

Besides the above-mentioned point, flushing can moreover have an environmental effect with high concentrated sediments destroying natural habitats of living organisms. In addition, sediment deposit may also alter the stream benthos (stream bed) long after flushing has been completed, reducing natural channel capacity and increase flood hazards.

2.3 Types of Flushing

Flushing can be classified into two general categories.

2.3.1 Empty or Free flow flushing

It involves emptying the reservoir to the level of flushing outlet and inflowing water from upstream is routed through the reservoir, resembling natural riverine conditions.

2.3.2 Pressure Flushing

It involves flushing under the pressurized conditions and a sustained reservoir water level. Under pressurized flushing conditions, all the settled sediments near the outlet opening of sluice gates are scoured within a very short time and funnel-shaped crater (flushing cone) will be formed by flushing flow. Once the cone is formed and is stable then there is no further movement of sediment from the cone. Figure 2.9 below illustrate the formation of flushing cone.

The flushing cone geometry which is developed after the pressurized flushing is influenced by the following factors.

- Submerged angle of repose of the sediments
- Inflow and outflow of water and sediment
- Outlet geometry
- Characteristics of the sediment

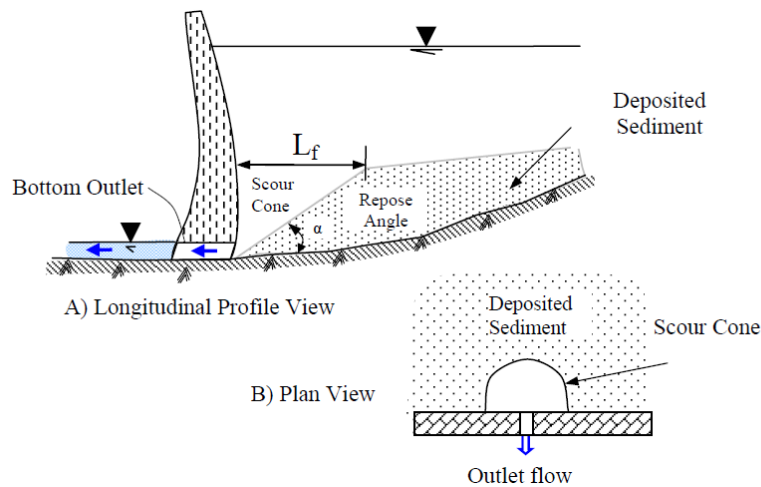


Figure 2.9 Longitudinal and Plan View of the pressure flushing (Samad Emamgholizadeh, 2006).

There have been broad studies about the pressurized flushing. Researchers have studied the extent of sediment deposit and develop a relation between reservoir depth, scour the length and outlet discharge. Moreover, their results showed that the formation of scour cone increases with a decrease in the water level in the reservoir. With the use of a physical model for research on pressure flushing researcher (Fang & Cao) concluded, with the release of the bottom intake funnel-shaped crater was developed with the angle of repose of the sediment (Fang and Cao, 1996); cited from (SHAHMIRZADI et al., 2010). Shen presented a dimensionless regression relation for determining the scoring depth of flushing cone in non-cohesive sediments (Shen et al., 1993); cited from (SHAHMIRZADI et al., 2010). Emamgholizadeh with his experimental studies also concluded that an increase is discharged at the outlet and lowering water level at reservoirs increases flushed sediments (Emamgholizadeh et al., 2006).

Even though with such intensive studies on pressurized flushing techniques, studies on the time-dependent analysis of flushing cone development are limited. Furthermore, lack of water resources and negative environmental impacts of pressure flushing makes the entire full flushing process impossible. Under such circumstances its vital to make establish a good harmony among sediment erosion, water resources on hand and one of the most important factors 'environmental impacts' (Meshkati et al., 2009).

2.4 Importance of Flushing Strategy

At present, almost all of the storage reservoir built are facing a common problem of sediment accumulation on its bed. Flow from the river system erodes and transports the bed materials with the flow and deposits it downstream where the flow velocity is low. This continuous action of disintegration, passage, and deposition over period result a considerable volume of storage lost every year. According to research undertaken by the World Commission of Dam reported that between 0.5 -0.1% of total storage is being lost every year due to sedimentation. Similarly, the International Commission on Large Dam (ICOLD) also estimated that 0.5 -0.75% of the total storage capacity is being lost each year because of the constant accumulation of debris. The researcher believes that reserves without proper watershed management in developing countries with a higher concentration of

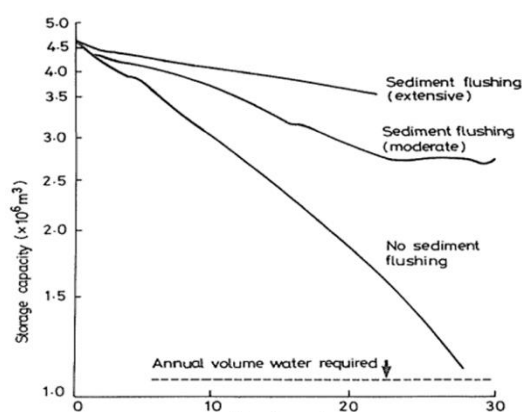
sediment load, loss of storage capacity are even at a much higher rate than other sediment affected areas. In addition, to rapidly filling the reservoirs, sediments are also causing a significant amount of damage to mechanical equipment due to the wearing of turbines. Such disintegration of turbine edges due to sediments significantly lowers the output production ability and are costly to repair and maintain for continuous production of energy in hydropower schemes.

Among different approaches which could be used to tackle the sedimentation issues in reservoirs, flushing may be one of the most economical technique to reclaim the lost storage without including another extra cost of dredging and other means of transporting and dumping to downstream Emamgholizadeh (2006)(Emamgholizadeh et al., 2006). Therefore, it has been successfully employed in many storage basins. Due to such advantages, flushing will further receive more attention in the future as well. There have been lots of extensive studies going on about sediment flushing schemes at different reservoirs around the world. At some reservoirs, it is proving to be very successful and in some, it showed little or no success as well.

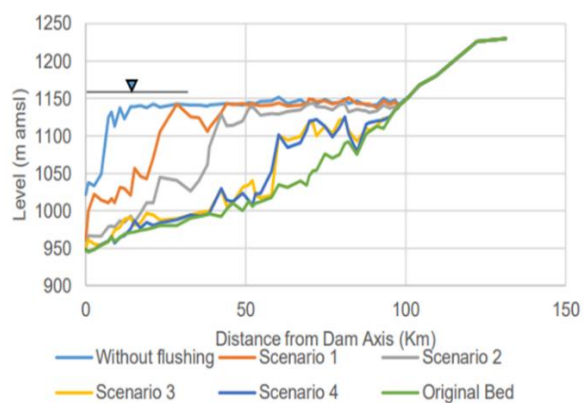
Hemphill (1931) (Hemphill, 1930); cited from (Brandt, 1999)stated that it is doubtful whether flushing is effective in larger reservoirs, but in most mountain hydropower reservoirs, flushing is the main and cheapest way of fighting against silting. Qain (1982) (Qian, 1982); cited from(Brandt, 1999)stated that flushing is only an option in reservoirs with small reservoirs capacity to water inflow and large capacity of sluices. However, flushing has been proved to be very effective at some reservoirs like Baira reservoir India, Gebidem reservoir Switzerland, Gmund reservoir in Austria, Mangahao reservoir in New Zealand, some reservoirs in China and Sefid Roud reservoir in Iran.

White (1990) also investigated the effect of flushing on the storage of the Kamativi dam, Zimbabwe and found out that the storage of the dam could be maintained for a considerable period of time with practical means of flushing. Figure 2.10 (a) below shows the graph of the storage capacity of the Kamativ dam with and without sediment flushing.

Similarly, Waqas Javed and Tawatchai Tingsanchali (2016) studied the impact of sediment flushing of Diamer Bhasha Dam in the Northern part of Pakistan. They found out that the reservoir could be used for a long term without any significant loss in storage capacity if the reservoir is operated with flushing. Figure 2.10 b below shows the profile of the river bed for different scenarios of flushing.



a. Kamativi FDam, Zimbabwe (White et al., 1990)



b. Diamer Bhasha Dam, Pakistan(Javed and Tingsanchali)

Figure 2.10 Effect of sediment flushing on the storage capacity of the reservoir.

Both figures are examples showing the importance of a flushing system in a reservoir to wash down the incoming sediments and prolong the reservoir's operation life. With such studies, we could

conclude that flushing strategy could be one of the most economical ways to tackle the ongoing sediment problems in the reservoir and responsible for operating and maintaining a hydraulic system without obstruction.

2.5 Flushing Procedures.

Flushing events has three stages. They are:

- Drawdown
- Erosion
- Refill

Figure 2.11 summarizes the characteristics behavior of hydraulic and sediment parameters during flushing. The drawdown stage can be further divided into two parts, preliminary drawdown, and final drawdown. Preliminary drawdown involves lowering down the reservoir to the minimum level of operation diverting available water for hydropower turbines to generate power. This process generally can occur for several days or weeks. Another stage of drawdown, final drawdown engages rapid emptying of the reservoir lower than the normal minimum operational level using the outlets installed at the bottom as a gate which occurs for a short period as compared to preliminary drawdown. For small reservoirs, this action of final drawdown could be completed within a few hours as well.

During the process of drawdown sediment from upstream of a dam or reservoir could be very active in motion and will get shifted from its initial position to further downstream where it again comes to rest and deposit. During such process, turbid current may be formed by the movement of eroded sediment and involves the various transition from erosion to deposition.

The erosion stage occurs when the riverine flow is established which producing high flow velocities that wash or rub the fine sediment deposits from the channel and transport those sediments through a dam. The duration of the process of erosion could last for a few days or a week, depending upon the sediment loads or flushing discharge. The refill stage begins with the closer of outlets installed at the bottom of dams or reservoirs and raising backwater causes sediment to deposit. When the sediment concentration is low, flow is released through outlets to help the sediment deposit further downstream of the river channel.

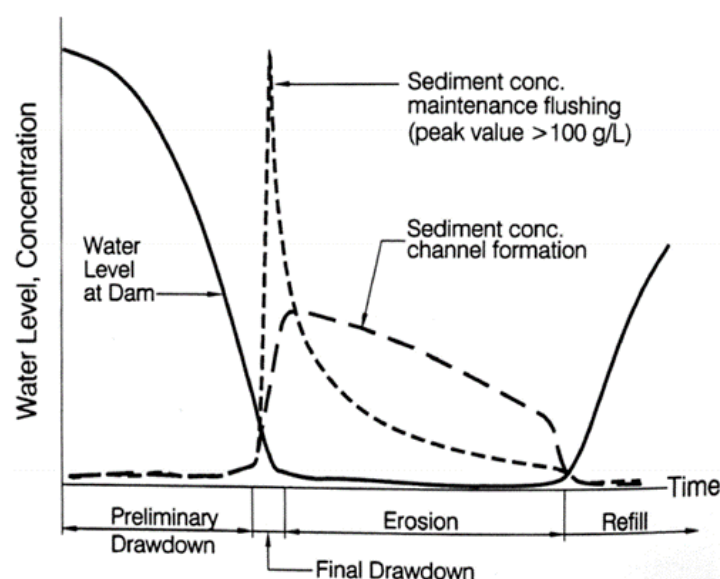


Figure 2.11 Hydraulic and sediment characteristics during flushing events at constant discharge (Morris and Fan, 1998).

2.6 Flushing Period

2.6.1 Flushing During Flood Season

The most common period of flushing is during flood season allowing the early-season flood to pass through the impoundment allowing the reservoir to refill with sediments during flood season. As it incorporates both the features of sediment routing and flushing, more effective than single routing and flushing used alone. Water reservoirs get dry with sediments due to flushing at an early stage through the operation of gates and during the end of the flood season, the outlet is closed to reserve the water for the dry season. This process of deposition and flushing has proved to be effective for many places with sediment problems.

2.6.2 Flushing During Nonflood Season

It is also possible to execute flushing during the non-flood season as well. During such period available discharge is small or lower than the flood season, making the flushing operation period longer and the rate of sediment deposition on flood plain can also be expected higher.

2.7 Erosion Process During Flushing

2.7.1 Slope Failure

Flushing action produces unstable banks that will slide and skid the side slope banks into the flushing channel. With frequent alternation of water level on the banks and widening of the flushing, the channel makes side slope vulnerable to the failure. The type of slope failure and angle of repose will depend upon the sediment characteristics. Figure 2.12 and Figure 2.13 below shows an example of slope failure during flushing.

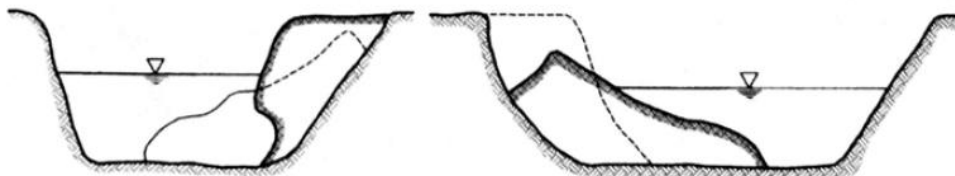


Figure 2.12 Slope failure in consolidated sediments (Morris and Fan, 1998).



Figure 2.13 Slope failure in unconsolidated silt and clay (Morris and Fan, 1998).

2.7.2 Retrogressive Erosion

A channel erosion process characterized by a zone of high slope and rapid erosion, moving upstream along a channel having a lower slope and erosion rate, is termed retrogressive erosion. The process of retrogressive erosion is illustrated in Figure 2.14.

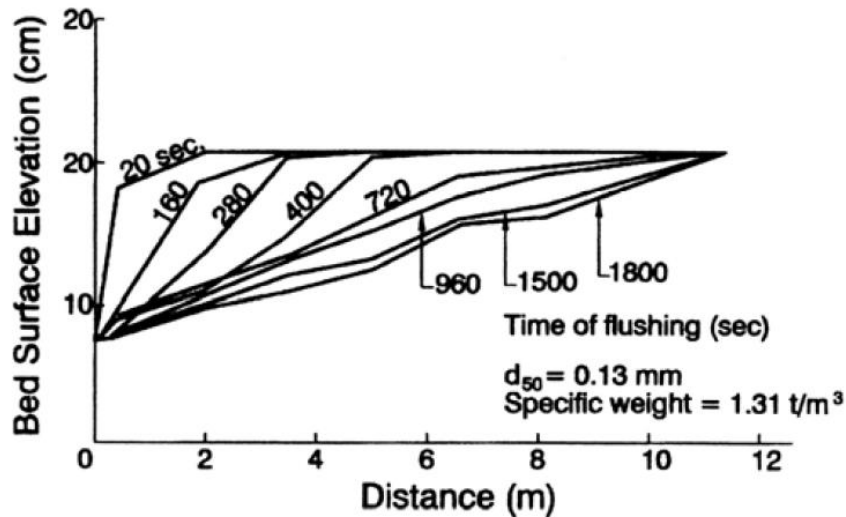


Figure 2.14 Process of Retrogressive erosion(Morris and Fan, 1998).

Retrogressive erosion is the principal method for the formation of flushing channels through reservoir deposits. The opening of deep outlets – which establishes flow across deposits having a relatively mild slope, with an abrupt drop or even a waterfall at the downstream end – initiates retrogressive erosion, creating a nick point that can move upstream rapidly depending on the nature of the deposits and the erosional forces.

Retrogressive erosion results from the change in hydraulic energy caused by the discontinuous longitudinal profile, and it is not dependent on any specific grain size in the deposit, although erosional patterns are influenced by the deposit characteristics. Retrogressive erosion can occur in coarse sediments on a river delta and in fine-grained and cohesive sediments.

2.7.3 Progressive Erosion

The term progressive erosion refers to a channel erosion process which occurs uniformly or progressively along the length of a channel instead of being concentrated at the downstream end. In general, when the suspended-sediment concentration in flowing water is less than the sediment carrying capacity, the flow will entrain sediment from the channel bed. When clear water enters a zone of erodible deposits having a uniform slope and grain size, it will progressively entrain sediment by eroding the deposit. The rate of bed erosion will initially be rapid because of the large available sediment-carrying capacity of clear water. As the flow progresses downstream and entrains sediment, its capacity to erode and transport additional sediment will decrease, eventually reaching zero. In this manner, progressive erosion can cause a high rate of bed erosion at the upstream end of a deposit and less erosion at the downstream end. This erosion pattern can be offset in reservoirs by the tendency for deposits to be coarser and less erodible at the upstream end.

3 Physical Modeling

3.1 Introduction

The physical model is a replica of an object or physical system that may be smaller or larger than the original one for laboratory studies. Usually, physical models are reduced to a smaller object for simplicity and easy to interpret how the prototype works in the real field. Physical modeling is a well-established approach for hydraulic studies which allows visualization, examination and gain information about prototype without spending a lot of money building a real object (prototype) in the field. It is used to visualize information about the context that the model represents. The main objective of physical modeling is to test a different aspect of a product or prototype as per the requirements of users.

In hydraulic engineering, physical models allow us to explore the fluid flows and its effects on the hydraulic structure during flow that enables them to improve the final design or product. It not only allows designers to explore and test their ideas but also presents them to others.

However, physical models are only good as assumptions and data on which they are based. It is one of the most cost-effective ways of providing this data. Physical hydraulic models which are well-founded and controlled laboratory experiments simulating hydraulic systems are therefore important to both our present and future research needs(Frostick et al., 2011).

Physical modeling tools have developed enormously during the last few decades. They have not only played an important role in the field of hydraulic engineering but provided us a good insight into the complex hydrodynamic regime and reliable and cost-economic solutions for different hydraulic problems as well. Furthermore, they also have provided valuable information about the problem that may arise in the future. Today we can find lots of engineering design solution or techniques which were developed using laboratory measurements and experiments for validation.

Laboratories around the world are performing physical modeling with their method for their model studies which resulted in the procedure of physical modeling to be different even for similar experiments. This limitation formed the result obtained from physical modeling to be empirical and very difficult in understanding and transferring the data. So, further tests and studies are required for a unified approach of physical modeling and to act as a reference for new researchers and studies new to the field. On the topic of physical modeling of pressurized flushing operation with lightweight material, this section will address how lightweight materials can be used for the study of sediment transport and how it can be related to natural sand sediments in scale models.



Figure 3.1 Example of Physical Modelling a & b.

3.2 Advantages and Disadvantages of Physical Modelling

3.2.1 Advantages

- Visual feedback from the model.
 - The immediate qualitative impression of the physical processes which can help to focus the study and reduce planned testing
 - Can help to reduce conflicts with stakeholders
 - Helpful for teaching and education
- Possibility to obtain measurements for extreme conditions not measured at the prototype.
 - High degree of experimental control allowing for the simulation of varied or sometimes rare environmental conditions (floods)
 - Safe design of spillway structure and energy dissipator
- Integration of governing physical processes without simplifying assumptions that have to be made for analytical or numerical models.
 - Provide measurements for complicated phenomena that have not yet been accessible for theoretical approaches
 - Can be used to obtain measurements to verify or disprove theoretical results
- Physical models can provide data for testing and verification of numerical models.

3.2.2 Disadvantages

- Scale effects occur in down-scaled models if all relevant variables are not correctly simulated.
- It is not possible to simulate all the relevant variables in the correct relationship with each other.
- Inefficiency to replicate the real forcing conditions leads to the progress of laboratory effects and impacts the process being simulated.
- Requires wider space and are time-consuming to build.
- High level of skill required to install and maintain and are also more expensive to operate than the numerical model.

3.3 Why Physical Modelling?

Although computational fluid dynamics (CFD) modeling is very common to simulate modern fluid mechanics problems, sometimes they lack to accurately predict some important physical phenomena. In addition, physical modeling analyses general hydraulic operation conditions and characterizes the hydrodynamic actions, providing the trust factor to ensure and increase the efficiency, safe and cost-effective design of the hydraulic system.

Another reason to pick physical modeling is it test alternatives which are not possible in CFD models. It is very easy to make alternation in physical modeling even in operation with small effort and time which could be difficult, and time-consuming to re-mesh and rerun the whole model in CFD.

If we compare the experience of physical modeling and CFD modeling, physical modeling has more than 100 years of research and knowledge with CFD striding from the last few decades. So, hydraulic engineers recommend physical modeling over CFD modeling in cases of irregular or non- standard site-specific conditions, complex hydraulic conditions, or the use of a non-standard design to improve project performance, constructability, or economics.

Focusing on why physical modeling with lightweight material, scaling of the prototype would be very simple except for very fine sediments. If the prototype turns out to be very small-sized sediments and its model scale would further become very small, which will behave as a cohesive material and its behavior could not be studied properly. For this reason, non-cohesive lightweight material could be used for the study process involving sediment transport of very fine and small-sized materials.

3.4 Some Definitions

3.4.1 Prototype

The object or the situation which is being modeled either in the same scale or most often at a reduced scale is called prototype.

3.4.2 Scale

According to Yalin 1971, a scale is a constant proportion of measurable characteristics between model and prototype (Yalin and Kamphuis, 1971). In simple words, we can define scale as a proportion between the prototype and model value of a certain parameter.

3.4.3 Similitude (or Scaling) Criteria

Formal mathematical definitions that must be met by the scale ratios between prototype and model.

3.4.4 Similarity

A condition that exists when a model gives a similar response as the prototype, even if the model is not in strict similitude with the prototype.

3.4.5 Scale Effects

Differences between the prototype and model response that result from the inability to simulate all relevant forces in the model at the proper scale dictated by the scaling criteria.

3.4.6 Laboratory Effects

Differences between the prototype and model response that arise from limitations of space, model constructability, instrument, or measurement techniques.

3.5 Basic Aspect of Physical Modeling

The basic aspect of the model is to have similarity with the prototype to find or confirm hydraulic solutions. Three basic types of similarities that must exist between model and prototype. They are.

- Geometric Similarity
- Kinematic Similarity
- Dynamic Similarity

In practice, it is not possible to have similarity in all values as some of these similarities are incompatible because of the same fluid or considering the same gravitational and other natural factors. Therefore, the most relevant forces present in the prototype must be selected and the model must be built according to the related similarity.

Gravitational, frictional and surface tension is the relevant forces for most of the hydrodynamics problems (Dalrymple, 1985)(Dalrymple, 2018). Thus, dimensional products are combinations of Froude, Reynolds, and Weber numbers. Other forces like compressibility and elasticity effects are neglected because these values are very small as compared to others and have a very small effect. Even though the same fluid is used in the model as a prototype, it prohibits satisfying all Froude, Reynolds and Weber number scaling criteria. Thus, most of the models are simulated with only Froude's similarity, implementing gravitational effects as the most significant criteria as compared to viscosity and other forces of water which does not have significant roles in models.

3.6 Previous Studies of Physical modeling of pressure flushing

Numerous studies had been carried out of the physical modeling of pressure flushing with different materials of sediments. Studies have shown that a sudden collapse of the deposited sediments near the outlets as soon as the bottom outlet was opened. This was due to the formation of a considerable pressure gradient through the outlet opening and sediment layer. Furthermore, the density of the drained material reduced over time and a stable flushing cone developed.

3.6.1 Experimental Investigation of Local Half-Cone Scouring Against Dam.

M. E. Meshkati Shahmirzadi, A. A. Dehghani, T. Sumi, Gh. Naser, A. Ahadpour in Hydraulic Laboratory of Gorgan University of Agricultural Science and Natural Resources, Iran 2010.

Experiment constraints and the result is shown below.

Experiment Constraints:

- Flume hexahedral shallow basin 2.0 m X 1.50 m X 3.0m (W X H X L)
- Outlet gate openings 2.54, 3.81, 5.08 and 7.62 cm
- Sediment size (d_{50}) 1mm
- Sediment thickness 16 cm
- Water depths (H_w) 36, 66, 99 mm
- Discharge (Q) 0.15 – 1.5 l/s

Table 3-1 Range of Dimensionless parameters

Parameters	Variations
$V_{scouring} / H_w^3$	0.00046-0.372
Fr^*	0.16 – 32.2
H_s / H_w	0.166 – 0.444
D_{outlet} / H_w	0.026 – 0.21

Experimental setup

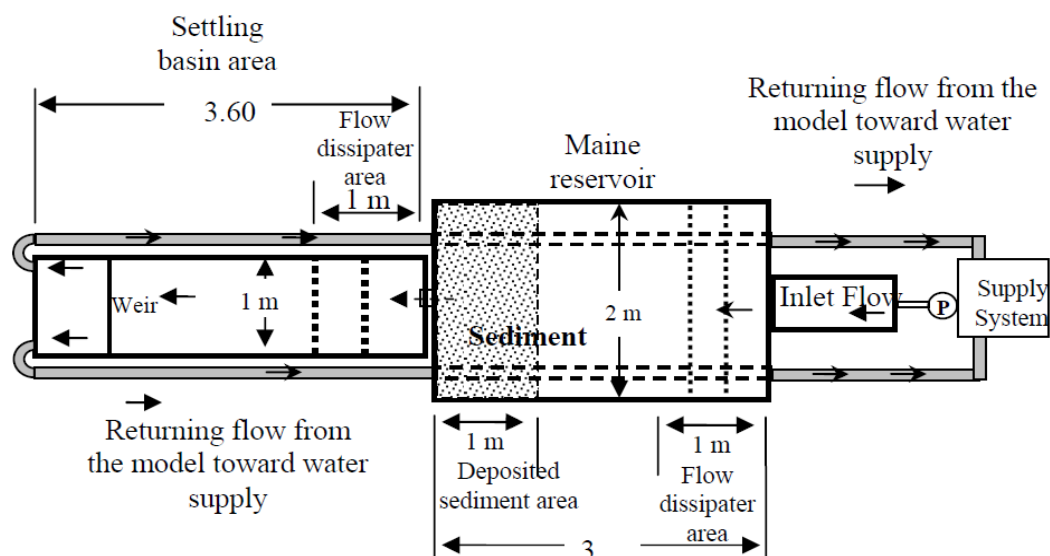


Figure 3.2 Experimental setup schematic plan view.

Results

Half cone shape scouring of the sediment bed is formed with the opening of the bottom outlet at the vicinity of the gate with pressure flushing. The maximum depth of the cone was found to be very near to the wall of the gate and the shape of the flushing cone over the deposited sediment was almost half of circumference. Figure 3.3 to Figure 3.7 below shows the variation of volume and width of flushing cone with different discharge and opening of the bottom outlet. From the figures, it was observed that for constant flow depth, there is an increase in the flushing cone dimension with an increase in discharge with almost the same trend. These result follows similar patterns with previous research works and can be summarized as there exist direct relation between the cross-section of the bottom outlet and dimensions of flushing cone. Dimensions of flushing cone increase with the increase in cross-section of bottom outlet for constant discharge and water depth.

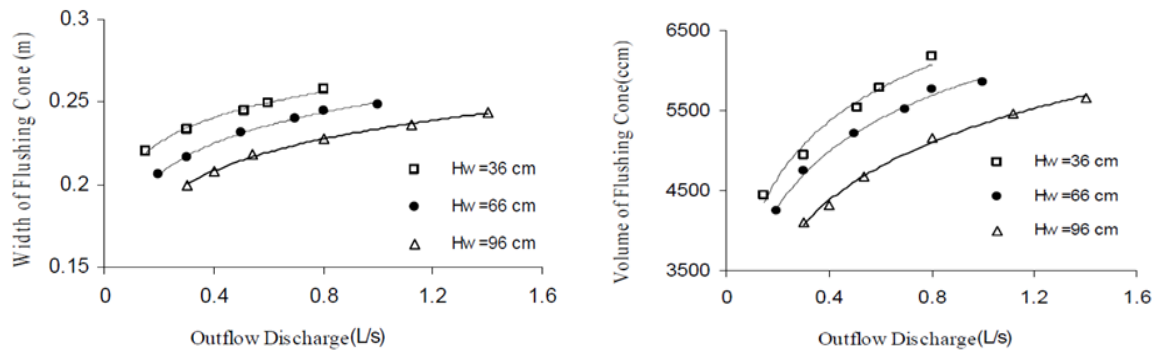


Figure 3.3 Variation of flushing cone volume and width of flushing cone versus outflow discharge for the bottom outlet of 2.54cm diameter.

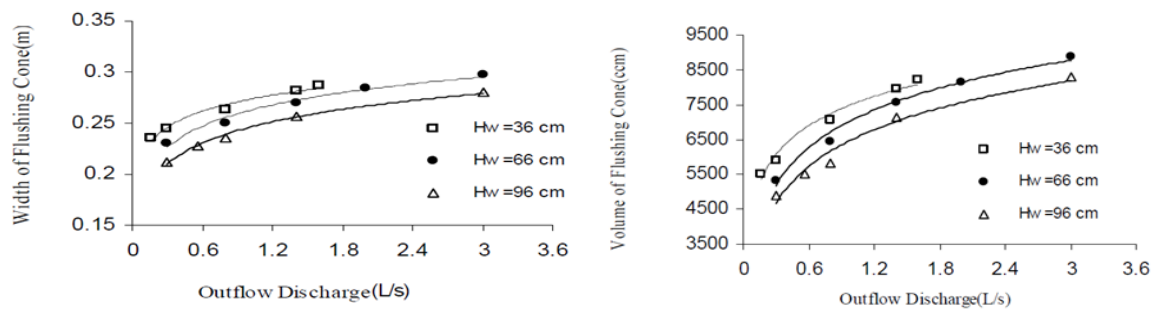


Figure 3.4 Variation of flushing cone volume and width of flushing cone versus outflow discharge for the bottom outlet of 3.81cm diameter.

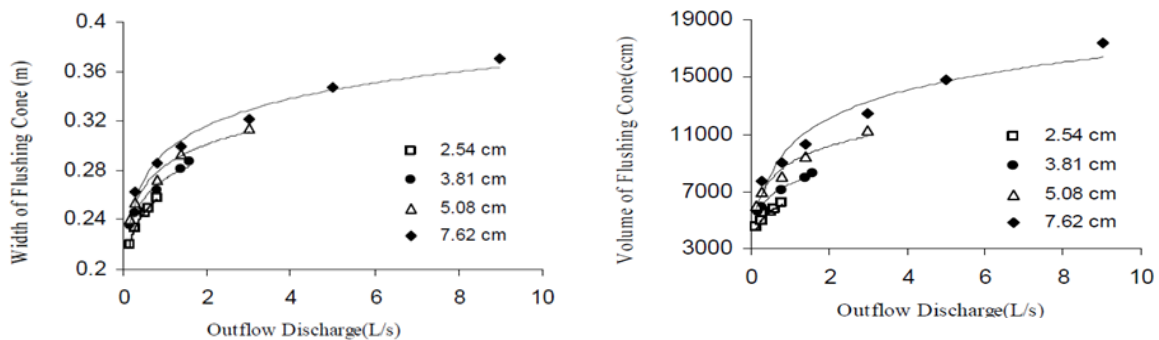


Figure 3.5 Variation of flushing cone volume and width of flushing cone versus outflow discharge for the bottom outlet of 36 cm diameter.

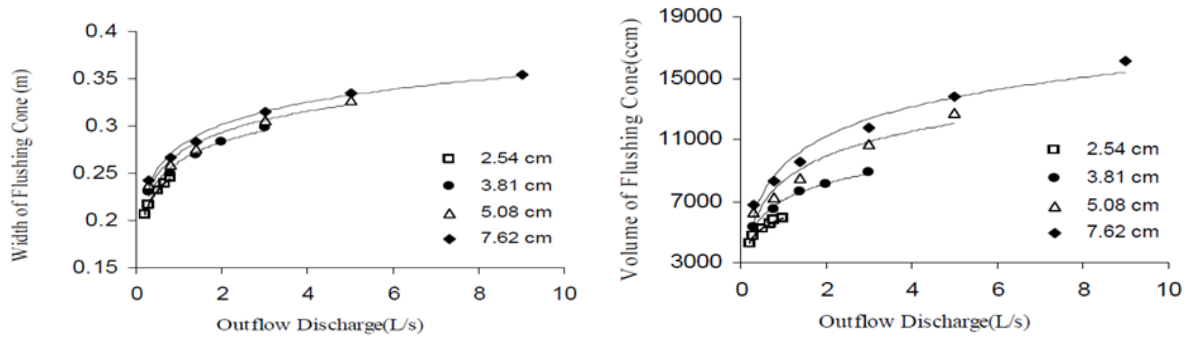


Figure 3.6 Variation of flushing cone volume and width of flushing cone versus outflow discharge for the bottom outlet of 66 cm diameter.

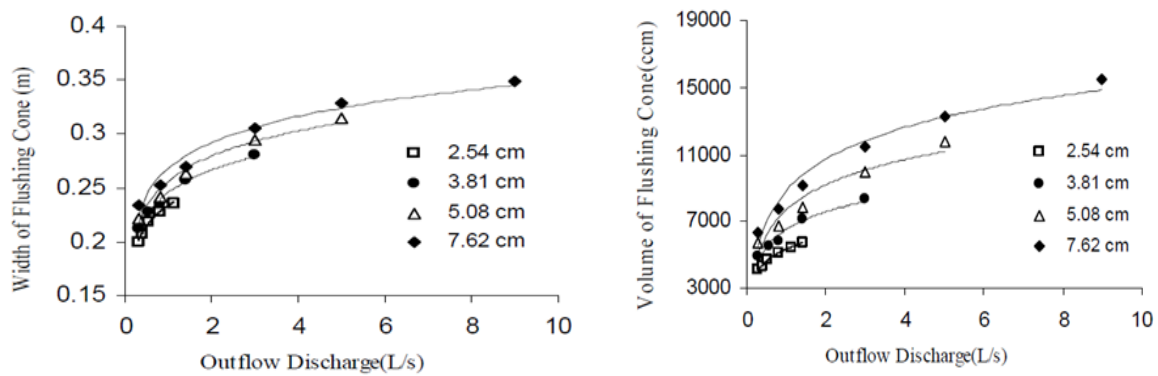


Figure 3.7 Variation of flushing cone volume and width of flushing cone versus outflow discharge for the bottom outlet of 96 cm diameter.

The proposed equation by multiple linear regression analysis is

$$\frac{V_{scouring}}{H_w^3} = 4.6 \left(\frac{u_{outlet}}{\sqrt{g(G_s - 1)d_{50}}} \right)^{0.21} \left(\frac{H_s}{H_w} \right)^{2.2} \left(\frac{D}{H_w} \right)^{0.89}$$

$$\frac{W_{scouring}}{H_w} = 0.02 \left(\frac{u_{outlet}}{\sqrt{g(G_s - 1)d_{50}}} \right)^{0.1} \left(\frac{H_s}{H_w} \right)^{0.75} \left(\frac{D}{H_w} \right)^{0.34}$$

Figure 3.8 depicts the results with the performance indices between estimated and observed experimental data for the testing data sets.

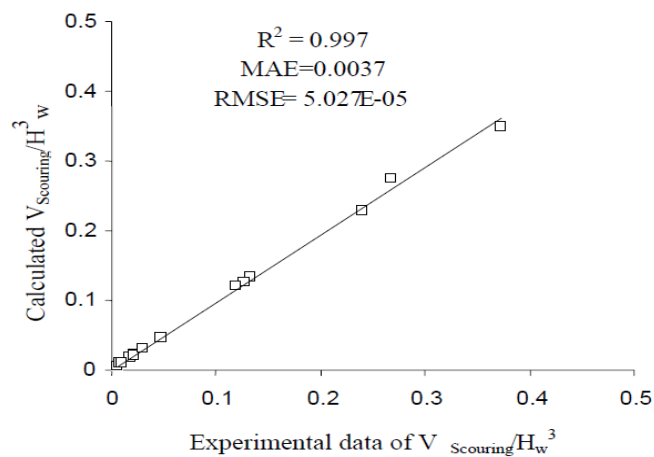


Figure 3.8 Observed and Dimensionless flushing cone volume using regressive model.

4 Theory

4.1 Dimensional Analysis

Dimensional Analysis can be simply defined as the interpretation of different physical quantities involved such as mass, length, time, temperature, force, area, volume, acceleration, velocity, and pressure and reduce complex physical problems to the simplest form. According to Henry Langhaar (1951) " The result of dimensional analysis of a problem is a reduction of the number of variables in the problem"(Langhaar, 1951); cited from (Hughes, 1993).

In other words, dimensional analysis could also be defined as techniques used in physical science and engineering to reduce physical properties such as force, area, acceleration, velocity and pressure and others to their fundamental dimensions of length (L), mass(M), and time(T) which further helps for the study of inter-relationships among the systems .In addition, it helps to escape the inconvenience of incompatible units.

Since it's not feasible to build an expensive full-scale prototype and study the effect of all the forces acting on porotype. There must be some way or conditions which can relate the relationship between the forces acting on the full-size prototype and the small-scale model of it. So, the question arises, what are those conditions, and what is the relationship between the forces? Dimensional analysis justifies both these questions and solves imposing problems with little and simple effort after applying dimensional analysis(Sonin, 2001) (Sonin, 2001).

Briefly, dimensional analysis involves the following steps:

1. Identify the important independent variables of the process.
2. Decide which variable is to be the dependent variable.
3. Determine how many independent dimensionless products can be formed from the variables.
4. Reduce the system variables to the proper number of independent dimensionless variables.

The main principle of dimensional analysis is that of dimensional homogeneity, which means the dimensions of each term in an equation on both sides are equal. In simple words, an equation is called dimensionally homogenous if dimensions of each term on both sides of an equation are the same. Such equations are independent of the system of units.

According to Langhaar (1951) " An equation is dimensionally homogenous if the form of the equation does not depend on the units of variables within the equation" (35); cited from (36). This means that if any system of units is dimensionally consistent, dimensionally homogenous equation is correct regardless of what system of units is used when substituting for the variables in the equation. Dimensionally homogeneous equations are very easy to work with and have fewer chances of error because it is very simple to check the consistency of dimensions when substituting the values for variables.

There are two important methods involved in dimensional analysis. They are:

1. Rayleigh's Method
2. Buckingham's Π - Theorem

As mentioned above during the pressurized flushing when the bottom outlets are opened the deposited sediments move due to flow and funnel shape cone is formed at the vicinity of the bottom outlet. The volume of the score cone (V_s) depends upon the factors such as geometrical conditions, hydraulic parameters, fluid properties and sediment properties such as water depth (H_w), flow discharge (Q), density of water (ρ_w), properties of sediments like depth of sediment deposit (H_s), size of sediment (d_s), density of sediment (ρ_s), dynamic viscosity (μ) and acceleration due to gravity (g).

Therefore, in pressure flushing volume of the cone may be written as a function of the following variables.

$$V_s = f(u, H_{w \text{ net}}, H_{w \text{ net}}, A, B, d_s, \rho_s - \rho_w, \rho_w, \mu, g) \quad 4-1$$

4.2 Hydraulic Similitude

The main objective of physical modeling is that the model should behave the same manner to the prototype it is intended to emulate. A properly designed model should have the same behavior which includes the velocity, acceleration, mass transport and the resultant forces that the fluid will exert in all respect in the controlled version of the prototype. This concept of performing hydraulic models test to obtain similar results to prototype can be achieved either by criteria of similitude or by conditions of similarity.

Similitude prescribes mathematical definition that must be met by the scale ratios of certain parameters between prototype and model. When all the major factors influencing reactions of the model resembles or in proportion to all major influencing reactions of a prototype then only similitude is achieved. Whereas, Similarity conditions is a condition that exists when a model gives a similar response as the prototype, even if the model is not in strict similitude with the prototype.

It is almost impossible to achieve complete similitude where all force ratios are constant and equal. So, it is important to choose those ratios which are more relevant and important parameters that need to be similitude. It is also necessary to maintain a balance between accuracy and making the problem simple.

According to Warnock 1950, in almost 90 percent of all hydraulic models forces associated with surface tension and elastic compression are relatively small and thus can be safely neglected (Warnock, 1950). This means for an appropriate hydrodynamic scaling law there are two lead forces one gravity and other viscous forces. Therefore, the Froude and Reynolds number are important because the similarity of one of these numbers, combined with geometric similarity provides the necessary conditions for hydrodynamic similitude in an overwhelming majority of models (Hughes, 1993) (Hughes 1993).

Thus, dimensional products chosen are combinations of Froude and Reynolds numbers. Other forces like compressibility and elasticity effects are neglected because these values are very small as compared to Froude and Reynolds number and have a very small effect.

4.2.1 Froude Criterion

Froude number is given by the square root of the ratio of inertial to gravity forces which can be written as,

$$Fr = \frac{\sqrt{\text{inertial force}}}{\sqrt{\text{gravity force}}} = \frac{\sqrt{\rho L^2 V^2}}{\sqrt{\rho L^3 g}} = \frac{V}{\sqrt{gL}} \quad 4-2$$

Where, Fr = Froude number L = Characteristic length (m) V = velocity (m/s)

g = acceleration due to gravity (9.81 m/s²)

Froude number expresses the relative influence of inertial and gravitational forces in hydraulic flow. Gravitational force is a dominating force for the flow with the free water surface. If Froude number is to be same for both in model and prototype then,

$$Fr_p = \left(\frac{V}{\sqrt{gl}} \right)_p = \left(\frac{V}{\sqrt{gl}} \right)_m = Fr_m \quad 4-3$$

$$\frac{Fr_p}{Fr_m} = \frac{\left(\frac{V}{\sqrt{gl}} \right)_p}{\left(\frac{V}{\sqrt{gl}} \right)_m} = 1 = Fr_r \quad 4-4$$

(Froude model criterion)

$$\frac{V_p}{V_m} = \sqrt{\left(\frac{g_p}{g_m} \right) \cdot \left(\frac{L_p}{L_m} \right)} \quad 4-5$$

$$V_r = \sqrt{g_r \cdot L_r} \quad 4-6$$

Almost all models of rivers and hydraulic structures are operated according to the Froude Model law. For given L_r it follows $V_r = \sqrt{L_r}$

4.2.2 Reynolds Criterion

Reynolds number is defined as the ratio of internal force to the viscous force. In Reynolds number, inertial and viscous forces are dominating. It is used first to distinguish between the laminar and turbulent flow. Reynolds number (Re) is important for laminar boundary layer problems and forces on cylinders with low Reynolds number.

$$Re = \frac{\text{inertial force}}{\text{viscous force}} = \frac{\rho L^2 V^2}{\mu VL} = \frac{\rho LV}{\mu} = \frac{LV}{\nu} \quad 4-7$$

Where, Re = Reynolds number L = Characteristic length(m) ρ = density (Kg/m³)

V = velocity (m/s) μ = Dynamic viscosity (Ns/m²) ν = μ/ ρ = kinematic viscosity (m²/s)

If Reynolds number is to be same for both in model and prototype then,

$$\left(\frac{\rho LV}{\mu}\right)_p = \left(\frac{\rho LV}{\mu}\right)_m \text{ or, } \left(\frac{V_p}{V_m}\right) \cdot \left(\frac{L_p}{L_m}\right) \cdot \left(\frac{\rho_p}{\rho_m}\right) = \left(\frac{\mu_p}{\mu_m}\right) \quad 4-8$$

In terms of Reynolds model criterion

$$Re_r = \frac{Re_p}{Re_m} = \frac{\rho_r L_r V_r}{\mu_r} = 1 \text{ (Reynolds model criterion)} \quad 4-9$$

Table 4-1 Froude Law versus Reynolds Law

Parameter	Symbol	Scale Ratio	
		Froude Law	Reynolds Law
Length	L_r	L_r	L_r
Area	A_r	L_r^2	L_r^2
Volume	V_r	L_r^3	L_r^3
Time	t_r	$L_r^{1/2}$	L_r^2
Velocity	V_r	$L_r^{1/2}$	L_r^{-1}
Acceleration	a_r	1	L_r^{-3}
Discharge	Q_r	$L_r^{2.5}$	L_r

Assuming $g_r = \rho_r = \mu_r = 1$

5 Scaling

Hydraulic models are designed based on scaling laws derived from dimensional analysis. Detail about dimensional analysis could be referred from "Physical Models and Laboratory Techniques In Costal Engineering" by Steven A. Hughes. For a design of the physical model, it is essential or mandatory to have dynamic similarity maintaining a consistent prototype to model the ratio of parameters acting on the system. In addition to this, all the derived dimensionless parameters are equal in prototype and model (Einstein & Chien 1956, Yalin a& Kamphuis 1971, Kobus 1984, Hughes 1993, Frostick 2011)(Einstein and Chien, 1956, Yalin and Kamphuis, 1971, Kobus, 1984, Hughes, 1993, Frostick et al., 2011); cited from (Hydralab+, 2016). It is almost impossible to achieve almost a perfect dynamic similarity between prototype and model. Therefore, the scale model is required to design in such a manner that all force ratios are retained while neglecting less important forces ratios. Neglecting of forces ratios may result in scale effects, there will be some alternation between prototype and scaled model observation. According to Heller 2011, scale effect becomes more significant with the increase in scale ratio and their relative importance depends on the investigated phenomenon. Which means that we have accepted scale effects for the scaled model.

Froude scaling is the most commonly used scaling law ensuring similarity in Froude number. Froude number is the ratio of the velocity of flow v to the root of gravitational acceleration g and depth of flow $Fr = \frac{v}{\sqrt{gh}}$. This scaling law ensures the constant ratio between inertial force and the gravitational force between model and prototype for open channel flow (Markofsky and Kobus, 1978) (Kobus 1978);cited from(Hydralab+, 2016).During the study of the model, it is assumed that water is used as a fluid to model so that the ratio of fluid density, kinematic viscosity, and dynamic viscosity are unity. Small subscript r represents the ratio between model(m) and prototype(p).

5.1 Fixed Bed Models

Fixed bed models are identified as a bed without any sediment transport or bed with constant or stable depth. If we consider a uniform open channel flow with a fixed bed in a very wide channel (channel having the ratio of width to depth ration greater than 30), so hydraulic radius (R) of the channel is equal to the depth of water (h) [R=h]. The expression for Froude number can be expressed with dimensional analysis as,

$$Fr = f\left(Re, \frac{K}{h}, S\right) \quad 5-1$$

Where Fr = Froude number
 Re = Reynolds number = $\frac{vh}{\nu}$
 $\frac{K}{h}$ = Relative roughness
 S = Slope

Considering the Froude-scaled model value of Reynolds number will be different for model and prototype. Therefore, there will be scale effects. To avoid it the model and prototype need to be fully turbulent. Roughness can be scaled by considering the Darcy-Weisbach friction factor or by Chezy - coefficient or by Manning's number. In a distorted model where horizontal and vertical scale is not equal leads to scale effects which replace geometric similarity by geometric affinity(De Vries and reports on Hydrology, 1993) (de Vries, 1993) ; cited from(Hydralab+, 2016) . According to Novak 2010, where the velocity component is important distortion is not acceptable but a vertically distorted model

is acceptable for uniform, non-uniform and unsteady flow conditions with relative slow vertical motion (Novak et al., 2018); cited from (Hydralab+, 2016).

Hydraulic time scale t_r can be derived based on Froude similarity as,

$$t_r = \frac{L_r}{\sqrt{h_r}} \quad 5-2$$

In the above equation L_r is the scale ratio for the horizontal length between model and prototype $\frac{L_m}{L_p}$ and h_r is the scale ratio for the height of flow $\frac{h_m}{h_p}$.

In the case of the non- distorted model ($L_r = h_r$). Therefore, hydraulic time scale t_r can be written as $t_r = \sqrt{L_r}$

5.2 Movable-Bed Models

5.2.1 Movable–Bed scaling Requirements

A movable-bed model should be able to model correctly all the complex interaction of short waves, long waves, unidirectional flows, sediment transport, solid structures and model boundaries. In our case, we are more interested in sediment transport, solid structures and model boundaries. It is almost impossible to simulate all interactions simultaneously with any scale relationship. Kamphuis 1985 stated that models have shown the most interaction is modeled incorrectly (Kamphuis, 1985); cited from (Hughes, 1993). There have been numerous developments of movable-bed scaling development in recent years which have provided scaling criteria but are limited to its advantages, assumptions, and constraints. Currently, there are so many scaling laws selecting an appropriate ser for a given model is sometimes very problematic (Hudson 1979); cited from (Hughes, 1993).

There two ways for determining the important parameters for sediment transport model:

- Assume that the sediment process is reacting primarily to a unidirectional flow situation with waves added.
- Assume that sediment is reacting primarily to waves with currents added.

The important physical parameters involved in sediment transport have been identified as follows (Kamphuis, 1985, Dalrymple, 1989); cited from (Hughes, 1993)(Kamphuis 1985; Dalrymple 1989).

• Hydrodynamic Parameters:		• Sediment Parameters:			
h	-	depth of flow	d	-	sediment diameter
σ	-	surface tension	ρ_s	-	sediment density
g	-	acceleration of gravity	τ_b	-	bottom shear stress
κ_s	-	bottom roughness	ω	-	sediment fall speed
ρ	-	fluid density			
ν	-	fluid kinematic viscosity			
u	-	velocity			
S_o	-	channel slope			

Sediment fall speed (ω) is not an independent parameter, as it is the function grain size, density, shape, fluid density and viscosity. And bottom shear stress is not a physical parameter but is a linkage between fluid and sediment.

5.2.2 Sediment Transport Similitude Requirements

The Physical parameter of the sediment can be combined with some physical properties of the fluid to form a set of dimensionless numbers commonly used for unidirectional flow. Flow in an open channel can generally be represented as a functional relationship of several variables (Ettema et al., 2000); cited from (Waldron, 2008) (Ettema 2000). This relationship can be expressed as

$$A = f_A(\rho, \nu, \sigma, \kappa, h, S_0, U, g) \quad 5-3$$

For a wide channel with uniform and steady flow ($R \approx H$). The expression can be written as

$$A = f_A(\rho, \nu, d, \rho_s, h, u_*, g\Delta p) \quad 5-4$$

Where, $\Delta p = (\rho_s - \rho)$ and $u_* = \sqrt{ghS_0}$

The above equation can be regrouped through Buckingham-Pi theory into a set of dimensionless parameters,

$$\pi_A = f_A \left[\frac{u_* d}{\nu}, \frac{\rho u_*^2}{g\Delta p d}, \frac{h}{d}, \frac{\rho_s}{\rho} \right] \quad 5-5$$

Where the dependent variable A in π_A could be any of flow resistance, sediment transport, etc. (Maynard, 2006); cited from (Waldron, 2008)(Maynard, 2006). If we add an extra parameter, $\frac{\omega}{u_*}$ which is the ratio of fall speed to the shear velocity. The above expression can be re-written as

$$\pi_A = f_A \left[\frac{u_* d}{\nu}, \frac{\rho u_*^2}{g\Delta p d}, \frac{h}{d}, \frac{\rho_s}{\rho}, \frac{\omega}{u_*} \right] \quad 5-6$$

The first parameter in the above equation is called grain size Reynolds number i.e.

$$R_* = \frac{u_* d}{\nu} \quad 5-7$$

Second is referred to as densimetric Froude number i.e.

$$F_* = \frac{\rho u_*^2}{g\Delta p d} \quad 5-8$$

These two parameters may be recognized as the coordinates of Shield's diagram for incipient motion in unidirectional flow as shown in the figure.

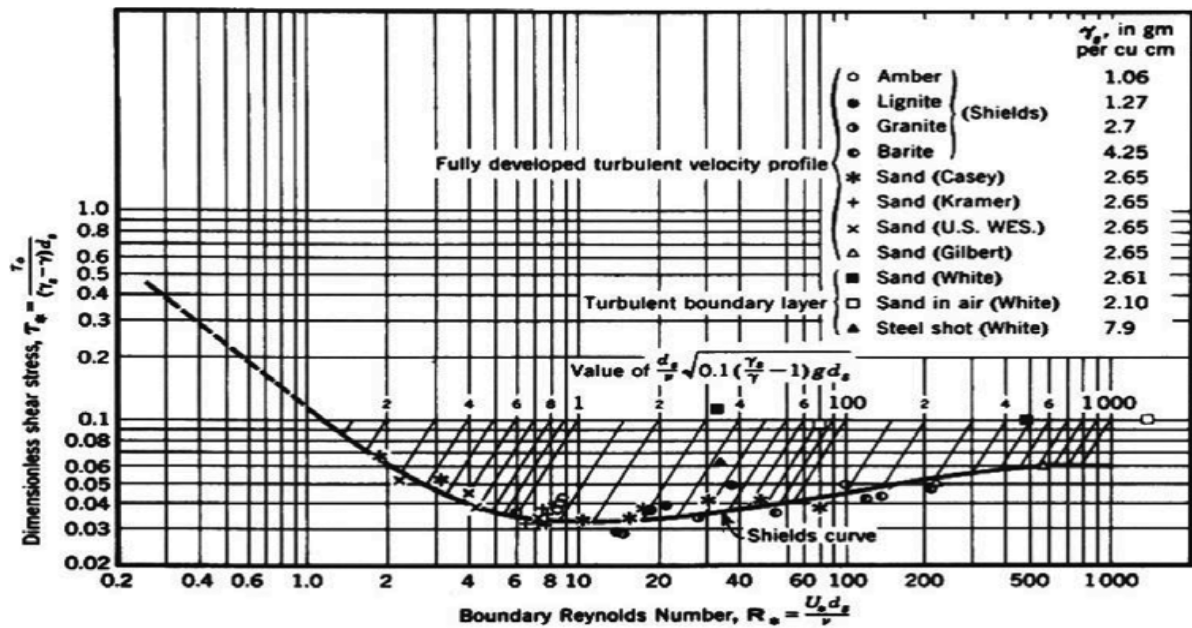


Figure 5.1 Shields Diagram for Unidirectional Flow (Vanoni,1975)(Vanoni, 1975).

The third term is relative density which is the ratio of the density of sediment to water density and it represents the buoyant force on the sediment. i.e.

$$S_s = \frac{\rho_s}{\rho} \quad 5-9$$

The fourth term (relative submergence) is the ratio of the depth to grain size h/d_s ; this term is important in consideration of surface tension effects, which are generally not considered to be important when modeling the bed. Such properties as this were excluded from the design of the SSPM (small scale physical model) as they are not considered to be important to scale (Ettema et al., 2000, Maynard, 2006); cited from (Waldron, 2008) (Maynard, 2006; Ettema et al., 2000).

$$\frac{h_r}{d_r} = 1 \quad 5-10$$

The last parameter is relative fall speed which accounts for suspended transport occurring simultaneously with bedload transport and could be used to evaluate scale effects for suspended load transport occurring in a model design for bedload transport. i.e.

$$V_w = \frac{\omega}{u_*} \quad 5-11$$

Values of all above mentioned five parameters must be the same in the model as in the prototype to achieve complete similitude in sediment transport generally which is not possible at scales other than the prototype.

Movable bed models represent two phases, flow with a solid particle and with fluid particles. Flow is generally Froude-scaled and the similarity in sediment movement depends upon a set of dimensional parameters which are,

- Grain size Reynolds number i.e. $Re_* = \frac{u_* d}{\nu}$
- Densimetric Froude number i.e. $Fr_* = \frac{\rho u_*^2}{g(\rho_s - \rho)d}$
- Relative sediment density i.e. $S_s = \frac{\rho_s}{\rho}$
- Relative submergence i.e. $\frac{h}{d}$
- Relative fall speed i.e. $V_w = \frac{\omega}{u_*}$

Where, ρ_s = density of sediment

u_* = shear velocity ($u_* = \sqrt{g h S}$)

ω = fall velocity

To obtain a perfect similitude for the sediment transport process, all these quantities would have to be equal in the model and prototype. Therefore, assuming the water is used in both models and prototypes ($\rho_r = \omega_r = 1$). Which gives

$$Re_{*r} = \frac{u_{*r} d_r}{\nu_r} = 1 \rightarrow u_{*r} d_r = 1 \quad 5-12$$

$$Fr_{*r} = \frac{\rho_r u_{*r}^2}{g_r (\rho_s - \rho)_r d_r} = 1 \rightarrow \frac{u_{*r}^2}{(G-1)_r d_r} = 1 \rightarrow u_{*r} = (G-1)_r^{1/2} d_r^{1/2} \quad 5-13$$

$$\left[(G-1) = \frac{(\rho_s - \rho)g}{\rho} \right]$$

$$\frac{\rho_{sr}}{\rho_r} = 1 \rightarrow \rho_{sr} = 1 \quad 5-14$$

$$\frac{h_r}{d_r} = 1 \rightarrow h_r = d_r \quad 5-15$$

$$\frac{\omega_r}{u_{*r}} = 1 = \frac{\sqrt{L_r}}{t_r} \quad 5-16$$

All the above equations have been formulated for unidirectional flow conditions. For unidirectional flows, the shear velocity can be expressed as $u_{*r} = \frac{h_r}{\sqrt{L_r}}$.

So,

$$Fr_{*r} = \frac{u_{*r}^2}{(G-1)_r d_r} = \frac{h_r^2}{(G-1)_r L_r d_r} = 1, d_r = h_r^2 L_r^{-1} (G-1)_r^{-1} \quad 5-17$$

$$\frac{h_r^2}{(G-1)_r L_r d_r} = 1$$

$$\frac{h_r^2}{L_r} = (G-1)_r d_r$$

$$\frac{h_r \cdot h_r}{L_r} = (G-1)_r d_r$$

$$h_r = \frac{L_r}{h_r} (G-1)_r d_r$$

$$h_r \cdot \frac{L_r}{h_r} = \frac{L_r}{h_r} \cdot \frac{L_r}{h_r} (G-1)_r d_r$$

[Multiplying by $\frac{L_r}{h_r}$ both sides]

$$L_r = \left(\frac{L_r}{h_r}\right)^2 \cdot (G-1)_r d_r$$

$$L_r = \delta^2 (G-1)_r d_r$$

$$[L_r h_r^{-1} = \delta]$$

$$L_r = \delta^2 (G-1)_r d_r$$

5-18

- Where L_r = Scale ratio
 δ = 1 for undistorted model
 d_r = Sediment size ratio

The dynamic of the suspended load transport can only be modeled exactly using an undistorted model. According to Low 1989 for lightweight materials with specific densities ρ_s/ρ ranging from 1 to 2.5 and grain diameter of $d=3.5\text{mm}$, the specific volumetric bedload transport rate q is related to $\frac{u_{*r}}{v_{sr}}$ by a simple relation i.e. $q_s \sim u_*^6$ and $\sim v_s^{-5}$ (Seng Low, 1989); cited from (Hydralab+, 2016). Zwamborn 1996 mentioned that Fr_* criterion is essentially the same as the $\frac{u_{*r}}{v_{sr}}$ criterion and a good similarity between model and prototype can be expected with an appropriate friction criterion and near similarity in Re_* (Zwamborn, 1966); cited from (Hydralab+, 2016).

As per the above equation for relative fall speed $V_w = \frac{\omega}{u_*}$ essentially corresponds to the ratio of the Rouse-number in the model and prototype and hence it is most important for suspended load transport when considering unidirectional flow. Putting the hydraulic time scale $t_r = \frac{L_r}{\sqrt{h_r}}$ in equation

$$\frac{\omega_r}{u_{*r}} = 1 = \frac{\sqrt{L_r}}{t_r},$$

we get

$$h_r = L_r$$

5-19

5.2.3 Dimensionless Unit Sediment Discharge

Taylor (1971) developed a dimensionless unit sediment discharge (q_{*S}) parameter known as Taylor's function defined as ratio of q_S and product of u_*d_S as $q_{*S} = \frac{q_S}{u_*d_S}$ (Pugh and Dodge, 1991, Taylor, 1971).

Where, q_S = unit sediment
 u_* = shear velocity
 d_S = sediment size

Dimensionless unit sediment discharge $q_{*SR} = \frac{q_{SR}}{u_*r d_{SR}} = 1$. Assuming similarity between model and prototype.

Where q_{*SR} = unit sediment discharge ratio $\frac{q_{*SM}}{q_{*SP}}$

$$\text{Since } u_{*r} = \sqrt{h_r S_r} = \sqrt{h_r h_r L_r^{-1}} = h_r L_r^{-1/2}$$

$$q_{SR} = u_{*r} d_{SR} = d_{SR} h_r L_r^{-1/2} \quad 5-20$$

5.3 Bedload Model Scale Requirements

As mentioned above the sediment movement of the bedload transport depends upon five dimensionless parameters mentioned in equation 5-6 and perfect similitude could be obtained if the prototype to model ratios of all parameters are unity. i.e.

$$R_{*r} = F_{*r} = S_{Sr} = \left(\frac{H}{d}\right) = V_{wr} = 1 \quad 5-21$$

But perfect similitude is almost impossible to achieve. Table 5-1 lists proposed scale requirements and indicate which parameters are preserved between prototype and model based on work done by Kamphuis.

Table 5-1 Classification of Models (Kamphuis 1985)

Model Class	$(R_*)_r = \left(\frac{u_* d}{v}\right)_r$	$(F_*)_r = \left(\frac{\rho u_*^2}{g(\rho_s - \rho)d}\right)_r$	$(S_s)_r = \left(\frac{\rho_s}{\rho}\right)_r$	$\left(\frac{H}{d}\right)_r$	$(V_w)_r = \left(\frac{\omega}{u_*}\right)_r$
Best Model (BM)	x	✓	✓	✓	x
Light Weight Model (LWM)	✓	✓	○	x	x
Densimetric Froude Model (DFM)	x	✓	○	x	x
Sand Models	x	x	✓	x	x

- ✓ Satisfied
- x Not Satisfied
- Not satisfied but limited to $1.05 < \rho_s/\rho < 2.65$

From these scaling relationships, it is possible to derive the complete scaling requirements for each of the models listed as the table above. As more of these criteria are left unfulfilled, less similar to the model will be to the prototype.

5.4 Best Model Requirements

Best Model is the model that satisfies most of the sediment transport parameters as shown in Table 1. As it satisfies the greatest number of parameters, it becomes more problematic to apply in the field because of restrictions that arise from fulfilling these criteria.

Maintaining the prototype to model ratio gives the ratio,

$$\left(\frac{H}{d}\right)_r = 1 \rightarrow H_r = d_r \quad 5-22$$

This means that sediment grains must be geometrically reduced according to the model length scale. Similarly, the scale ratio of relative sediment density yields as

$$\left(\frac{\rho_s}{\rho}\right)_r = 1 \rightarrow \rho_{s,r} = \rho_r \text{ or } (\rho_s - \rho)_r = 1 \quad 5-23$$

As water is used as a fluid in the model, then $\rho_r = 1$ and the model sediment should have nearly the same density as the prototype. As fluid and sediment densities in the model and the prototype is the same which means submerged sediment specific weight ratio will also be unity. i.e.

$$(F_*)_r = \left(\frac{\rho u_*^2}{g \Delta p d}\right)_r = 1 \rightarrow (\Delta p g)_r = 1, \quad \Delta p = (\rho_s - \rho), \quad \gamma = \Delta p g$$

For the best model $\gamma_r = \rho_r = v_r = 1$, resulting in $u_{*r} = \sqrt{d_r}$ and substituting it into the expression for

$$(R_*)_r = \left(\frac{u_* d}{v}\right)_r, \quad \text{we get } (R_*)_r = \left(\frac{u_* d}{v}\right)_r$$

$$(R_*)_r = \sqrt{d_r} \cdot d_r = d_r^{3/2} \quad 5-24$$

5.5 Lightweight Model Requirements (LWM)

As mentioned above in Table 5-1, it maintains its similarity of both R_* and F_* for sediment density ranging from 1.05 to 2.65 (limited to $1.05 < \rho_s/\rho < 2.65$). Sediment density other than this range is not satisfied. The other three parameters relative length and the relative fall speed are not counted for the model. The requirements of the lightweight model can be found by solving $Re_{*r} = \left(\frac{u_* d}{v}\right)_r = 1$ and $F_{*r} = \left(\frac{\rho u_*^2}{g \Delta p d}\right)_r = 1$

Assuming the water in the model fluid having $\rho_r = v_r = 1$ and putting these values in the above equation.

$$\text{We get, } Re_{*r} = \left(\frac{u_* d}{v}\right)_r = 1 \rightarrow u_{*r} = \frac{1}{d_r}$$

$$F_{*r} = \left(\frac{\rho u_*^2}{g(\rho_s - \rho)d}\right)_r = 1 \rightarrow \frac{u_{*r}^2}{(G-1)_r d_r} = 1 \rightarrow \frac{\frac{1}{d_r^2}}{(G-1)_r d_r} = 1 \rightarrow d_r^3 = \frac{1}{(G-1)_r}$$

$$(G-1) = \frac{(\rho_s - \rho)}{\rho}$$

5.6 Lightweight Model Scale Effects

Lightweight materials can maintain similarity in practical Reynolds and Froude number between model and prototype and furthermore holds prototype and model sediment at the same position on the Shield's diagram Figure 5.1. By saying this we should expect that the incipient motion of the model sediment will be correctly simulated. Nonetheless, it may cause distortions in other important scale factors with significant scale effects which is pointed out by Kamphuis as,

- a) Improper acceleration of particles may result due to incorrect scaling of relative density, which may lead to underrating of sediment transport rate and there are possibilities of particles in model entering in suspension state lot earlier than prototype.
- b) The relative length scale is not correctly scaled because the lightweight particles are quite bigger than they should be which causes sediment movement relatively less than what should occur.
- c) As lightweight sediments are bigger than it should be, they are somewhat more porous. This increase in porosity will allow absorbing more wave energy by the model.
- d) Liquefaction of bed in lightweight material occurs sooner which is a problem if bottom resting weights are being supported by the movable-bed.
- e) The Lightweight material does not simulate the relative fall speed. So, suspended sediment transport will not be modeled properly.

5.7 Densimetric Froude Model

Densimetric Froude models are similar to lightweight models except for that similitude in Practical Reynolds number is relaxed to pick up more flexibility in specifying model parameters as only similitude in Froude number is required. Substituting the value of $F_{*r} = 1$ in equation 5-13, we get

$$\frac{u_{*r}^2}{(G-1)_r d_r} = 1, d_r = \frac{u_{*r}^2}{(G-1)_r} \quad 5-25$$

And for unidirectional flow from equation 5-17, we get

$$\frac{h_r^2}{(G-1)_r L_r d_r} = 1, d_r = \frac{h_r^2}{(G-1)_r L_r} \quad 5-26$$

5.8 Sand Model Requirements

Sand model fulfills only one scaling criteria of the same density as prototype form the criteria mention from equation 5-7 to 5-11. According to Kamphuis 1985, the non-similarity of Re_* and Fr_* in such a model will result in erroneous modeling of sediment transport at low flow velocities (Kamphuis, 1985, Hughes, 1993). Assuming water is used in the model which means,

$$S_s = \frac{\rho_s}{\rho} \quad 5-27$$

Any scale ratios being defined in terms of length and sediment diameter scale.

5.9 Selected similarity conditions:

- Similarity in Froude number
- Similarity in Shields parameter

- Similarity in dimensionless unit sediment discharge
- Fully turbulent flow, $Re > 2000$ in both model and prototype.
- Density of model sediments between 1050 – 2650 kg/m³
- Boundary Reynolds number > 70 in both model and prototype.

5.10 Summary for scale ratios.

Description	Scale ratio	Equation number
Horizontal Length	L_r	
Vertical Depth	h_r	
Distortion	$\delta = L_r h_r^{-1}$	
Slope	$S_r = h_r L_r^{-1}$	
Flow Velocity	$u_r = \sqrt{h_r}$	
Flow Discharge	$Q_r = B_r h_r u_r = L_r h_r \sqrt{h_r} = L_r h_r^{3/2}$	
Manning's	$n_r = \frac{h_r^{2/3}}{L_r^{1/2}}$	
Bed Shear Velocity	$u_{*r} = d_{sr}^{1/2} (G - 1)_r^{1/2}$	5-13
Sediment size	$d_{sr} = h_r^2 L_r^{-1} (G - 1)_r^{-1}$	5-17
Scale ratio	$L_r = \delta^2 (G - 1)_r d_r$	5-18
Dimensionless unit sediment discharge	$q_{sr} = u_{*r} d_{sr} = d_{sr} h_r L_r^{-1/2}$	5-20
Best Model Requirement	$(R_*)_r = \sqrt{d_r} \cdot d_r = d_r^{3/2}$	5-24

6 Method

6.1 Experimental Setup

Two sets of laboratory experiments were carried out with different lightweight (low-density) materials at two places; one in Hydraulic Laboratory of NTNU, Norway and another at Hydraulic Laboratory of Hydro Lab, Nepal. Each set of the experiment was carried out by varying flushing discharge, reservoir water level, the thickness of the sediment deposit layer and opening height of bottom orifice. To make the results from both sets of experiments comparable, the sizing of the sediments was chosen in such a way that they could be scaled up to represent a common arbitrary prototype.

For experimenting, an existing flume in the hydraulic Laboratory of NTNU, Norway was used. A 12 m long flume with 0.6 X 0.75 m rectangular cross-section was used to simulate a reservoir and cone formation due to pressure flushing. At 8m chainage from inlet box, a flushing gate was installed. Details dimensions of the flume are shown in Figure 6.1 below. Experimenting in Hydro Lab, Nepal was also conducted with a similar setup of flume as in the Hydraulic Laboratory of NTNU.

The flushing opening of 50mm wide was mounted in the middle of the flushing gate for flushing simulation with variable opening height. The outlet was provided such that its sill was 60 mm above the flume bed. The details of the flushing gate as shown in Figure 6.2.

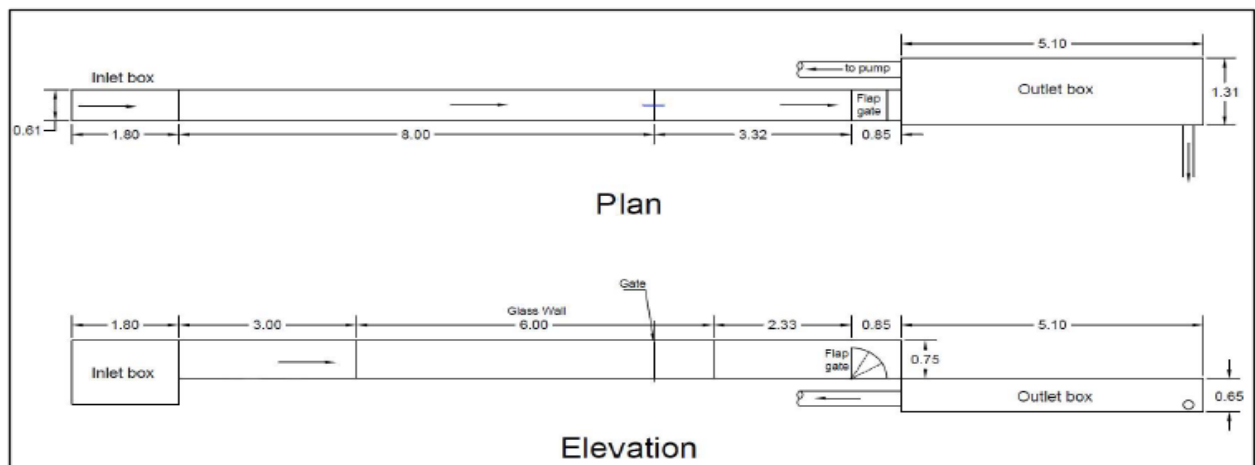


Figure 6.1 Plan and Longitudinal view of the model and its details.

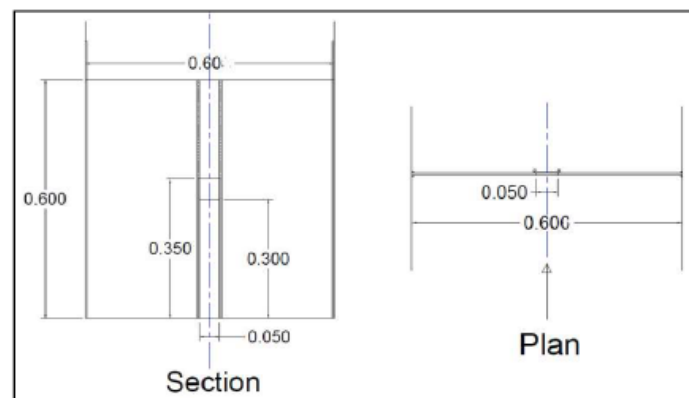


Figure 6.2 Details of the flushing gate.

6.2 Experimental procedure

To begin with, experiment firstly desired sediments were evenly distributed over the model with required thickness of 120 and 140mm maintaining a specific same level above the bottom level to the desired length upstream. Then the model was slowly filled with water until the water level reached to requisite surface level. After the water level reached to intended discharge through inlet bottom outlet (gate opening) was opened manually. As soon as the downstream outlet would be opened, sediments start to discharge through the opening under water flow pressure. The sediment is discharged with high concentration at the beginning of experiments with the gate opening and the concentration of flushing decreases with time. The experiment was continued until the flushing rate stops completely or reaches an equilibrium condition with negligible flushing to downstream. A flushing cone is formed as soon as the sediment discharge reaches a stable stage. The time required for the formation of the flushing cone and its balancing depends upon the hydraulic conditions. To retain the shape of developed flushing cone, flushing outlet is closed and water was slowly and carefully drained out from the model and the measurement of flushed cone bed was done.

6.2.1 Types and size distribution of the sediments.

Sand and non-cohesive lightweight plastic materials were used for experiments. Details of sediment being used during experiments are shown below. Figure 6.3 shows the experimental setup of the sediments being used for experiments.

Table 6-1 Types of sediments used for experiments.

Sediment Types	Density [kg/m ³]	Mean size d_{50} [mm]	Sediment Thickness [mm]
Sand	2650	1	120 & 140
Blue Lightweight Material	1400	4	120 & 140
Yellow Lightweight Material	1058	2	120 & 140

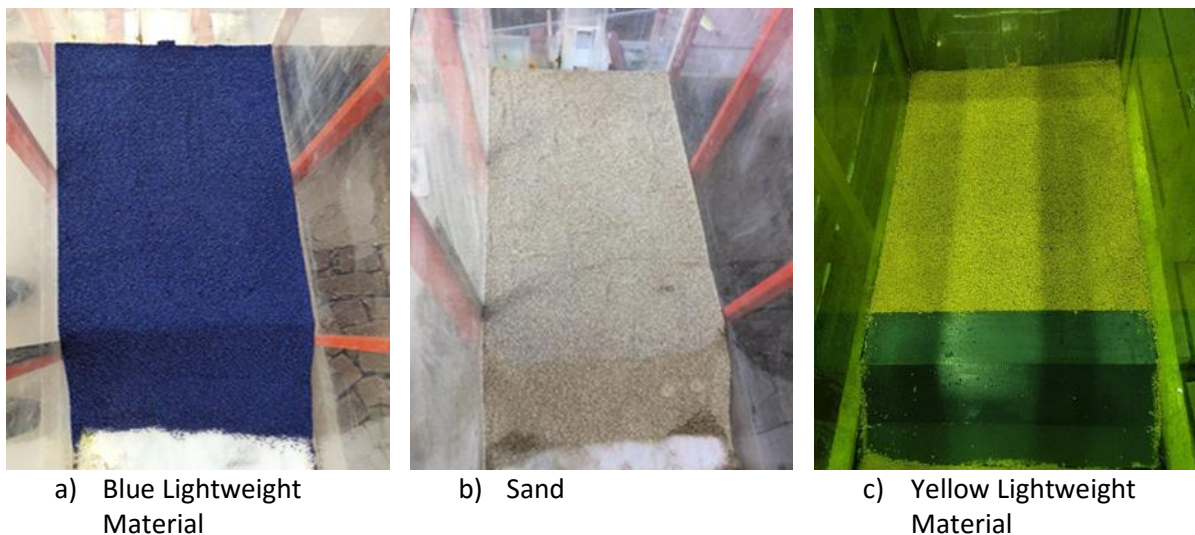
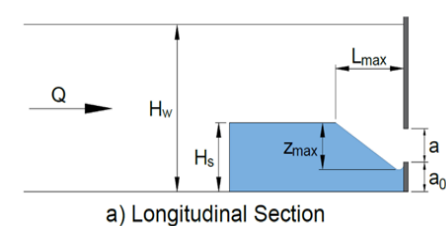
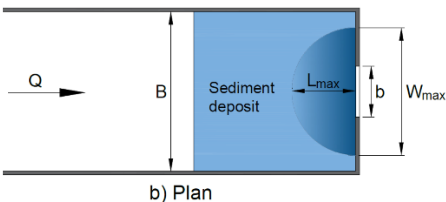


Figure 6.3 Initial bed for different sediment material during experiments.

6.2.2 Experimental Setup

<p>Q = Discharge</p> <p>H_w = Flow depth above bed level</p> <p>H_s = Sediment height above bed level</p> <p>a = Height of bottom outlet</p> <p>a_0 = Height of bottom outlet</p> <p>b = Width of bottom outlet</p> <p>B = Width of reservoir(flume)</p> <p>h_s = Height of Sediment above outlet sill</p> <p>$H_{s\ net}$ = Net sediment height above the center of the outlet opening</p> <p>$H_{w\ net}$ = Net flow depth above the center of the outlet opening</p> <p>L_{max} = Maximum length of flushing cone</p> <p>W_{max} = Maximum width of flushing cone</p> <p>Z_{max} = Maximum depth of flushing cone</p> <p>V_s = Volume of flushing cone</p>	 <p>a) Longitudinal Section</p>  <p>b) Plan</p> <p style="text-align: center;">Where,</p> <p style="text-align: center;">$h_s = H_s - a_0$</p> <p style="text-align: center;">$H_{s\ net} = h_s - a/2$</p> <p style="text-align: center;">$H_{w\ net} = H_w - a/2$</p>
---	---

6.2.3 Number of Experiments and it's constraints.

Table 6-2 Different test constraints.

Test no.	a_0 , [mm]	a , [mm]	b , [mm]	B , [mm]	H_s , [mm]	Q , [l/s]	H_w , [mm]
1	60	20	50	600	140,120	1.30	267
2	60	20	50	600	140,120	1.70	373
3	60	20	50	600	140,120	2.00	523
4	60	20	50	600	140,120	1.80	453
5	60	30	50	600	140,120	1.80	244
6	60	30	50	600	140,120	2.20	326
7	60	30	50	600	140,120	2.60	414
8	60	30	50	600	140,120	3.00	518
9	60	40	50	600	140,120	2.50	244
10	60	40	50	600	140,120	3.20	352
11	60	40	50	600	140,120	3.90	450
12	60	40	50	600	140,120	4.30	565
13	60	50	50	600	140,120	3.20	258
14	60	50	50	600	140,120	3.80	325
15	60	50	50	600	140,120	4.50	417
16	60	50	50	600	140,120	5.00	499

Note: All 16 experiments mentioned above were done for sand and for two lightweight materials mentioned above. All total there was 3 x 16 number experiments conducted for this study.

6.2.4 Measuring of flushing cone volume.

Hydraulic Laboratory NTNU, Norway

After a slow and careful drawdown of water to the required depth in the model, measurement of flushed bed was done by a multi-transducers array system, recording bed levels with 32 acoustics transducers. Seatek transducers with an electronics package were used for this purpose in our case. The numbering of 32 different transducers and its positioning is shown in Figure 6.4. A program was written using LabVIEW 2017 software for the acquisition of data from the Seatek MHz Ultrasonic Ranging System Figure 6.5.

A Simple code was written in MATLAB for post-processing of data to calculate the volume and 3-Dimensional view of the flushing cone after the experiment.

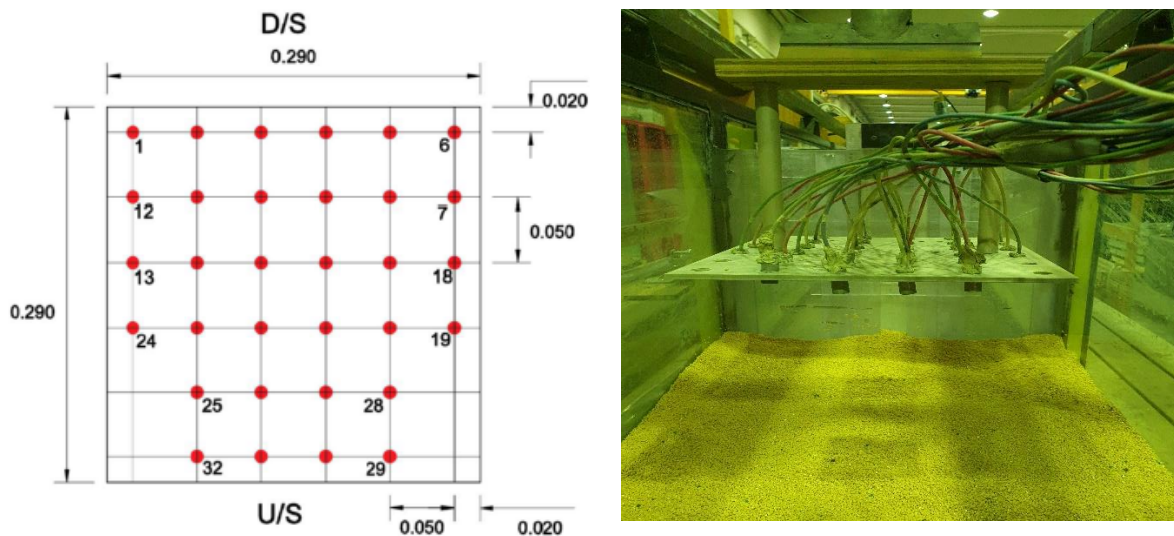


Figure 6.4 Arrangement of Multiple Transducers.

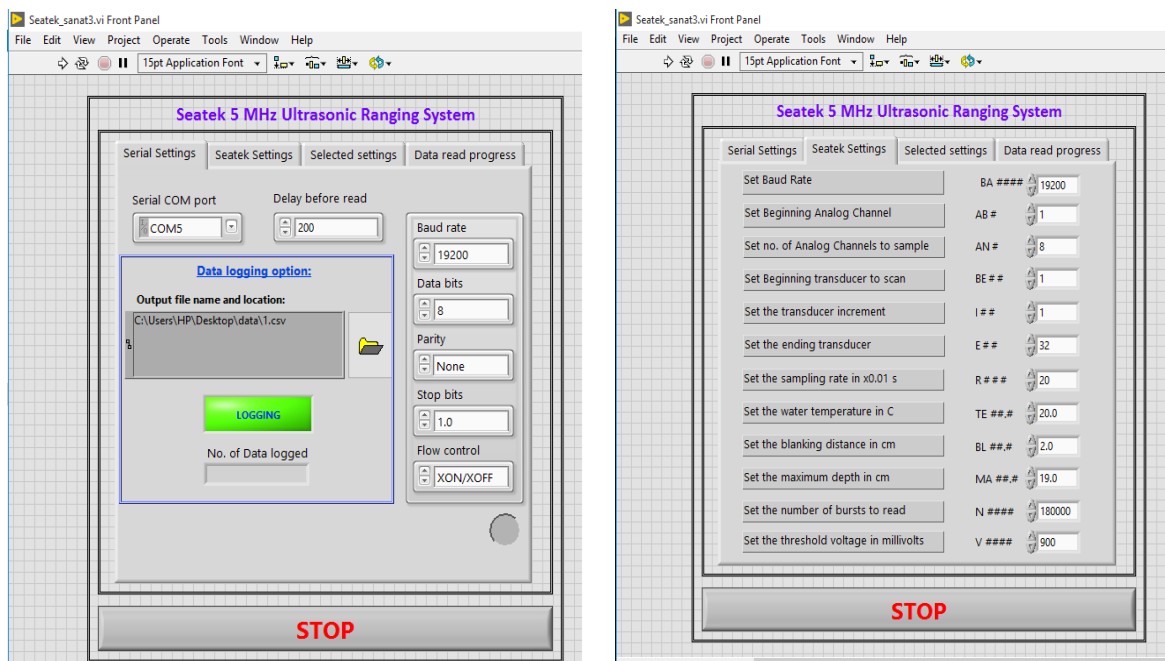


Figure 6.5 Data acquisition software.

Hydro Lab, Nepal

In Hydro Lab, Nepal, the measurement of flushed bed was done manually with staff gauge. Measurements at a suitable interval were done to measure the cone formed on the bed after the opening of the flushing gates.

Simple code was written in MATLAB for post-processing of data to calculate the volume and 3-Dimensional view of the flushing cone after the experiment. Figure 6.6 and Figure 6.7 shows the 3 D points and the 3D surface of the flushing cone after the experiment with 1.30 l/s outflow discharge, 140 mm sediment thickness, 267mm water depth and 20 mm X 50mm bottom outlet of yellow lightweight material.

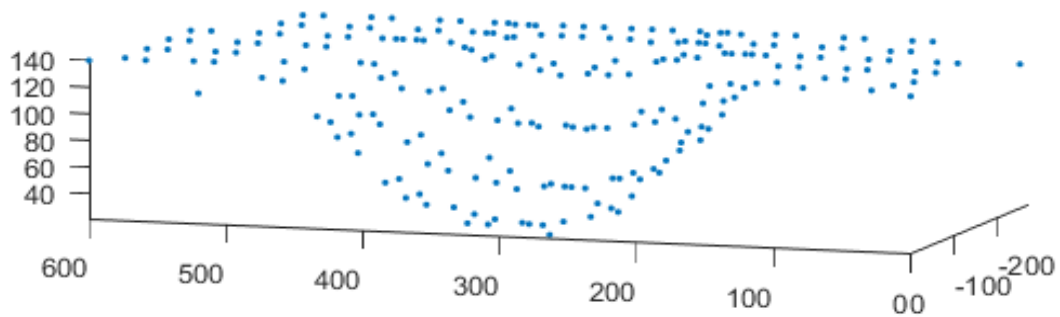


Figure 6.6 3-Dimensional view of the flushing cone after the experiment with 1.30 l/s outflow discharge, 140 mm sediment thickness, 267mm water depth and 20 mm X 50mm bottom outlet of yellow lightweight material.

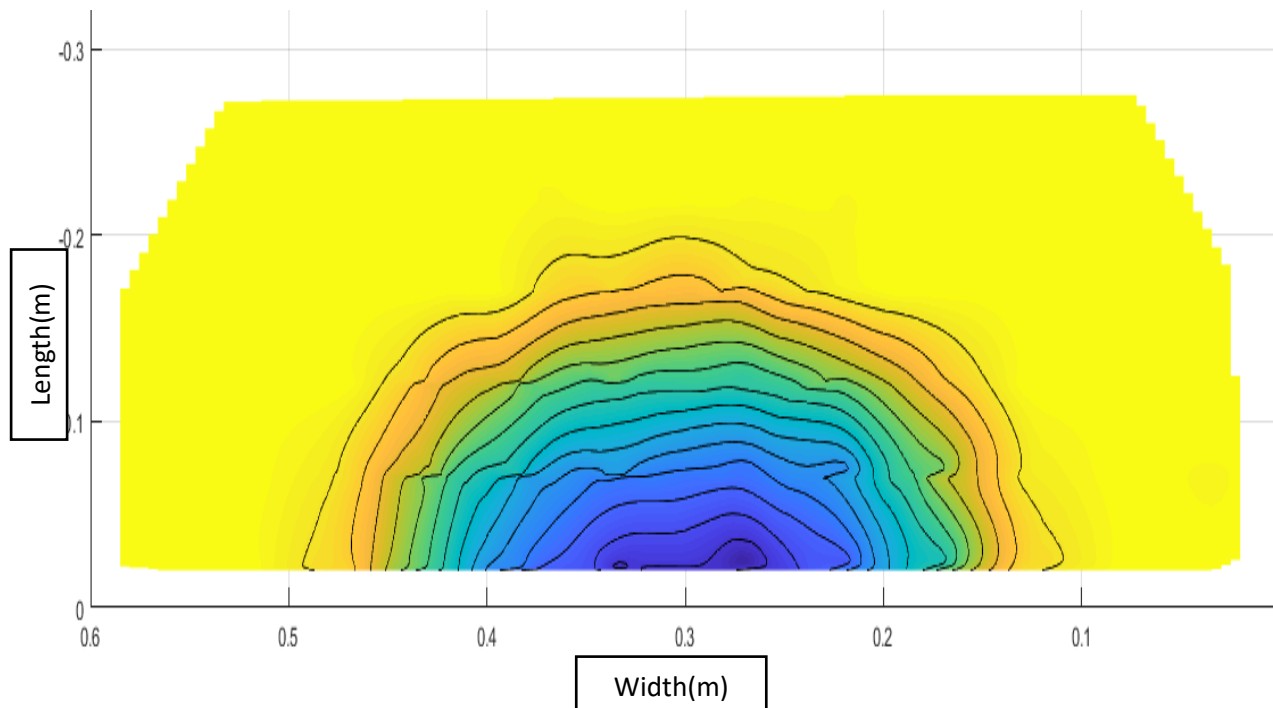


Figure 6.7 The bed topographic view of the flushing cone after the experiment with 1.30 l/s outflow discharge, 140 mm sediment thickness, 267mm water depth and 20 mm X 50mm bottom outlet of yellow lightweight material.

7 Results and Discussion

During the pressure, the flushing operation collapse of the deposited material was noticed forming a funnel-shaped scoured cone near the outlet as soon as the gate was opened. Furthermore, flushing acceleration was very intense during the start of the experiment and the intensity of drained material reduced over time and a stable flushing cone was developed over time with a very fast forming process less than a minute.

The shape of the cone formed was almost symmetrical (half circumference) to the center of the bottom outlet with maximum cone depth close to the bottom outlet wall. Besides, the width of the flushed cone was almost twice the length and the dimension of depth and length increases with the increase in discharge. Figure 7.1 and Figure 7.2 below shows the shape of the flushing cone near the bottom outlet.

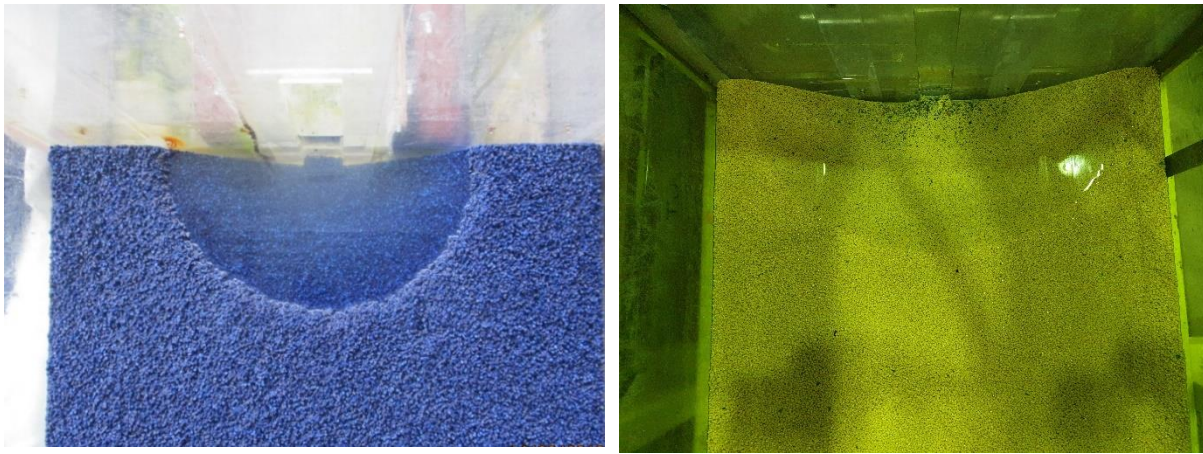


Figure 7.1 Flushing cone at the vicinity of bottom outlet with Blue & Yellow Lightweight Material.

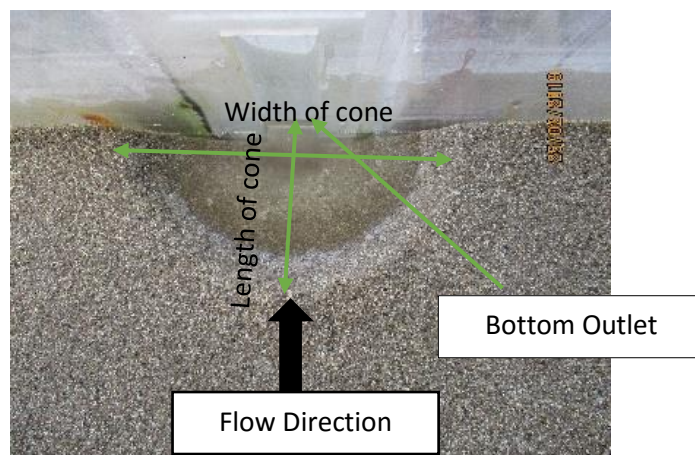


Figure 7.2 Flushing cone at the vicinity of the bottom outlet with Sand.

7.1 Comparison with empirical relations

Measured flushed cone volume was compared and analyzed with different empirical relationships proposed by four different types of research. Among them, Meshkati (2010) were selected for further companions because the empirical relation to determining the volume of flushing cone was determined considering diameter of the circular bottom outlet (D), specific gravity of sediment particles (G_s) and the particle size of sediment (d_s), even though only one sediment thickness was used during experiments and fits better with our data. Therefore, the measured $\frac{V_s}{H_{w\ net}^3}$ was further compared with the calculated $\frac{V_s}{H_{w\ net}^3}$ the empirical relation proposed by Meshkati in 2010.

Summary of results obtained from the experiments.

Table 7-1 Result summary

Test	$H_{w\ net}$ [mm]	H_w [mm]	$H_{s\ net}$ [mm] [Hs = 140 mm]	$H_{s\ net}$ [mm] [Hs = 120 mm]	A_{outlet}	Q, [lps]	Measured Volume of flushed cone (V_s) [m^3]					
							Blue Lightweight Material		Sand		Yellow Lightweight Material	
							Hs = 140 mm	Hs = 120 mm	Hs = 140 mm	Hs = 120 mm	Hs = 140 mm	Hs = 120 mm
1	267	197	70	50	0.001	1.3	0.00126	0.00083	0.00113	0.00079	0.00290	0.00155
2	373	303	70	50	0.001	1.7	0.00158	0.00100	0.00122	0.00087	0.00350	0.00188
3	523	453	70	50	0.001	2	0.00162	0.00113	0.00141	0.00112	0.00337	0.00229
4	453	383	70	50	0.001	1.8	0.00171	0.00112	0.00129	0.00098	0.00342	0.00213
			0	0								
5	244	169	65	45	0.0015	1.8	0.00160	0.00108	0.00135	0.00089	0.00362	0.00219
6	326	251	65	45	0.0015	2.2	0.00192	0.00127	0.00163	0.00107	0.00361	0.00249
7	414	339	65	45	0.0015	2.6	0.00217	0.00131	0.00167	0.00111	0.00428	0.00293
8	518	443	65	45	0.0015	3	0.00244	0.00147	0.00179	0.00124	0.00485	0.00322
			0	0								
9	244	164	60	40	0.002	2.5	0.00178	0.00131	0.00170	0.00107	0.00483	0.00269
10	352	274	60	40	0.002	3.2	0.00225	0.00154	0.00195	0.00120	0.00537	0.00318
11	455	375	60	40	0.002	3.9	0.00247	0.00172	0.00204	0.00128	0.00537	0.00373
12	570	490	60	40	0.002	4.3	0.00287	0.00180	0.00216	0.00144	0.00685	0.00425
			0	0								
13	264	179	55	35	0.0025	3.2	0.00206	0.00148	0.00194	0.00118	0.00581	0.00349
14	327	242	55	35	0.0025	3.8	0.00259	0.00163	0.00203	0.00129	0.00580	0.00395
15	424	339	55	35	0.0025	4.7	0.00275	0.00182	0.00223	0.00141	0.00674	0.00457
16	502	417	55	35	0.0025	5	0.00304	0.00198	0.00234	0.00150	0.00735	0.00477

7.2 The variation of flushing cone volume versus $H_{w\ net}$ for different water depth and the bottom outlet.

From the experiment, it was observed that the volume of flushing cone increases with an increase in flow depth and followed almost the same progression for both two lightweight materials (blue and yellow) and sand (representation of blue lightweight material). During the experiment, it was also observed that the higher sediment thickness resulted in higher flushing volume for all three cases. Because of time constraints, sand representing the yellow lightweight material could not be done. However, with the result found we could predict that the volume of flushing cone of sand which will represent the yellow material would also follow the same behavior.

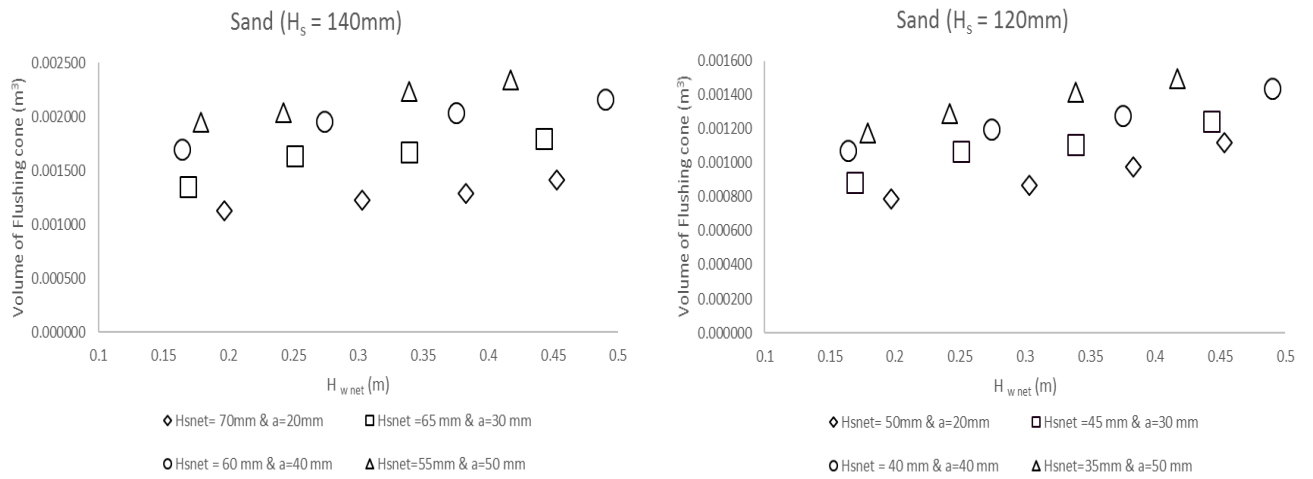


Figure 7.3 Sand H_s 140 mm (left) and 120 mm (right)

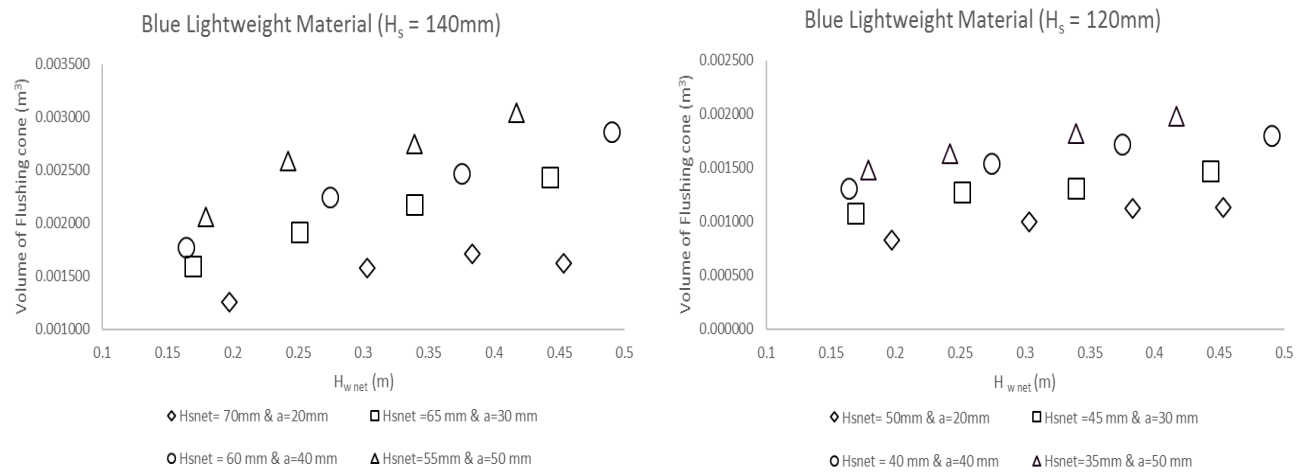


Figure 7.4 Blue Lightweight Material H_s 140 mm (left) and 120 mm (right)

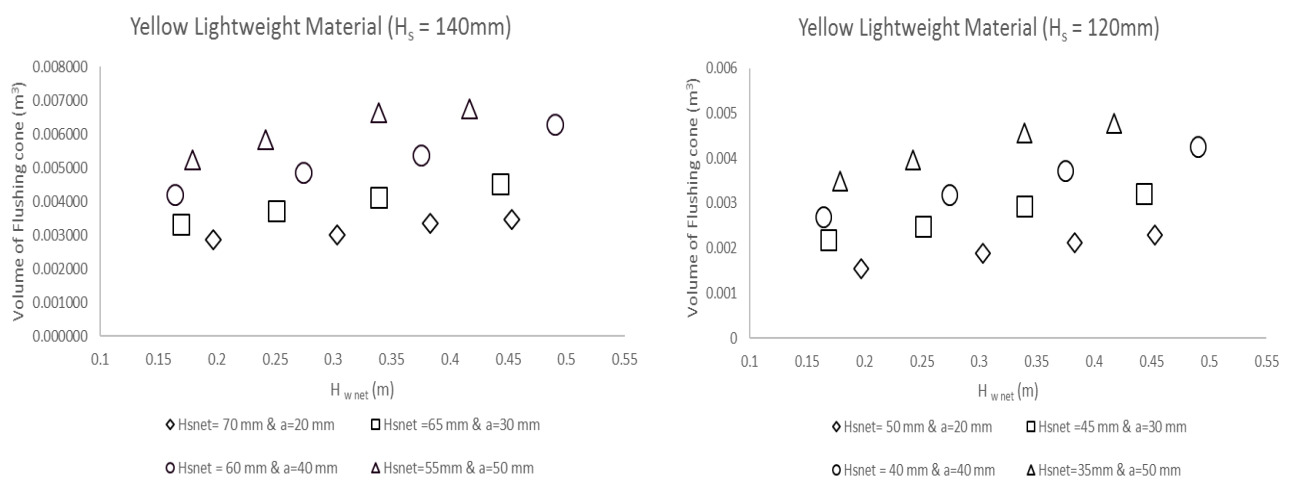


Figure 7.5 Yellow Plastic Material H_s 140 mm (left) and 120 mm (right)

7.3 The variation of flushing cone width versus outflow discharge

Meshakati in 2010 investigated the effect of discharge and water depth for the development of flushing cone. According to his studies for constant water depth dimensions of flushing, cone increases with increasing outflow discharge and follows the same trend between all outlet sizes. Besides that, they also mentioned that there will be wider flushing at lower water depth for constant outflow discharge.

In this study, the discharge was dependent on flow depth for each outlet opening size. Hence, the effect of varying discharge and flow depth could not be studied independently. Despite that, studies showed that there is an increase in the dimension of a flushed cone with an increase in outflow discharge. Figure 7.6 depicts the variation of the flushing cone dimension (width) with the outflow discharge of the bottom outlet. Furthermore, from Figure 7.6 it can be observed that higher sediment depth composes wider or bigger flushing cone depth.

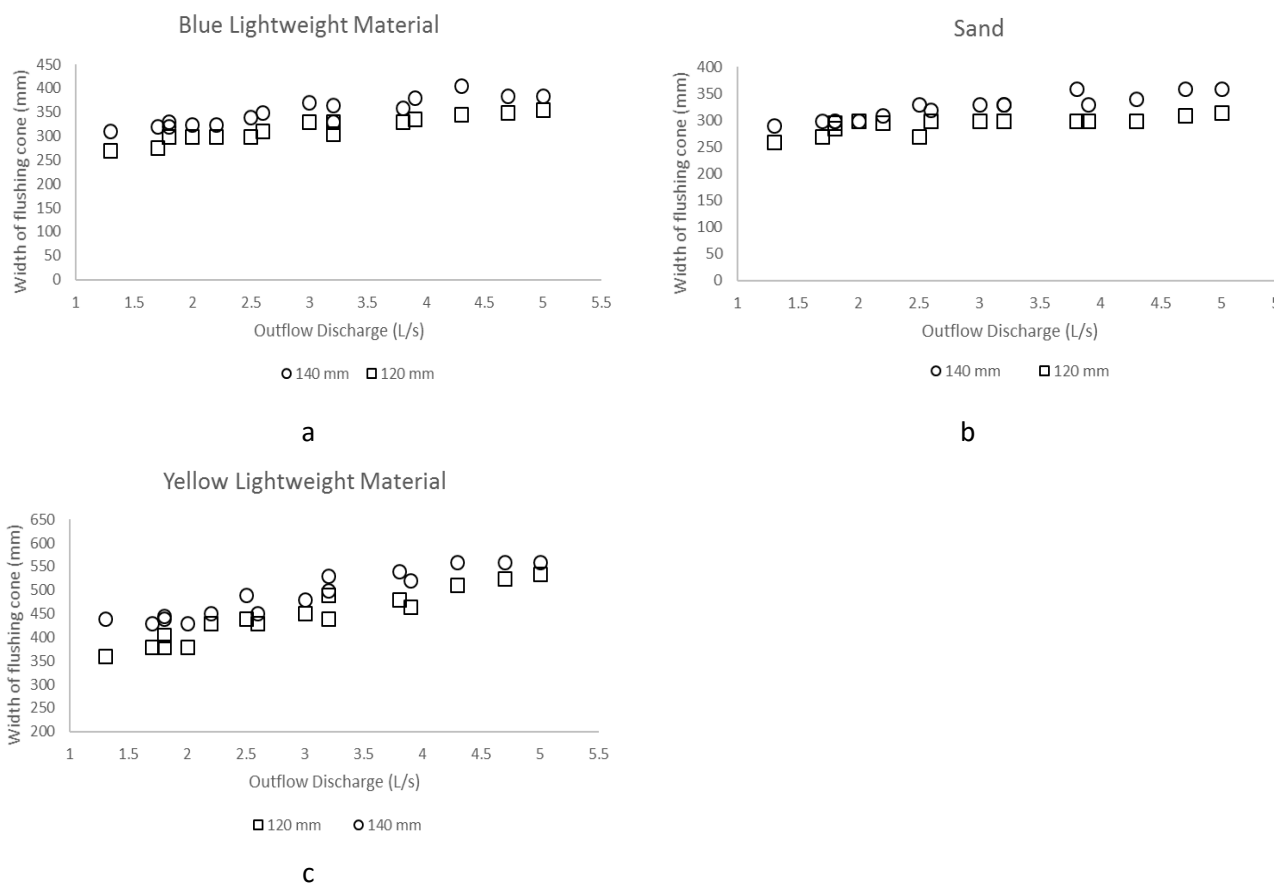
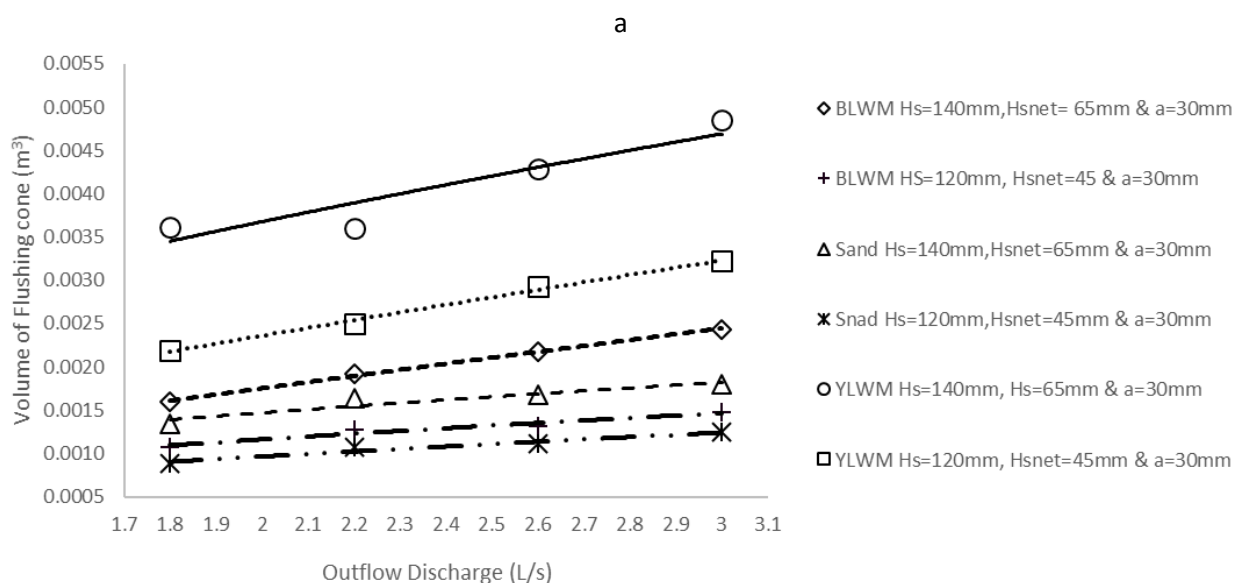
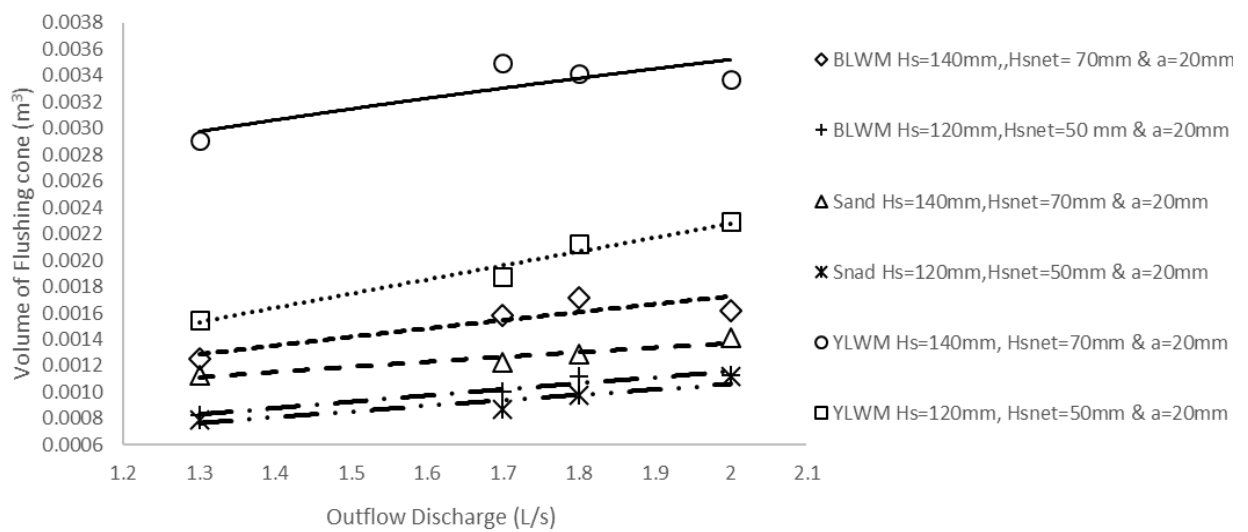


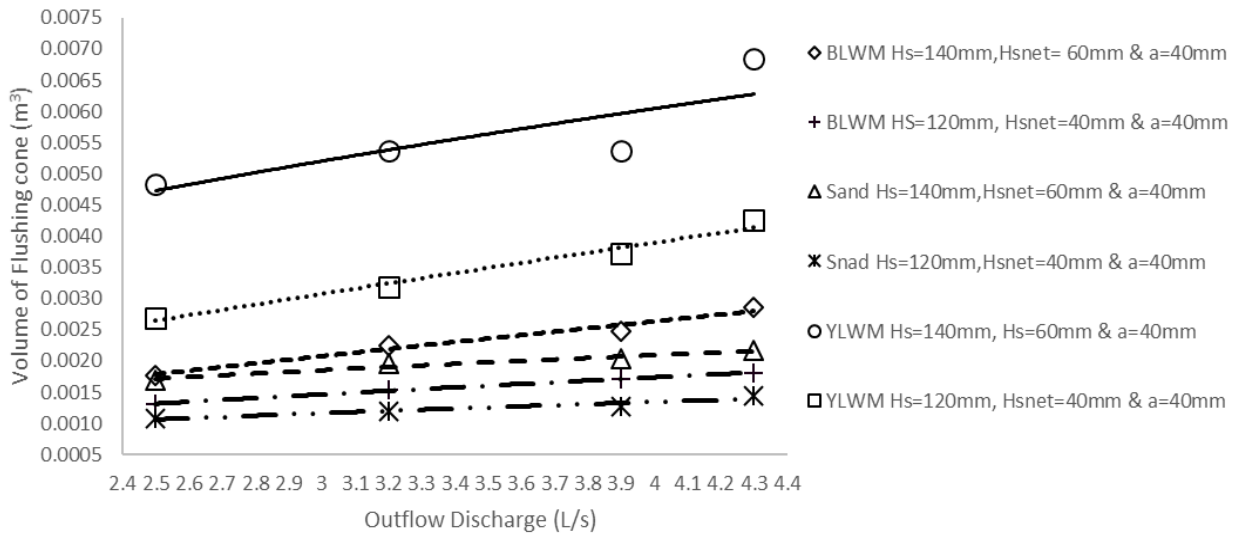
Figure 7.6 Flushing cone width versus outflow discharge for Blue Lightweight material (a), sand (b) & Yellow Lightweight material(c)

7.4 The variation of Outflow discharge versus volume of flushing cone and sediment height

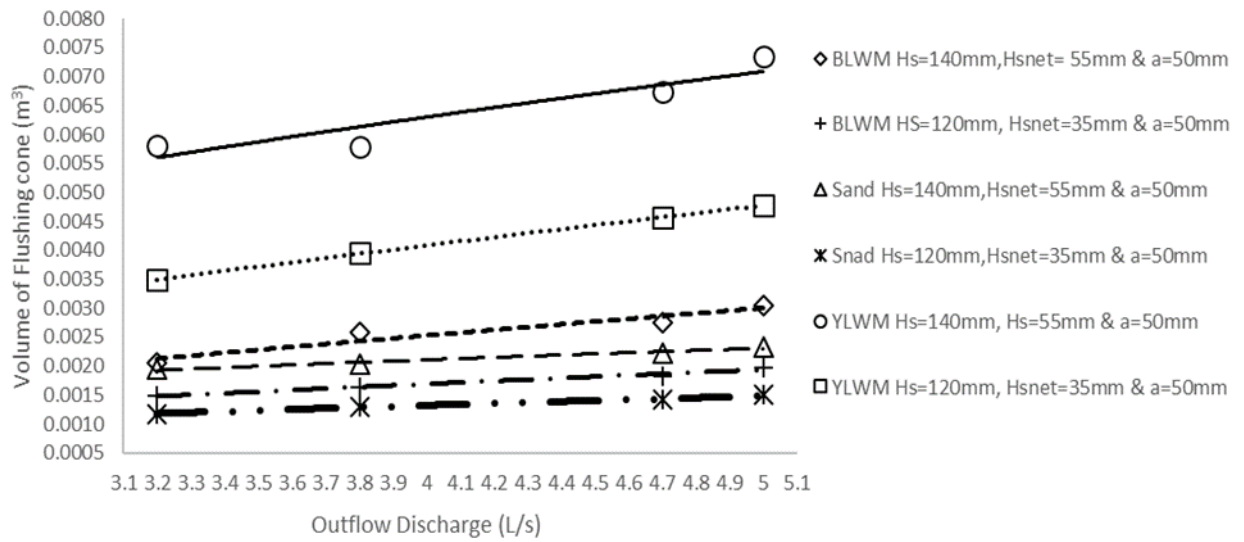
Meshkati (2010) investigated that with constant water depth, with an increase of outflow discharge the volume of flushing cone increase and the trend will be the same for all the outlets. Even though this study was conducted with varying water depth from (244 mm to 570 mm), the volume of flushed cones increased with an increase in outflow discharge like the study conducted by the Meshkati. Figure 7.7 (a, b, c, & d) below illustrates the relation between the volume of flushed cone and outflow discharge for three different materials Blue lightweight material (BLWM), Sand and Yellow lightweight material (YLWM) of sediment thickness 140 and 120 mm.

In addition, Figure 7.7 shows the effect of sediment height on the volume of flushing cone for different sediments being used in experiments. The figure below illustrates that increasing the height of sediment from 120 mm to 140mm causes an increase in the volume of flushing.





c



d

Figure 7.7 The variation of flushing cone volume versus outflow discharge for different depth of sediment and different outlet openings.

7.5 Comparison between Blue lightweight material and sand

Figure 7.8 below shows the comparison of Blue lightweight material and its corresponding sand of sediment thickness 140 and 120 mm. If we compare R² value for both sediment thickness (140 mm & 120 mm), it shows a high correlation with the value of almost 1.

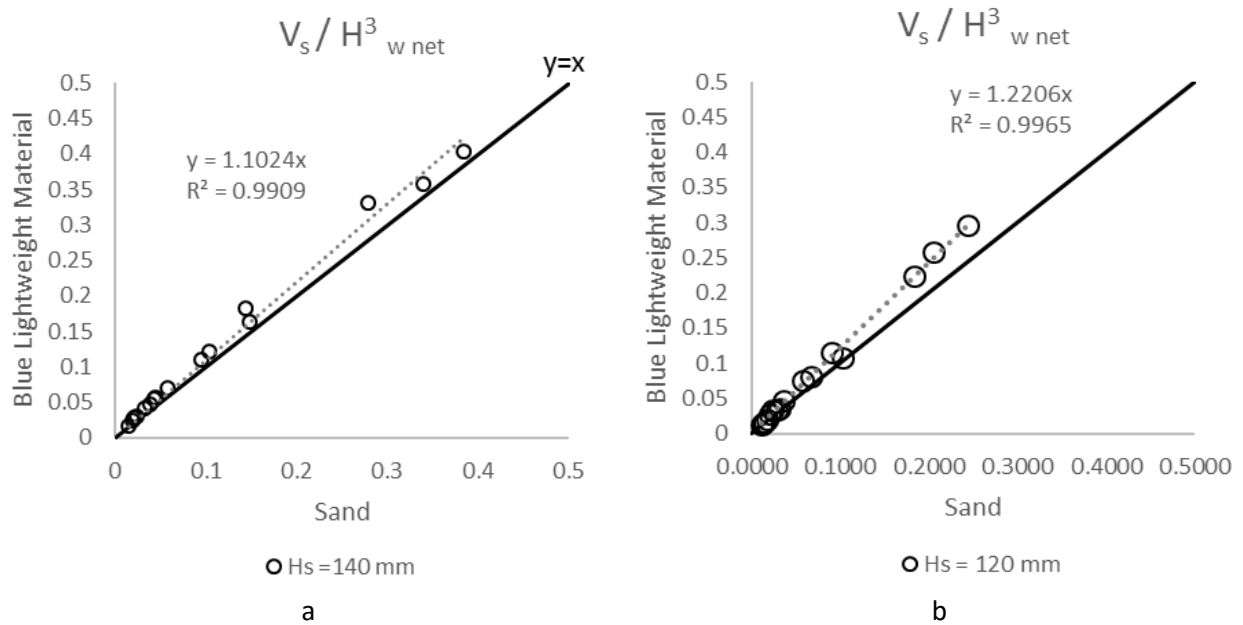


Figure 7.8 Comparison between Blue lightweight material and sand for (a) 140 mm& (b) 120 mm sediment thickness.

7.6 Statistical analysis for estimating ratio flushing cone volume and $H_w \text{ net} \left(\frac{V_s}{H_w^3 \text{ net}} \right)$

Meshkati (2010) conducted his study with sediment consisting of silica particles with a median diameter of $d_{50}=1\text{mm}$ with a circular outlet of the main reservoir with different diameters. With his experimental data, the following equation was suggested for the volume of flushing cone.

$$\frac{V_s}{H_w^3 \text{ net}} = 4.6 \left(\frac{u_{\text{outlet}}}{\sqrt{g(G_s - 1)d_{50}}} \right)^{0.21} \left(\frac{H_s}{H_w} \right)^{2.2} \left(\frac{D}{H_w} \right)^{0.89}$$

Figure 7.9 shows the comparison between the measured and calculated ratio of $\frac{V_s}{H_w^3 \text{ net}}$ proposed by Meshkati (2010) and the experimental data conducted during this study. The slope line represents the $\frac{V_s}{H_w^3 \text{ net}}$ as suggested by Meshkati (2010), whereas the dots with different shapes (triangle, square, diamond, circle and asterisk) represents the variation of measured versus calculated $\frac{V_s}{H_w^3 \text{ net}}$ ratio obtained during this study with different sediment samples with two different depth. It illustrates that sand which was used as a sediment sample (represented by diamond and asterisk-shape) in Figure 7.9 shows some better prediction with the equation suggested by the Meshkati (2010). But other than that the other two lightweight materials do not show any better prediction. Meshkati (2010) equation prediction for sand is better than for lightweight materials.

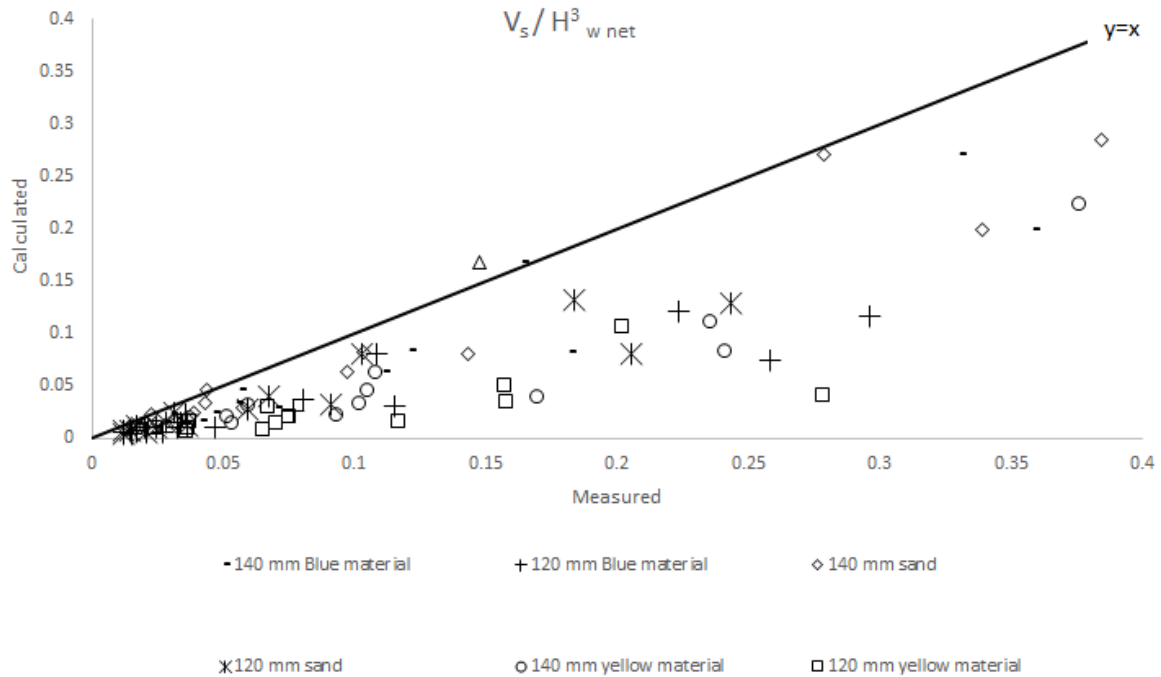


Figure 7.9 Comparison of $V_s / H^3_{w net}$ of Blue Material, Sand and Yellow Material of sediment thickness 140 & 120 mm.

Since lightweight material is a scaled model of sand a common equation representing both sand and lightweight material is proposed. As mentioned above, during the experiment conducted by Meshkati in 2010, a circular outlet opening of the main reservoir was used for flushing purpose which is not in our case. In our case, we used a rectangular opening of the different cross-sectional areas for the flushing purpose. Therefore, the parameter $\frac{A_{outlet}}{H_{w net}^2}$ was considered instead of $\frac{D}{H_{w net}}$ ratio. This could be one of the reasons for the deviation between the measured and calculated volume of the dimensionless flushing cone volume proposed by Meshkati. Another possible reason for the deviation could be the use of single sediment thickness and the use of only natural sand for the experiments to develop the empirical equations which might not be used for the different range of parameters used in this study.

Hence, multiple regression analysis was carried out to develop a relationship between the non-dimensional parameters for the flushing scour cone volume $V_{scouring}$ and other independent parameters of $\frac{u_{outlet}}{\sqrt{g(G_s-1)d_{50}}}, \frac{H_s}{H_{w net}}$ and $\frac{A_{outlet}}{H_{w net}^2}$ as other hydraulic, fluid and sediment properties were constant (B =flume width, ρ_s = sediment density, ρ_w = water density and μ = dynamic viscosity). Software called Eureka was used to derive an empirical relationship between these independent parameters and the following equation was derived.

New proposed an empirical formula for calculation of $\frac{V_{scouring}}{H_{w net}^3}$ by using software Eureka

$$\frac{V_s}{H_{w net}^3} = 3.211 \left(\frac{u_{outlet}}{\sqrt{g(G_s - 1)d_{50}}} \right)^{0.662} \frac{A_{outlet}}{H_{w net}^2} \cdot \frac{H_s}{H_{w net}} \quad 7-1$$

For verification of results, the statistical parameters such as mean squared error (MSE), mean absolute error (MAPE) and R squared value were calculated for the above equations are presented in Table 7-2.

Table 7-2 Statistical verification for presented equation

Equation	Parameters	MSE	MAE	R ²
1	$\frac{V_s}{H_{w\ net}^3} = f\left(\frac{u_{outlet}}{\sqrt{g(G_s-1)d_{50}}}, \frac{A_{outlet}}{(H_{w\ net})^2}, \frac{H_s}{H_{w\ net}}\right)$	0.000415	0.01157	0.9828

With the R squared value of 0.9828, it suggests a close fit will be obtained if we plot the values which were measured during experiments against the values obtained from the suggested empirical formula. Additionally, with RMSE value of 0.000415 and the MAE value of 0.01157 Table 7-2 also suggest the errors in predicting the $\frac{V_s}{H_{w\ net}^3}$ is very low. In spite, the suggested equation shows a high correlation their applicability should be tested using other experimental data as well.

7.7 Comparison between Yellow lightweight material and sand

Because of the time constraints experiment for the sand representing the yellow lightweight material could not be done. Since the suggested empirical equation showed a high correlation coefficient, the volume of flushing cone of sand representing the yellow lightweight material could be predicted and could be correlated with the yellow lightweight material which is discussed below.

Figure 7.10 shows the comparison of Yellow lightweight material and its corresponding predicted sand of sediment thickness 140 and 120 mm. If we compare R² value for both sediment thickness (140 mm & 120 mm), it shows a high correlation with the value of almost 1.

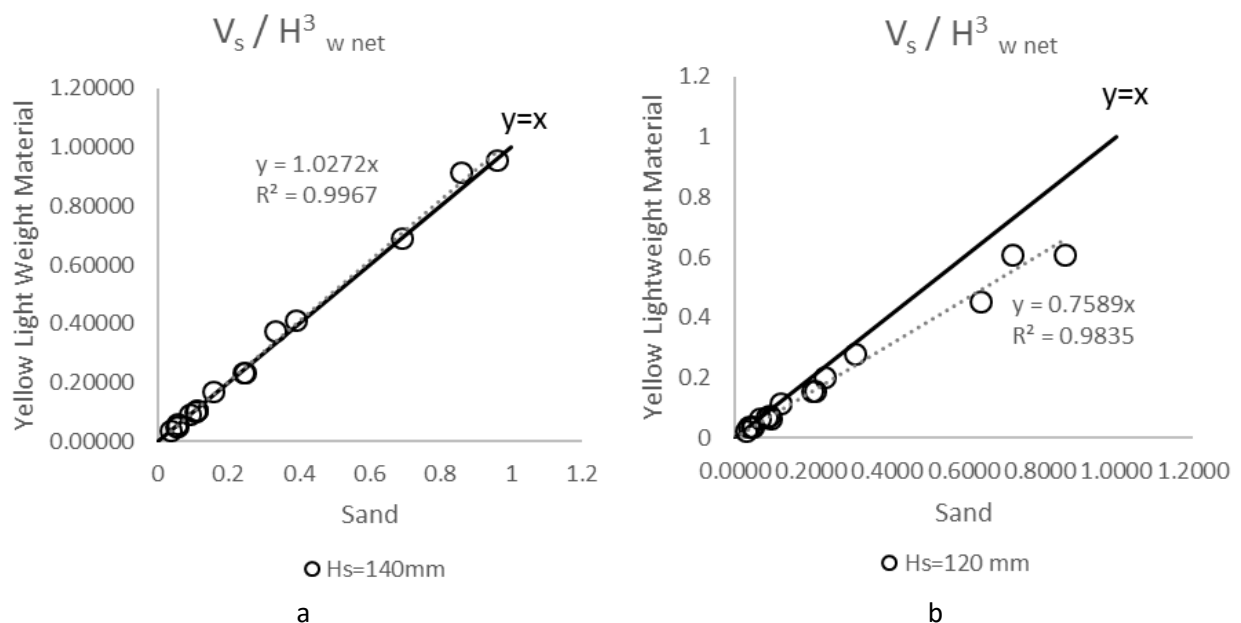


Figure 7.10 Comparison between Yellow lightweight material and sand for 140 mm (a) & 120 mm (b) sediment thickness.

8 Conclusion

Physical models have been used for decades by different hydraulic laboratories to study different processes that involve in hydraulic structures under controlled laboratory environment. Still, there is a limited number of studies about lightweight materials. The main objective of this study is to find how lightweight materials response to pressurized flushing under different hydraulic parameters of outlet discharge, sediment depth, flow depth and different bottom outlet with the use of a physical model. In addition, the other objective of this study is also to develop scaling relation among parameters of the prototype and lightweight model for the quantitative study of sediment transport. To fulfill this aim, experiments were conducted with two separate lightweight materials and sand with different test constraints under pressurized flushing.

As previously mentioned, the asymmetrical flushing cone is developed in front of the gate in the pressure flushing operation. The scouring depth was found to be maximum in the vicinity of the dam wall. Visually side slopes of the cone formed after flushing were approximately equal of the submerged sediments. During the experiment, it was observed that flushing of sediments accelerates very fast for the first one to two minutes and slows down slowly and finally reach to hydraulically equilibrium conditions. After which the flushing operation is very slowed or stops.

This study shows that outflow discharge(Q), flow depth (H_w), area of the outlet (A_{outlet}) and sediment thickness (H_s) is the main parameters correlating the flushing cone dimensions. The result of the study shows the dimension of flushing cone increases with an increase in flow depth, outflow discharge, and cross-section of the bottom outlet. In addition, the study also reveals that an increase in sediment thickness (height), increases the volume of the flushed cone as well. Another interesting thing which was observed during the comparison between two lightweight materials was that materials with finer grains yellow lightweight material in this case study formed wider cones due to the lower angle of repose and higher buoyancy effect.

This study was compared with the study done by Meshkati (2010) with sediment consisting of silica particles with a circular outlet of the main reservoir. While this study is done with two different lightweight materials and one sand sample of thickness 140 and 120mm with the rectangular opening as an outlet.

Comparison between the measured and calculated ratio of $\frac{V_s}{H_{w\ net}^3}$ proposed by Meshkati (2010) and the experimental data conducted during this study was conducted in this study. During the comparison, it was noted Meshkati equations' prediction for sand is better than for lightweight material. The Possible reason for deviation could be the use of the diameter of a circular outlet as an equivalent area, the use of the same sediment thickness and the use of only natural sand to develop the empirical equations which have been mentioned above.

As lightweight material is a scaled model of the sand, a common equation was proposed which can represent both sand as well as lightweight materials. Multiple regression was carried out based upon the experimental data under clear water flow condition and dimensionless equation for predicting the volume of flushing cone was presented. The presented 7-1 equation was found to have a high correlation coefficient with a statistical parameter such as root mean square error of 0.000415, mean absolute error of 0.01157 and an R-squared value of 0.9828.

Furthermore, a comparison of the dimensionless ratio $\frac{V_s}{H_{w\ net}^3}$ between sand and lightweight material was also done. During the analysis of experimental data, a high correlated relationship was noticed

between these two materials with R-squared value of almost 1. With the time constraints, experiment with sand samples for yellow lightweight material could not be conducted. Since the suggested equation showed a high correlation value, the volume of flushing cone was predicted using this equation and compared with the volume of a flushed cone of its respective lightweight material. This comparison also showed the high correlated relationship between each other. Figure 8.1 below presents the comparison of $\frac{V_{scouring}}{H_{w net}^3}$ ratio between sand and two different lightweight material.

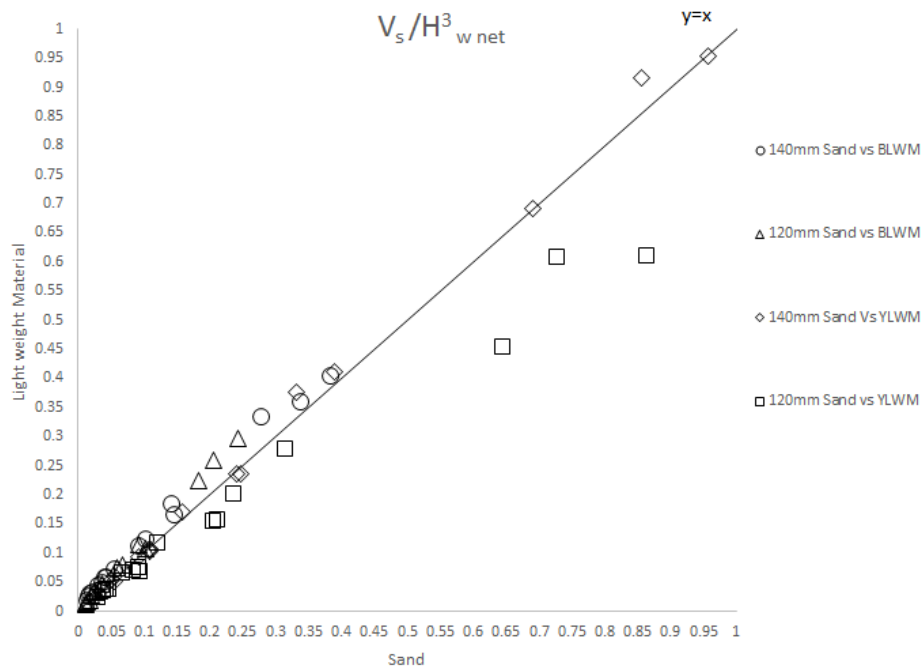


Figure 8.1 Comparison of $\frac{V_s}{H_{w net}^3}$ ratio between sand and lightweight material.

With the experimental data related to this research study a summary can be drawn that with the use of proper scaling relations among parameters of the prototype, the lightweight model can be conveniently used for quantitative studies of a process involving sediment transport. Despite the suggested equations for predicting of flushing cone appeared to have a high correlation their applicability should be tested using other experimental data. Supplementary experiments are recommended by using different sizes, shapes, and thicknesses of sediment materials under different hydraulic conditions to confirm the results obtained from this study.

9 Future Work

Hydraulic flushing is the most common and effective measures to flush the deposited sediments from reservoirs. This study was carried out for investigation of cone development upstream of sluice gate under pressurized flushing condition using both sand and lightweight material for varying discharge, water depth, thickness of sediment layer and height of gate opening with an objective to develop scaling relation among parameters of prototype and lightweight model so that such models could be used for studies of sediment transport process. During the study, it was ascertained that there exists a high correlation between lightweight material and prototype material (sand). Since this study was limited to only two types of lightweight materials, further experiments are necessary with different setups and gradation of bed materials under different hydraulic conditions to comply with the result obtained from this study.

Furthermore, experiments run with different sill height above the bottom of the bed level which could show different approach flows and their effect on the scour development would be another area of study. A sloping bed upstream of the orifice and its effect on the flushing volume could be another interesting topic.

It would be also very interesting to study the effect of having multiple opening outlets with different shapes on sediment volume flushed with the same setup. For example, having two separate openings of 0.001 m² spaced at equidistance instead of having one 0.002 m² opening. Setup of multiple outlets could have different velocity fields and may show different flushed cone structures.

Future work can be performed under the following topics

1. Conducting similar experiments with different materials at different hydraulic conditions.
2. The experiment runs with different locations of outlet opening at a variable distance above the bed.
3. A sloping bed upstream of the orifice.
4. Multiple outlet configurations setup.

10 References:

- ANNANDALE, G. W., MORRIS, G. L. & KARKI, P. 2016. *Extending the life of reservoirs: sustainable sediment management for dams and run-of-river hydropower*, The World Bank.
- BRANDT, S. A. 1999. *Reservoir desiltation by means of hydraulic flushing: sedimentological and geomorphological effects in reservoirs and downstream reaches as illustrated by the Cachi Reservoir and the Reventazon River, Costa Rica*, University of Copenhagen, Copenhagen (Dinamarca). Institute of Geography.
- BROWN, C. B. 1944. *The control of reservoir silting*, US Govt. print. off.
- CENTER, E. A. E. W. *Dredging* [Online]. Available: https://www.navfac.navy.mil/navfac_worldwide/specialty_centers/exwc/products_and_services/ev/erb/tech/rem/dredge.html [Accessed].
- CHHETTRY, B., THAPA, B., THAPA, B. J. I. J. O. H. & DAMS 2014. Assembly design to ease turbine maintenance in sediment-laden conditions. 2, 84-88.
- DALRYMPLE, R. 1989. Physical modelling of littoral processes. *Recent advances in Hydraulic physical modelling*. Springer.
- DALRYMPLE, R. A. 2018. *Physical modelling in coastal engineering: Proceedings of an international conference, Newark, Delaware, August 1981*, Routledge.
- DE VRIES, M. J. S. & REPORTS ON HYDROLOGY 1993. Use of models for river problems.
- EINSTEIN, H. A. & CHIEN, N. J. T. O. T. A. S. O. C. E. 1956. Similarity of distorted river models with movable beds. 121, 440-457.
- EMAMGHOLIZADEH, S., BINA, M., FATHI-MOGHADAM, M., GHOMEYSHI, M. J. A. J. O. E. & SCIENCES, A. 2006. Investigation and evaluation of the pressure flushing through storage reservoir. 1, 7-16.
- EMAMGHOLIZADEH, S. & FATHI-MOGHDAM, M. J. J. O. H. E. 2014. Pressure flushing of cohesive sediment in large dam reservoirs. 19, 674-681.
- ETTEMA, R., ARNDT, R., ROBERTS, P. & WAHL, T. 2000. *Hydraulic modeling: Concepts and practice*.
- FANG, D. & CAO, S. An experimental study on scour funnel in front of a sediment flushing outlet of a reservoir. Proceedings of the 6th Federal Interagency Sedimentation Conference, Las Vegas, 1996.
- FROSTICK, L. E., MCLELLAND, S. J. & MERCER, T. G. 2011. *Users Guide to Physical Modelling and Experimentation: Experience of the HYDRALAB Network*, Taylor & Francis.
- GARCIA, M. Sedimentation engineering: processes, measurements, modeling, and practice. 2008. American Society of Civil Engineers.
- GUMMER, J. H. J. H. R. W. 2009. Combating Silt Erosion in Hydraulic Turbines-Some of the most attractive hydro sites are plagued by silt. While silt erosion of hydraulic turbines at these sites can be managed, further work is needed to better predict and control this erosion. 17, 28.
- HEMPHILL, R. Silting and life of southwestern reservoirs. Proceedings of the American Society of Civil Engineers, 1930. ASCE, 967-980.
- HUGHES, S. A. 1993. *Physical models and laboratory techniques in coastal engineering*, World Scientific.
- HYDRALAB+ 2016. Critical review of challenges for representing climate change in physical models. In: BAYNES(UNIVERSITÉ, S. M. U. W. V. D. L. U. E. & RENNES, D. (eds.).
- JAVED, W. & TINGSANCHALI, T. SEDIMENT FLUSHING STRATEGY FOR RESERVOIR OF PROPOSED BHASHA DAM, PAKISTAN.
- KAMBLE, S., KUNJEER, P. & ISAAC, N. J. I. J. O. H. E. 2018. Hydraulic model studies for estimating scour cone development during pressure flushing of reservoirs. 24, 337-344.
- KAMPHUIS, J. J. P. M. I. C. E. 1985. On understanding scale effect in coastal mobile bed models. 141-162.
- KOBUS, H. 1984. Local air entrainment and detrainment.

- KONDOLF, G. M., GAO, Y., ANNANDALE, G. W., MORRIS, G. L., JIANG, E., ZHANG, J., CAO, Y., CARLING, P., FU, K. & GUO, Q. J. E. S. F. 2014. Sustainable sediment management in reservoirs and regulated rivers: Experiences from five continents. 2, 256-280.
- LANGHAAR, H. L. 1951. *Dimensional analysis and theory of models*, Wiley New York.
- MARKOFSKY, M. & KOBUS, H. 1978. Unified presentation of weir-aeration data.
- MAYNORD, S. T. J. J. O. H. E. 2006. Evaluation of the micromodel: An extremely small-scale movable bed model. 132, 343-353.
- MESHKATI, M., DEGHANI, A., NASER, G., EMAMGHOLIZADEH, S., MOSAEDI, A. J. W. A. O. S., ENGINEERING & TECHNOLOGY 2009. Evolution of developing flushing cone during the pressurized flushing in reservoir storage. 58, 1107-1111.
- MILLIMAN, J. D. & MEADE, R. H. J. T. J. O. G. 1983. World-wide delivery of river sediment to the oceans. 91, 1-21.
- MOHAMMAD, B. T., DAHAM, F. A., BILAL, Z. Z. J. Z. J. O. P. & SCIENCES, A. 2018. Experimental Investigation to study the Hydraulic Performance of Pressure Flushing in Straight Wall Reservoirs. 30, 113-121.
- MORRIS, G. L. 2014. Sediment management and sustainable use of reservoirs. *Modern water resources engineering*. Springer.
- MORRIS, G. L. & FAN, J. 1998. *Reservoir sedimentation handbook: design and management of dams, reservoirs, and watersheds for sustainable use*, McGraw Hill Professional.
- NEOPANE, H. P. 2010. Sediment erosion in hydro turbines.
- NOVAK, P., GUINOT, V., JEFFREY, A. & REEVE, D. E. 2018. *Hydraulic modelling: An introduction: Principles, methods and applications*, CRC Press.
- PARI, S. A., KASHEFIPOUR, S., GHOMESHI, M., BAJESTAN, M. S. J. J. O. F., AGRICULTURE & ENVIRONMENT 2010. Effects of obstacle heights on controlling turbidity currents with different concentrations and discharges. 8, 930-935.
- PUGH, C. A. & DODGE, R. A. J. S. M. 1991. DESIGN OF SEDIMENT NODELS. 61.
- QIAN, N. Reservoir sedimentation and slope stability; technical and environmental effects. Fourteenth International Congress on Large Dams, Transactions, Rio de Janeiro, Brazil, 1982. 639-690.
- RANDLE, T., KIMBREL, S., COLLINS, K., BOYD, P., JONAS, M., VERMEEREN, R., EIDSON, D., COOPER, D., SHELLEY, J. & JURACEK, K. 2017. Frequently Asked Questions about Reservoir Sedimentation and Sustainability. Subcommittee on Sedimentation, National Reservoir Sedimentation and
- SAMAD EMAMGHOLIZADEH, M. B., M. FATHI-MOGHADAM AND M. GHOMEYSHI 2006. INVESTIGATION AND EVALUATION OF THE PRESSURE FLUSHING THROUGH STORAGE RESERVOIR *ARPN Journal of Engineering and Applied Sciences* 8.
- SCHELLENBERG, G., DONNELLY, C., HOLDER, C. & AHSAN, R. J. H. R. W. 2017. Dealing with Sediment: Effects on Dams and Hydropower Generation.
- SENG LOW, H. J. J. O. H. E. 1989. Effect of sediment density on bed-load transport. 115, 124-138.
- SHAHMIRZADI, M. M., DEGHANI, A., SUMI, T., MOSAEDI, A. J. W. & GEOSCIENCE 2010. Experimental Investigation of Pressure Flushing Technique in Reservoir Storages. 1.
- SHAHMIRZADI, M. M., DEGHANI, A., SUMI, T., NASER, G. & AHADPOUR, A. Experimental investigation of local half-cone scouring against dam.
- SHARMA, H. J. T. I. J. O. H. & DAMS 2010. Power generation in sediment laden rivers: The case of Nathpa Jhakri. 17, 112.
- SHEN, H. W., LAI, J.-S. & ZHAO, D. Hydraulic desiltation for noncohesive sediment. *Hydraulic Engineering*, 1993. ASCE, 119-124.
- SONIN, A. A. 2001. The Physical Basis of Dimensional Analysis, Ain A. Sonin.
- SUMI, T., HIROSE, T. J. W. S., TRANSPORT,, DISTRIBUTION, E. O. L. S. S. & TAKAHASI, Y., ED 2009. Accumulation of sediment in reservoirs. 224-252.
- TAYLOR, B. D. 1971. Temperature effects in alluvial streams.
- VANONI, V. J. S. E. 1975. Sediment discharge formulas. 190-229.

- WALDRON, R. L. 2008. Physical modeling of flow and sediment transport using distorted scale modeling.
- WARNOCK, J. Chapter II Hydraulic Similitude. Proceedings, 1950. The University, 136.
- WHITE, W. J. H. I. M. R. A. R., WATER & PUBL, S. I. 1990. Reservoir sedimentation and flushing.
- YALIN, M. & KAMPHUIS, J. J. J. O. H. R. 1971. Theory of dimensions and spurious correlation. 9, 249-265.
- ZWAMBORN, J. J. L. H. B. 1966. Reproducibility in hydraulic models of prototype river morphology. 291-298.

11 Appendix A Basic Formulas & Calculations

Basic Formula

No	Parameters	Symbol	Formula	Unit
1	Manning's value	n	$n = \frac{d^{\frac{1}{6}}}{21.1}$	$s/m^{1/3}$
2	Unit Discharge	q	$q = \frac{Q}{B}$	$m^3/s/m$
3	Bed Shear Velocity	u_*	$u_* = \sqrt{gRS}$ $= \sqrt{ghS}$ (wide channel)	m/s
4	Bead Shear Stress	τ	$\tau = u_*^2 \cdot \rho$	N/m^2
5	Settling Velocity (Soulsby 1997)	w	$w = \frac{\vartheta}{d} [(10.36^2 + 1.049D_*^3)^{0.5} - 10.36]$	m/s

Dimensionless Parameters

No	Parameters	Symbol	Formula	Unit
1	Submerged specific gravity of sediment particles	$(G - 1)$	$(G - 1) = \left(\frac{\rho_s - \rho}{\rho} \right)$	-
2	Froude Number	Fr	$Fr = \frac{u}{\sqrt{gL}}$	-
3	Reynolds Number	Re	$re = \frac{\rho Lv}{\mu} = \frac{Lu}{\vartheta}$	-
4	Shield Number	Fr_*	$Fr_* = \frac{u_*^2 \rho}{(\rho_s - \rho) \cdot g \cdot d}$ $= \frac{u_*^2}{(G - 1) \cdot g \cdot d}$	-
5	Grain Reynolds Number	Re_*	$Re_* = \frac{u_* d}{\vartheta}$	-
6	Dimensionless Grain Size	D_*	$D_* = \left(\frac{Re_*^2}{Fr_*} \right)^{\frac{1}{3}}$	-
7	Darcy Weisbach Friction Factor	f	$f = 8 \cdot g \cdot R \cdot S \cdot \frac{1}{u^2}$	-
8	Dimensionless Sediment Discharge	q_{s*}	$q_{s*} = \frac{q_s}{u_* \cdot d}$	-

Where,

d	Sediment particle size	(m)
Q	Flow discharge	(m^3/s)
B	Flow width	(m)
g	acceleration due to gravity	(m/s^2)
h	Flow depth	(m)
S	Slope	
w	Settling velocity	(m/s)
ρ	Density of water	(kg/m^3)
ρ_s	Density of sediment particle	(kg/m^3)
u	Flow velocity	(m/s)
ϑ	Kinematic viscosity of water	(m^2/s)

Basic calculations

Using equation 5-18, Prototype with model with scaling ratio of 1:5 of blue lightweight material.

Input parameters	Model value		
	Symbol	Value	Units
Sediment particle size	d	4.000	mm
Density of sediment particle	ρ_s	1400.00	kg/m ³
Length in horizontal direction	L	1.00	m
Width of the flume	B	0.60	m
Submerged specific gravity of sediment particles	G-1	0.40	-

we get

$$L_r = \delta^2 (G - 1)_r d_r$$

$$\frac{L_m}{L_p} = \delta^2 \cdot \frac{(G - 1)_m}{(G - 1)_p} \cdot \frac{d_m}{d_p}$$

$$\frac{1}{5} = \frac{0.4}{1.65} \cdot \frac{4}{d_p}$$

$$d_p = \frac{5 \cdot 0.4 \cdot 4}{1.65} = 4.848$$

Using equation 5-18, Prototype with model with scaling ratio of 1:5 of yellow lightweight material.

Input parameters	Model value		
	Symbol	Value	Units
Sediment particle size	d	2.000	mm
Density of sediment particle	ρ_s	1058.00	kg/m ³
Length in horizontal direction	L	1.00	m
Width of the flume	B	0.60	m
Submerged specific gravity of sediment particles	G-1	0.058	-

we get

$$L_r = \delta^2 (G - 1)_r d_r$$

$$\frac{L_m}{L_p} = \delta^2 \cdot \frac{(G - 1)_m}{(G - 1)_p} \cdot \frac{d_m}{d_p}$$

$$\frac{1}{5} = \frac{0.058}{1.65} \cdot \frac{2}{d_p}$$

$$d_p = \frac{5 \cdot 0.058 \cdot 2}{1.65} = 0.352$$

Table 11-1 Test parameters and scaling ratios for blue lightweight material and sand

Parametrs	Symbols	Prototype		Model (Blue Lightweight Material)			Undistorted Sand Model		
		Value	Units	Scale Ratio	Value	Units	Scale Ratio	Value	Units
Parameters usually taken as constant									
Density of water	ρ_w	1000	kg/m ³	1	1000	kg/m ³	1	1000	kg/m ³
Kinematic viscosity of water	ν	0.000001	m ² /s	1	0.000001	m ² /s	1	0.000001	m ² /s
Gravitational acceleration	g	9.81	m/s ²	1	9.81	m/s ²	1	9.81	m/s ²
Bed porosity, λ	$(1-\lambda)$	1	--	1	1	--	1	1	--
Input parameters									
Sediment particle size	d	4.848004687	mm	1.212001172	4	mm	5	0.969600937	mm
Density of sediment particle	ρ_s	2650	kg/m ³	1.892857143	1400	kg/m ³	1	2650	kg/m ³
Length in horizontal direction	L	5	m	5	1	m	5	1	m
Width of the flume	B	3	m	5	0.6	m	5	0.6	m
Calculated Parametrs									
Specific gravity of sediment particles	G	2.65	--	1.892857143	1.4	--	1	2.65	--
Manning's n	n	0.024691163	s/m ^{1/3}	1.307617317	0.01888256	s/m ^{1/3}	1.307660486	0.018881937	s/m ^{1/3}
Flow depth	h	1.249938103	m	4.999752411	0.25	m	5	0.249987621	m
Flow velocity	u	0.044720252	m/s	2.236012614	0.02	m/s	2.236067977	0.019999505	m/s
Settling velocity (calculated using Soulsby 1997)	w	0.28478103	m/s	2.264614214	0.125752558	m/s	2.411980586	0.118069371	m/s
Flow discharge	Q	0.167692642	m ³ /s	55.89754729	0.003	m ³ /s	55.90169944	0.002999777	m ³ /s
unit discharge (flow)	q	0.055897547	m ³ /s/m	11.17950946	0.005	m ³ /s/m	11.18033989	0.004999629	m ³ /s/m
Bed shear velocity	u_*	0.003332209	m/s	2.235957252	0.001490283	m/s	2.236067977	0.001490209	m/s
Bed shear stress	τ	0.011103615	N/m ²	4.999504833	0.002220943	N/m ²	5	0.002220723	N/m ²
unit sediment discharge	q_s	0.000108399	m ³ /s/m	2.70998281	0.00004	m ³ /s/m	11.18033989	9.69553E-06	m ³ /s/m
Bed development in vertical direction	z	0	m	0.293789368		m	5	0	m
Dimensionless parameters									
Submerged specific gravity of sediment particles	$G-1$	1.65	--	4.125	0.4	--	1	1.65	--
Distortion	δ	--	--	1.00004952	--	--	1	--	--
Energy Slope	S	9.05538E-07	--	0.999950482	9.05583E-07	--	1	9.05538E-07	--
Froude number	Fr	0.012771017	--	1	0.012771017	--	1	0.012771017	--
Reynolds number	Re	55897.54729	--	11.17950946	5000	--	11.18033989	4999.62862	--
Shields parameter	Fr_* or θ	0.000141497	--	1	0.000141497	--	1	0.000141497	--
Grain Reynolds number	Re_*	16.15456377	--	2.70998281	5.961131457	--	11.18033989	1.44490811	--
Dimensionless grain size	D_*	122.6348813	--	1.943767683	63.09132635	--	5	24.52697625	--
Darcy Weisbach friction factor	f	0.044416661	--	0.999950482	0.04441886	--	1	0.044416661	--
Dimensionless unit sediment discharge	q_{s*}	6.710135532	--	1	6.710135532	--	1	6.710135532	--

Table 11-2 Test parameters and scaling ratios for yellow lightweight material and sand.

Parameters	Symbols	Prototype		Model (Yellow Lightweight Material)			Undistorted Sand Model		
		Value	Units	Scale Ratio	Value	Units	Scale Ratio	Value	Units
Density of water	ρ_w	1000	kg/m ³	1.00	1000	kg/m ³	1.00	1000	kg/m ³
Kinematic viscosity of water	ν	0.000001	m ² /s	1.00	0.000001	m ² /s	1.00	0.000001	m ² /s
Gravitational acceleration	g	9.81	m/s ²	1.00	9.81	m/s ²	1.00	9.81	m/s ²
Bed porosity, λ	$(1-\lambda)$	1	--	1.00	1	--	1.00	1	--
Input parameters									
Sediment particle size	d	0.3515	mm	0.18	2	mm	5.00	0.0703	mm
Density of sediment particle	ρ_s	2650	kg/m ³	2.50	1058	kg/m ³	1.00	2650	kg/m ³
Length in horizontal direction	L	5	m	5.00	1	m	5.00	1	m
Width of the flume	B	3		5.00	0.6		5.00	0.6	
Calculated Parameters									
Specific gravity of sediment particles	G	2.65	--	2.50	1.058	--	1.00	2.65	--
Manning's n	n	0.021998051	s/m ^{1/3}	1.31	0.016822449	s/m ^{1/3}	1.31	0.016822449	s/m ^{1/3}
Flow depth	h	1.25	m	5.00	0.25	m	5.00	0.25	m
Flow velocity	u	0.04472136	m/s	2.24	0.02	m/s	2.24	0.02	m/s
Settling velocity (calculated using Soulsby 1997)	w	0.053212717	m/s	1.79	0.029756406	m/s	13.32	0.003995776	m/s
Flow discharge	Q	0.167705098	m ³ /s	55.90	0.003	m ³ /s	55.90	0.003	m ³ /s
unit discharge (flow)	q	0.055901699	m ³ /s/m	11.18	0.005	m ³ /s/m	11.18	0.005	m ³ /s/m
Bed shear velocity	u_*	0.002968808	m/s	2.24	0.001327691	m/s	2.24	0.001327691	m/s
Bed shear stress	τ	0.008813818	N/m ²	5.00	0.001762764	N/m ²	5.00	0.001762764	N/m ²
unit sediment discharge	q_s	1.57196E-05		0.39	0.00004	m ³ /s/m	11.18	0.000001406	m ³ /s/m
Bed development in vertical direction	z	0		0.01			5.00	0	
Dimensionless parameters									
Submerged specific gravity of sediment particles	$G-1$	1.65	--	28.45	0.058	--	1.00	1.65	--
Distortion	δ	--	--	1.00	--	--	1.00	--	--
Energy Slope	S	7.18762E-07	--	1.00	7.18762E-07	--	1.00	7.18762E-07	--
Froude number	Fr	0.012771017	--	1.00	0.012771017	--	1.00	0.012771017	--
Reynolds number	Re	55901.69944	--	11.18	5000	--	11.18	5000	--
Shields parameter	Fr_* or θ	0.001549123	--	1.00	0.001549056	--	1.00	0.001549123	--
Grain Reynolds number	Re_*	1.04353585	--	0.39	2.655382187	--	11.18	0.093336684	--
Dimensionless grain size	D_*	8.891526214	--	0.54	16.57279135	--	5.00	1.778305243	--
Darcy Weisbach friction factor	f	0.035255273	--	1.00	0.035255273	--	1.00	0.035255273	--
Dimensionless unit sediment discharge	q_{s*}	15.06374495		1.00	15.06374495		1.00	15.06374495	

12 Appendix B. Measured volume of sediment flushed

Blue Lightweight Material

Table 12-1 Measured volume of BLWM flushed. (Hs = 140mm)

Test	a ₀ , [mm]	a, [mm]	b, [mm]	B, [mm]	H _s , [mm]	Q, [lps]	H _w , [mm]	A _{outlet}	Volume of cone [mm ³]	Volume of cone [m ³]	Width of cone [mm]	Length of cone [mm]	H _{w net} [m]	H _{s net} [m]	V _s /H _{w net} ³
1	60	20	50	600	140	1.3	267	0.001	1.26E+06	0.00126	310	150	0.197	0.07	0.164178
2	60	20	50	600	140	1.7	373	0.001	1.58E+06	0.00158	320	165	0.303	0.07	0.056851
3	60	20	50	600	140	2	523	0.001	1.62E+06	0.00162	325	160	0.453	0.07	0.017426
4	60	20	50	600	140	1.8	453	0.001	1.71E+06	0.00171	330	160	0.383	0.07	0.030513
5	60	30	50	600	140	1.8	244	0.0015	1.60E+06	0.00160	320	160	0.169	0.065	0.33086
6	60	30	50	600	140	2.2	326	0.0015	1.92E+06	0.00192	325	170	0.251	0.065	0.121215
7	60	30	50	600	140	2.6	414	0.0015	2.17E+06	0.00217	350	170	0.339	0.065	0.055757
8	60	30	50	600	140	3	518	0.0015	2.44E+06	0.00244	370	190	0.443	0.065	0.028033
9	60	40	50	600	140	2.5	244	0.002	1.78E+06	0.00178	340	165	0.164	0.06	0.402726
10	60	40	50	600	140	3.2	352	0.002	2.25E+06	0.00225	365	190	0.274	0.06	0.109422
11	60	40	50	600	140	3.9	455	0.002	2.47E+06	0.00247	380	195	0.375	0.06	0.046854
12	60	40	50	600	140	4.3	570	0.002	2.87E+06	0.00287	405	205	0.49	0.06	0.024353
13	60	50	50	600	140	3.2	264	0.0025	2.06E+06	0.00206	330	165	0.179	0.055	0.358619
14	60	50	50	600	140	3.8	327	0.0025	2.59E+06	0.00259	360	190	0.242	0.055	0.182607
15	60	50	50	600	140	4.7	424	0.0025	2.75E+06	0.00275	385	200	0.339	0.055	0.070499
16	60	50	50	600	140	5	502	0.0025	3.04E+06	0.00304	385	200	0.417	0.055	0.041899

Table 12-2 Measured volume of BLWM flushed. (Hs =120 mm)

Test	a ₀ , [mm]	a, [mm]	b, [mm]	B, [mm]	H _s , [mm]	Q, [lps]	H _w , [mm]	A _{outlet}	Volume of cone [mm ³]	Volume of cone [m ³]	Width of cone [mm]	Length of cone [mm]	H _{w net} [m]	H _{s net} [m]	V _s /H _{w net} ³
1	60	20	50	600	120	1.3	267	0.001	8.27E+05	0.00083	270	135	0.197	0.05	0.108136
2	60	20	50	600	120	1.7	373	0.001	1.00E+06	0.00100	275	140	0.303	0.05	0.03602
3	60	20	50	600	120	2	523	0.001	1.13E+06	0.00113	300	150	0.453	0.05	0.01214
4	60	20	50	600	120	1.8	453	0.001	1.12E+06	0.00112	300	145	0.383	0.05	0.019912
5	60	30	50	600	120	1.8	244	0.0015	1.08E+06	0.00108	300	145	0.169	0.045	0.223377
6	60	30	50	600	120	2.2	326	0.0015	1.27E+06	0.00127	300	150	0.251	0.045	0.08054
7	60	30	50	600	120	2.6	414	0.0015	1.31E+06	0.00131	310	155	0.339	0.045	0.033726
8	60	30	50	600	120	3	518	0.0015	1.47E+06	0.00147	330	170	0.443	0.045	0.016964
9	60	40	50	600	120	2.5	244	0.002	1.31E+06	0.00131	300	155	0.164	0.04	0.296331
10	60	40	50	600	120	3.2	352	0.002	1.54E+06	0.00154	305	155	0.274	0.04	0.074883
11	60	40	50	600	120	3.9	455	0.002	1.72E+06	0.00172	335	150	0.375	0.04	0.032573
12	60	40	50	600	120	4.3	570	0.002	1.80E+06	0.00180	345	165	0.49	0.04	0.015318
13	60	50	50	600	120	3.2	264	0.0025	1.48E+06	0.00148	330	165	0.179	0.035	0.258415
14	60	50	50	600	120	3.8	327	0.0025	1.63E+06	0.00163	330	165	0.242	0.035	0.115294
15	60	50	50	600	120	4.7	424	0.0025	1.82E+06	0.00182	350	170	0.339	0.035	0.046719
16	60	50	50	600	120	5	502	0.0025	1.98E+06	0.00198	355	175	0.417	0.035	0.027288

Sand

Table 12-3 Measured volume of sand flushed. (H_s=140 mm)

Test	a ₀ , [mm]	a, [mm]	b, [mm]	B, [mm]	H _s , [mm]	Q, [lps]	H _w , [mm]	A _{outlet}	Volume of cone [mm ³]	Volume of cone [m ³]	Width of cone [mm]	Length of cone [mm]	H _{w net} [m]	H _{s net} [m]	V _s /H _{w net} ³
1	60	20	50	600	140	1.3	267	0.001	1.13E+06	0.00113	290	130	0.197	0.07	0.147763
2	60	20	50	600	140	1.7	373	0.001	1.22E+06	0.00122	300	140	0.303	0.07	0.04391
3	60	20	50	600	140	2	523	0.001	1.41E+06	0.00141	300	150	0.453	0.07	0.015182
4	60	20	50	600	140	1.8	453	0.001	1.29E+06	0.00129	300	140	0.383	0.07	0.02297
5	60	30	50	600	140	1.8	244	0.0015	1.35E+06	0.00135	300	140	0.169	0.065	0.278963
6	60	30	50	600	140	2.2	326	0.0015	1.63E+06	0.00163	310	150	0.251	0.065	0.10328
7	60	30	50	600	140	2.6	414	0.0015	1.67E+06	0.00167	320	150	0.339	0.065	0.042931
8	60	30	50	600	140	3	518	0.0015	1.79E+06	0.00179	330	160	0.443	0.065	0.020634
9	60	40	50	600	140	2.5	244	0.002	1.70E+06	0.00170	330	155	0.164	0.06	0.384521
10	60	40	50	600	140	3.2	352	0.002	1.95E+06	0.00195	330	160	0.274	0.06	0.094984
11	60	40	50	600	140	3.9	455	0.002	2.04E+06	0.00204	330	165	0.375	0.06	0.038609
12	60	40	50	600	140	4.3	570	0.002	2.16E+06	0.00216	340	165	0.49	0.06	0.0184
13	60	50	50	600	140	3.2	264	0.0025	1.94E+06	0.00194	330	160	0.179	0.055	0.339004
14	60	50	50	600	140	3.8	327	0.0025	2.03E+06	0.00203	360	165	0.242	0.055	0.14351
15	60	50	50	600	140	4.7	424	0.0025	2.23E+06	0.00223	360	170	0.339	0.055	0.057231
16	60	50	50	600	140	5	502	0.0025	2.34E+06	0.00234	360	180	0.417	0.055	0.032215

Table 12-4 Measured volume of sand flushed. (H_s=120 mm)

Test	a ₀ , [mm]	a, [mm]	b, [mm]	B, [mm]	H _s , [mm]	Q, [lps]	H _w , [mm]	A _{outlet}	Volume of cone [mm ³]	Volume of cone [m ³]	Width of cone [mm]	Length of cone [mm]	H _{w net} [m]	H _{s net} [m]	V _s /H _{w net} ³
1	60	20	50	600	120	1.3	267	0.001	7.89E+05	0.00079	260	125	0.197	0.05	0.103154
2	60	20	50	600	120	1.7	373	0.001	8.67E+05	0.00087	270	135	0.303	0.05	0.031169
3	60	20	50	600	120	2	523	0.001	1.12E+06	0.00112	300	140	0.453	0.05	0.012018
4	60	20	50	600	120	1.8	453	0.001	9.76E+05	0.00098	285	135	0.383	0.05	0.017381
5	60	30	50	600	120	1.8	244	0.0015	8.86E+05	0.00089	295	120	0.169	0.045	0.18366
6	60	30	50	600	120	2.2	326	0.0015	1.07E+06	0.00107	295	140	0.251	0.045	0.067412
7	60	30	50	600	120	2.6	414	0.0015	1.11E+06	0.00111	300	140	0.339	0.045	0.028392
8	60	30	50	600	120	3	518	0.0015	1.24E+06	0.00124	300	145	0.443	0.045	0.014304
9	60	40	50	600	120	2.5	244	0.002	1.07E+06	0.00107	270	135	0.164	0.04	0.243304
10	60	40	50	600	120	3.2	352	0.002	1.20E+06	0.00120	300	140	0.274	0.04	0.058218
11	60	40	50	600	120	3.9	455	0.002	1.28E+06	0.00128	300	140	0.375	0.04	0.024244
12	60	40	50	600	120	4.3	570	0.002	1.44E+06	0.00144	300	145	0.49	0.04	0.012228
13	60	50	50	600	120	3.2	264	0.0025	1.18E+06	0.00118	300	140	0.179	0.035	0.205254
14	60	50	50	600	120	3.8	327	0.0025	1.29E+06	0.00129	300	140	0.242	0.035	0.091184
15	60	50	50	600	120	4.7	424	0.0025	1.41E+06	0.00141	310	145	0.339	0.035	0.036313
16	60	50	50	600	120	5	502	0.0025	1.50E+06	0.00150	315	150	0.417	0.035	0.020642

Yellow Lightweight Material

Table 12-5 Measured volume of YLWM flushed. (Hs=140 mm)

Test	a ₀ , [mm]	a, [mm]	b, [mm]	B, [mm]	H _s , [mm]	Q, [lps]	H _w , [mm]	A _{outlet}	Volume of cone [mm ³]	Volume of cone [m ³]	Width of cone [mm]	Length of cone [mm]	H _{w net} [m]	H _{s net} [m]	V _s /H _{wnet} ³
1	60	20	50	600	140	1.3	267	0.001	2.90E+06	0.00290	44	22	0.197	0.07	0.376044
2	60	20	50	600	140	1.7	373	0.001	3.50E+06	0.00350	43	22	0.303	0.07	0.108634
3	60	20	50	600	140	2	523	0.001	3.37E+06	0.00337	43	23	0.453	0.07	0.037457
4	60	20	50	600	140	1.8	453	0.001	3.42E+06	0.00342	44	23.5	0.383	0.07	0.059806
5	60	30	50	600	140	1.8	244	0.0015	3.62E+06	0.00362	44.5	23	0.169	0.065	0.69114
6	60	30	50	600	140	2.2	326	0.0015	3.61E+06	0.00361	45	23	0.251	0.065	0.235625
7	60	30	50	600	140	2.6	414	0.0015	4.28E+06	0.00428	45	25	0.339	0.065	0.105626
8	60	30	50	600	140	3	518	0.0015	4.85E+06	0.00485	48	26.5	0.443	0.065	0.052002
9	60	40	50	600	140	2.5	244	0.002	4.83E+06	0.00483	49	23.5	0.164	0.06	0.954671
10	60	40	50	600	140	3.2	352	0.002	5.37E+06	0.00537	50	25	0.274	0.06	0.236354
11	60	40	50	600	140	3.9	455	0.002	5.37E+06	0.00537	52	27	0.375	0.06	0.101945
12	60	40	50	600	140	4.3	570	0.002	6.85E+06	0.00685	56	28	0.49	0.06	0.053481
13	60	50	50	600	140	3.2	264	0.0025	5.81E+06	0.00581	53	25.5	0.179	0.055	0.915726
14	60	50	50	600	140	3.8	327	0.0025	5.80E+06	0.00580	54	25.5	0.242	0.055	0.411995
15	60	50	50	600	140	4.7	424	0.0025	6.74E+06	0.00674	56	27	0.339	0.055	0.170131
16	60	50	50	600	140	5	502	0.0025	7.35E+06	0.00735	56	28.5	0.417	0.055	0.093295

Table 12-6 Measured volume of YLWM flushed. (Hs=120 mm)

Test	a ₀ , [mm]	a, [mm]	b, [mm]	B, [mm]	H _s , [mm]	Q, [lps]	H _w , [mm]	A _{outlet}	Volume of cone [mm ³]	Volume of cone [m ³]	Width of cone [mm]	Length of cone [mm]	H _{w net} [m]	H _{s net} [m]	V _s /H _{wnet} ³
1	60	20	50	600	120	1.3	267	0.001	1.55E+06	0.00155	36	18	0.197	0.05	0.202214
2	60	20	50	600	120	1.7	373	0.001	1.88E+06	0.00188	38	20	0.303	0.05	0.067438
3	60	20	50	600	120	2	523	0.001	2.29E+06	0.00229	38	20	0.453	0.05	0.024645
4	60	20	50	600	120	1.8	453	0.001	2.13E+06	0.00213	38	20	0.383	0.05	0.037841
5	60	30	50	600	120	1.8	244	0.0015	2.19E+06	0.00219	40.5	19.5	0.169	0.045	0.45413
6	60	30	50	600	120	2.2	326	0.0015	2.49E+06	0.00249	43	21	0.251	0.045	0.157716
7	60	30	50	600	120	2.6	414	0.0015	2.93E+06	0.00293	43	23	0.339	0.045	0.07526
8	60	30	50	600	120	3	518	0.0015	3.22E+06	0.00322	45	23	0.443	0.045	0.037061
9	60	40	50	600	120	2.5	244	0.002	2.69E+06	0.00269	44	20.5	0.164	0.04	0.609393
10	60	40	50	600	120	3.2	352	0.002	3.18E+06	0.00318	44	21	0.274	0.04	0.154782
11	60	40	50	600	120	3.9	455	0.002	3.73E+06	0.00373	46.5	24.5	0.375	0.04	0.070751
12	60	40	50	600	120	4.3	570	0.002	4.25E+06	0.00425	51	25	0.49	0.04	0.036133
13	60	50	50	600	120	3.2	264	0.0025	3.49E+06	0.00349	49	23	0.179	0.035	0.607636
14	60	50	50	600	120	3.8	327	0.0025	3.95E+06	0.00395	48	23	0.242	0.035	0.278991
15	60	50	50	600	120	4.7	424	0.0025	4.57E+06	0.00457	52.5	24	0.339	0.035	0.117331
16	60	50	50	600	120	5	502	0.0025	4.77E+06	0.00477	53.5	24	0.417	0.035	0.065782

13 Appendix C Calculation and comparison of Parameter $\frac{V_s}{H_{w net}^3}$ with M. E. Meshkati (2010) equation & new empirical relation.

Blue Lightweight Material

Table 13-1 Comparison and computation of BLWM (Hs = 140 mm).

Test	a ₀ , [mm]	a, [mm]	b, [mm]	H _s , [mm]	d _s , [mm]	Q, [lps]	H _w , [mm]	h _s , [mm]	H _{snet} , [m]	H _{snet} , [m]	H _{wnet} , [mm]	H _{wnet} , [m]	V _s , [m ³]	Q, [m ³ /s]	u _{out} , [m/s]
1	60	20	50	140	4	1.30	267	80	70	0.070	197	0.197	0.0013	0.0013	1.300
2	60	20	50	140	4	1.70	373	80	70	0.070	303	0.303	0.0016	0.0017	1.700
3	60	20	50	140	4	2.00	523	80	70	0.070	453	0.453	0.0016	0.002	2.000
4	60	20	50	140	4	1.80	453	80	70	0.070	383	0.383	0.0017	0.0018	1.800
5	60	30	50	140	4	1.80	244	80	65	0.065	169	0.169	0.0016	0.0018	1.200
6	60	30	50	140	4	2.20	326	80	65	0.065	251	0.251	0.0019	0.0022	1.467
7	60	30	50	140	4	2.60	414	80	65	0.065	339	0.339	0.0022	0.0026	1.733
8	60	30	50	140	4	3.00	518	80	65	0.065	443	0.443	0.0024	0.003	2.000
9	60	40	50	140	4	2.50	244	80	60	0.060	164	0.164	0.0018	0.0025	1.250
10	60	40	50	140	4	3.20	352	80	60	0.060	272	0.272	0.0023	0.0032	1.600
11	60	40	50	140	4	3.90	455	80	60	0.060	375	0.375	0.0025	0.0039	1.950
12	60	40	50	140	4	4.30	570	80	60	0.060	490	0.49	0.0029	0.0043	2.150
13	60	50	50	140	4	3.20	264	80	55	0.055	179	0.179	0.0021	0.0032	1.280
14	60	50	50	140	4	3.80	327	80	55	0.055	242	0.242	0.0026	0.0038	1.520
15	60	50	50	140	4	4.47	424	80	55	0.055	339	0.339	0.0027	0.004474	1.790
16	60	50	50	140	4	5.02	502	80	55	0.055	417	0.417	0.0030	0.005019	2.008

Fr = u_{out} / (Sqrt(g(G_s-1)d₅₀)))

**EMP = (A / (H_{wnet})²) * (H_s / H_{wnet}) * ((5.82207907097161 * Fr)¹³ * 0.060915993091)^{0.0509040671365669}

Gs	Gs-1	A _{out}	D	D / (H _{wnet})	H _{snet} / H _{wnet}	*Fr	V _s / H _{wnet} ³		A / (H _{wnet})	A / (H _{wnet}) ²	**EMP
							Calculated	Measured			
1.4	0.4	0.001	0.0357	0.1811	0.3553	10.3765	0.1687	0.1642	0.0051	0.0258	0.1384
1.4	0.4	0.001	0.0357	0.1178	0.2310	13.5692	0.0472	0.0569	0.0033	0.0109	0.0454
1.4	0.4	0.001	0.0357	0.0788	0.1545	15.9638	0.0141	0.0174	0.0022	0.0049	0.0151
1.4	0.4	0.001	0.0357	0.0932	0.1828	14.3674	0.0232	0.0305	0.0026	0.0068	0.0234
1.4	0.4	0.0015	0.0437	0.2586	0.3846	9.5783	0.2711	0.3309	0.0089	0.0525	0.2896
1.4	0.4	0.0015	0.0437	0.1741	0.2590	11.7068	0.0833	0.1212	0.0060	0.0238	0.1010
1.4	0.4	0.0015	0.0437	0.1289	0.1917	13.8353	0.0341	0.0558	0.0044	0.0131	0.0458
1.4	0.4	0.0015	0.0437	0.0986	0.1467	15.9638	0.0154	0.0280	0.0034	0.0076	0.0226
1.4	0.4	0.002	0.0505	0.3077	0.3659	9.9774	0.2859	0.4027	0.0122	0.0744	0.4007
1.4	0.4	0.002	0.0505	0.1855	0.2206	12.7710	0.0631	0.1119	0.0074	0.0270	0.1034
1.4	0.4	0.002	0.0505	0.1346	0.1600	15.5647	0.0244	0.0469	0.0053	0.0142	0.0450
1.4	0.4	0.002	0.0505	0.1030	0.1224	17.1611	0.0109	0.0244	0.0041	0.0083	0.0215
1.4	0.4	0.0025	0.0564	0.3152	0.3073	10.2168	0.2000	0.3586	0.0140	0.0780	0.3587
1.4	0.4	0.0025	0.0564	0.2331	0.2273	12.1325	0.0817	0.1826	0.0103	0.0427	0.1627
1.4	0.4	0.0025	0.0564	0.1664	0.1622	14.2844	0.0298	0.0705	0.0074	0.0218	0.0659
1.4	0.4	0.0025	0.0564	0.1353	0.1319	16.0244	0.0161	0.0419	0.0060	0.0144	0.0382

Calculated V_s / H_{wnet}³ = 4.6 (Fr)^{0.21} (H_{snet} / H_{wnet})^{2.2} (D / (H_{wnet}))^{0.89}

Table 13-2 Comparison and computation of BLWM (Hs = 120 mm).

Test	a ₀ , [mm]	a, [mm]	b, [mm]	H _s , [mm]	d _s , [mm]	Q, [lps]	H _w , [mm]	h _s , [mm]	H _{snet} , [m]	H _{snet} , [m]	H _{wnet} , [mm]	H _{wnet} , [m]	V _s , [m ³]	Q, [m ³ /s]	u _{out} , [m/s]
1	60	20	50	120	4	1.30	267	60	50	0.050	197	0.197	0.0008	0.0013	1.300
2	60	20	50	120	4	1.70	373	60	50	0.050	303	0.303	0.0010	0.0017	1.700
3	60	20	50	120	4	2.00	523	60	50	0.050	453	0.453	0.0011	0.002	2.000
4	60	20	50	120	4	1.80	453	60	50	0.050	383	0.383	0.0011	0.0018	1.800
5	60	30	50	120	4	1.80	244	60	45	0.045	169	0.169	0.0011	0.0018	1.200
6	60	30	50	120	4	2.20	326	60	45	0.045	251	0.251	0.0013	0.0022	1.467
7	60	30	50	120	4	2.60	414	60	45	0.045	339	0.339	0.0013	0.0026	1.733
8	60	30	50	120	4	3.00	518	60	45	0.045	443	0.443	0.0015	0.003	2.000
9	60	40	50	120	4	2.50	244	60	40	0.040	164	0.164	0.0013	0.0025	1.250
10	60	40	50	120	4	3.20	352	60	40	0.040	272	0.272	0.0015	0.0032	1.600
11	60	40	50	120	4	3.90	455	60	40	0.040	375	0.375	0.0017	0.0039	1.950
12	60	40	50	120	4	4.30	570	60	40	0.040	490	0.49	0.0018	0.0043	2.150
13	60	50	50	120	4	3.20	264	60	35	0.035	179	0.179	0.0015	0.0032	1.280
14	60	50	50	120	4	3.80	327	60	35	0.035	242	0.242	0.0016	0.0038	1.520
15	60	50	50	120	4	4.47	424	60	35	0.035	339	0.339	0.0018	0.004474	1.790
16	60	50	50	120	4	5.02	502	60	35	0.035	417	0.417	0.0020	0.005019	2.008

Fr = u_{out} / (Sqrt(g(G_s-1)d₅₀))) **EMP = (A/(H_{wnet})²)*(H_s/H_{wnet})*((5.82207907097161*fr)¹³.0060915993091)⁰.0509040671365669

G _s	G _s -1	A _{out}	D	D/(H _{wnet})	H _{snet} /H _{wnet}	*Fr	V _s /H ³ _{wnet}		A/(H _{wnet})	A/(H _{wnet}) ²	**EMP
							Calculated	Measured			
1.4	0.4	0.001	0.0357	0.1811	0.2538	10.3765	0.0805	0.1081	0.0051	0.0258	0.0989
1.4	0.4	0.001	0.0357	0.1178	0.1650	13.5692	0.0225	0.0360	0.0033	0.0109	0.0325
1.4	0.4	0.001	0.0357	0.0788	0.1104	15.9638	0.0067	0.0121	0.0022	0.0049	0.0108
1.4	0.4	0.001	0.0357	0.0932	0.1305	14.3674	0.0110	0.0199	0.0026	0.0068	0.0167
1.4	0.4	0.0015	0.0437	0.2586	0.2663	9.5783	0.1207	0.2234	0.0089	0.0525	0.2005
1.4	0.4	0.0015	0.0437	0.1741	0.1793	11.7068	0.0371	0.0805	0.0060	0.0238	0.0699
1.4	0.4	0.0015	0.0437	0.1289	0.1327	13.8353	0.0152	0.0337	0.0044	0.0131	0.0317
1.4	0.4	0.0015	0.0437	0.0986	0.1016	15.9638	0.0068	0.0170	0.0034	0.0076	0.0156
1.4	0.4	0.002	0.0505	0.3077	0.2439	9.9774	0.1172	0.2963	0.0122	0.0744	0.2671
1.4	0.4	0.002	0.0505	0.1855	0.1471	12.7710	0.0258	0.0765	0.0074	0.0270	0.0690
1.4	0.4	0.002	0.0505	0.1346	0.1067	15.5647	0.0100	0.0326	0.0053	0.0142	0.0300
1.4	0.4	0.002	0.0505	0.1030	0.0816	17.1611	0.0045	0.0153	0.0041	0.0083	0.0143
1.4	0.4	0.0025	0.0564	0.3152	0.1955	10.2168	0.0740	0.2584	0.0140	0.0780	0.2283
1.4	0.4	0.0025	0.0564	0.2331	0.1446	12.1325	0.0302	0.1153	0.0103	0.0427	0.1035
1.4	0.4	0.0025	0.0564	0.1664	0.1032	14.2844	0.0110	0.0467	0.0074	0.0218	0.0420
1.4	0.4	0.0025	0.0564	0.1353	0.0839	16.0244	0.0060	0.0273	0.0060	0.0144	0.0243

Calculated V_s/H³_{wnet} = 4.6 (Fr)^{0.21}(H_{snet}/H_{wnet})^{2.2}(D/(H_{wnet}))^{0.89}

Sand

Table 13-3 Comparison and computation of Sand (Hs = 140 mm).

Test	a ₀ , [mm]	a, [mm]	b, [mm]	H _s , [mm]	d _s , [mm]	Q, [lps]	H _w , [mm]	h _s , [mm]	H _{snet} , [m]	H _{snet} , [m]	H _{wnet} , [mm]	H _{wnet} , [m]	V _s , [m ³]	Q, [m ³ /s]	u _{out} , [m/s]
1	60	20	50	140	1	1.30	267	80	70	0.070	197	0.197	0.0011	0.0013	1.300
2	60	20	50	140	1	1.70	373	80	70	0.070	303	0.303	0.0012	0.0017	1.700
3	60	20	50	140	1	2.00	523	80	70	0.070	453	0.453	0.0014	0.002	2.000
4	60	20	50	140	1	1.80	453	80	70	0.070	383	0.383	0.0013	0.0018	1.800
5	60	30	50	140	1	1.80	244	80	65	0.065	169	0.169	0.0013	0.0018	1.200
6	60	30	50	140	1	2.20	326	80	65	0.065	251	0.251	0.0016	0.0022	1.467
7	60	30	50	140	1	2.60	414	80	65	0.065	339	0.339	0.0017	0.0026	1.733
8	60	30	50	140	1	3.00	518	80	65	0.065	443	0.443	0.0018	0.003	2.000
9	60	40	50	140	1	2.50	244	80	60	0.060	164	0.164	0.0017	0.0025	1.250
10	60	40	50	140	1	3.20	352	80	60	0.060	272	0.272	0.0020	0.0032	1.600
11	60	40	50	140	1	3.90	455	80	60	0.060	375	0.375	0.0020	0.0039	1.950
12	60	40	50	140	1	4.30	570	80	60	0.060	490	0.49	0.0022	0.0043	2.150
13	60	50	50	140	1	3.20	264	80	55	0.055	179	0.179	0.0019	0.0032	1.280
14	60	50	50	140	1	3.80	327	80	55	0.055	242	0.242	0.0020	0.0038	1.520
15	60	50	50	140	1	4.47	424	80	55	0.055	339	0.339	0.0022	0.004474	1.790
16	60	50	50	140	1	5.02	502	80	55	0.055	417	0.417	0.0023	0.005019	2.008
Fr = u _{out} / (Sqrt (g (G _s - 1) d ₅₀)))						**EMP = (A / (H _{wnet}) ²) * (H _s / H _{wnet}) * ((5.82207907097161 * fr) ¹³ * 0.060915993091) ^{0.0509040671365669}									

Gs	Gs -1	A _{out}	D	D / (H _{w net})	H _{snet} / H _{w net}	*Fr	V _s / H _{w net} ³		A / (H _{w net})	A / (H _{w net}) ²	**EMP
							Calculated	Measured			
2.65	1.65	0.001	0.0357	0.1811	0.3553	10.2180	0.1682	0.1478	0.0051	0.0258	0.1370
2.65	1.65	0.001	0.0357	0.1178	0.2310	13.3620	0.0470	0.0439	0.0033	0.0109	0.0450
2.65	1.65	0.001	0.0357	0.0788	0.1545	15.7200	0.0140	0.0152	0.0022	0.0049	0.0150
2.65	1.65	0.001	0.0357	0.0932	0.1828	14.1480	0.0231	0.0230	0.0026	0.0068	0.0231
2.65	1.65	0.0015	0.0437	0.2586	0.3846	9.4320	0.2702	0.2790	0.0089	0.0525	0.2867
2.65	1.65	0.0015	0.0437	0.1741	0.2590	11.5280	0.0830	0.1033	0.0060	0.0238	0.0999
2.65	1.65	0.0015	0.0437	0.1289	0.1917	13.6240	0.0340	0.0429	0.0044	0.0131	0.0453
2.65	1.65	0.0015	0.0437	0.0986	0.1467	15.7200	0.0153	0.0206	0.0034	0.0076	0.0223
2.65	1.65	0.002	0.0505	0.3077	0.3659	9.8250	0.2850	0.3845	0.0122	0.0744	0.3967
2.65	1.65	0.002	0.0505	0.1855	0.2206	12.5760	0.0629	0.0971	0.0074	0.0270	0.1024
2.65	1.65	0.002	0.0505	0.1346	0.1600	15.3270	0.0243	0.0386	0.0053	0.0142	0.0445
2.65	1.65	0.002	0.0505	0.1030	0.1224	16.8990	0.0109	0.0184	0.0041	0.0083	0.0213
2.65	1.65	0.0025	0.0564	0.3152	0.3073	10.0608	0.1993	0.3390	0.0140	0.0780	0.3551
2.65	1.65	0.0025	0.0564	0.2331	0.2273	11.9472	0.0814	0.1435	0.0103	0.0427	0.1610
2.65	1.65	0.0025	0.0564	0.1664	0.1622	14.0663	0.0297	0.0572	0.0074	0.0218	0.0653
2.65	1.65	0.0025	0.0564	0.1353	0.1319	15.7798	0.0161	0.0322	0.0060	0.0144	0.0378
Calculated V _s / H _{w net} ³ = 4.6 (Fr) ^{0.21} (H _{snet} / H _{w net}) ^{2.2} (D / (H _{w net})) ^{0.89}											

Table 13-4 Comparison and computation of Sand (H_s = 120 mm).

Test	a ₀ , [mm]	a, [mm]	b, [mm]	H _s , [mm]	d _s , [mm]	Q, [lps]	H _w , [mm]	h _s , [mm]	H _{snet} , [m]	H _{snet} , [m]	H _{wnet} , [mm]	H _{wnet} , [m]	V _s , [m ³]	Q, [m ³ /s]	u _{out} , [m/s]
1	60	20	50	120	1	1.30	267	60	50	0.050	197	0.197	0.0008	0.0013	1.300
2	60	20	50	120	1	1.70	373	60	50	0.050	303	0.303	0.0009	0.0017	1.700
3	60	20	50	120	1	2.00	523	60	50	0.050	453	0.453	0.0011	0.002	2.000
4	60	20	50	120	1	1.80	453	60	50	0.050	383	0.383	0.0010	0.0018	1.800
5	60	30	50	120	1	1.80	244	60	45	0.045	169	0.169	0.0009	0.0018	1.200
6	60	30	50	120	1	2.20	326	60	45	0.045	251	0.251	0.0011	0.0022	1.467
7	60	30	50	120	1	2.60	414	60	45	0.045	339	0.339	0.0011	0.0026	1.733
8	60	30	50	120	1	3.00	518	60	45	0.045	443	0.443	0.0012	0.003	2.000
9	60	40	50	120	1	2.50	244	60	40	0.040	164	0.164	0.0011	0.0025	1.250
10	60	40	50	120	1	3.20	352	60	40	0.040	272	0.272	0.0012	0.0032	1.600
11	60	40	50	120	1	3.90	455	60	40	0.040	375	0.375	0.0013	0.0039	1.950
12	60	40	50	120	1	4.30	570	60	40	0.040	490	0.49	0.0014	0.0043	2.150
13	60	50	50	120	1	3.20	264	60	35	0.035	179	0.179	0.0012	0.0032	1.280
14	60	50	50	120	1	3.80	327	60	35	0.035	242	0.242	0.0013	0.0038	1.520
15	60	50	50	120	1	4.47	424	60	35	0.035	339	0.339	0.0014	0.004474	1.790
16	60	50	50	120	1	5.02	502	60	35	0.035	417	0.417	0.0015	0.005019	2.008

Fr = u_{out} / (sqrt(g(G_s-1)d₅₀)))

**EMP = (A/(H_{wnet})^2) * (H_s/H_{wnet}) * ((5.82207907097161*fr)^13.0060915993091)^0.0509040671365669

G _s	G _s -1	A _{out}	D	D/(H _{wnet})	H _{snet} /H _{wnet}	*Fr	V _s /H ³ _{wnet}		A/(H _{wnet})	A/(H _{wnet}) ²	**EMP
							Calculated	Measured			
2.65	1.65	0.001	0.0357	0.1811	0.2538	10.2180	0.0802	0.1032	0.0051	0.0258	0.0979
2.65	0.896075	0.001	0.0357	0.1178	0.1650	18.1319	0.0239	0.0312	0.0033	0.0109	0.0393
2.65	1.09565	0.001	0.0357	0.0788	0.1104	19.2912	0.0070	0.0120	0.0022	0.0049	0.0123
2.65	1.007447	0.001	0.0357	0.0932	0.1305	18.1062	0.0116	0.0174	0.0026	0.0068	0.0195
2.65	0.669216	0.0015	0.0437	0.2586	0.2663	14.8103	0.1323	0.1837	0.0089	0.0525	0.2676
2.65	0.815567	0.0015	0.0437	0.1741	0.1793	16.3971	0.0398	0.0674	0.0060	0.0238	0.0874
2.65	0.947813	0.0015	0.0437	0.1289	0.1327	17.9757	0.0160	0.0284	0.0044	0.0131	0.0377
2.65	1.08349	0.0015	0.0437	0.0986	0.1016	19.3992	0.0071	0.0143	0.0034	0.0076	0.0178
2.65	0.659242	0.002	0.0505	0.3077	0.2439	15.5437	0.1286	0.2433	0.0122	0.0744	0.3583
2.65	0.848999	0.002	0.0505	0.1855	0.1471	17.5320	0.0276	0.0595	0.0074	0.0270	0.0851
2.65	0.99687	0.002	0.0505	0.1346	0.1067	19.7188	0.0105	0.0242	0.0053	0.0142	0.0351
2.65	1.139517	0.002	0.0505	0.1030	0.0816	20.3350	0.0046	0.0122	0.0041	0.0083	0.0160
2.65	0.688731	0.0025	0.0564	0.3152	0.1955	15.5722	0.0808	0.2053	0.0140	0.0780	0.3018
2.65	0.800812	0.0025	0.0564	0.2331	0.1446	17.1492	0.0325	0.0912	0.0103	0.0427	0.1302
2.65	0.947813	0.0025	0.0564	0.1664	0.1032	18.5592	0.0117	0.0363	0.0074	0.0218	0.0499
2.65	1.051214	0.0025	0.0564	0.1353	0.0839	19.7696	0.0062	0.0206	0.0060	0.0144	0.0280
Calculated V _s /H ³ _{wnet} = 4.6 (Fr) ^{0.21} (H _{snet} /H _{wnet}) ^{2.2} (D/(H _{wnet})) ^{0.89}											

Yellow Lightweight Material

Table 13-5 Comparison and computation of YLWM (H_s = 140mm)

Test	a ₀ , [mm]	a, [mm]	b, [mm]	H _s , [mm]	d _s , [mm]	Q, [lps]	H _w , [mm]	h _s , [mm]	H _{snet} , [m]	H _{snet} , [m]	H _{wnet} , [mm]	H _{wnet} , [m]	V _s , [m ³]	Q _r , [m ³ /s]	u _{out} , [m/s]
1	60	20	50	140	2	1.30	267	80	70	0.070	197	0.197	0.0029	0.0013	1.300
2	60	20	50	140	2	1.70	373	80	70	0.070	303	0.303	0.0030	0.0017	1.700
3	60	20	50	140	2	2.00	523	80	70	0.070	453	0.453	0.0035	0.002	2.000
4	60	20	50	140	2	1.80	453	80	70	0.070	383	0.383	0.0034	0.0018	1.800
5	60	30	50	140	2	1.80	244	80	65	0.065	169	0.169	0.0033	0.0018	1.200
6	60	30	50	140	2	2.20	326	80	65	0.065	251	0.251	0.0037	0.0022	1.467
7	60	30	50	140	2	2.60	414	80	65	0.065	339	0.339	0.0041	0.0026	1.733
8	60	30	50	140	2	3.00	518	80	65	0.065	443	0.443	0.0045	0.003	2.000
9	60	40	50	140	2	2.50	244	80	60	0.060	164	0.164	0.0042	0.0025	1.250
10	60	40	50	140	2	3.20	352	80	60	0.060	272	0.272	0.0049	0.0032	1.600
11	60	40	50	140	2	3.90	455	80	60	0.060	375	0.375	0.0054	0.0039	1.950
12	60	40	50	140	2	4.30	570	80	60	0.060	490	0.49	0.0063	0.0043	2.150
13	60	50	50	140	2	3.20	264	80	55	0.055	179	0.179	0.0053	0.0032	1.280
14	60	50	50	140	2	3.80	327	80	55	0.055	242	0.242	0.0058	0.0038	1.520
15	60	50	50	140	2	4.47	424	80	55	0.055	339	0.339	0.0066	0.004474	1.790
16	60	50	50	140	2	5.02	502	80	55	0.055	417	0.417	0.0068	0.005019	2.008

Fr = u_{out} / (Sqrt (g (G_s -1) d₅₀))) **EMP= (A/(H_{wnet})^2)*(H_s/H_{wnet})*((5.82207907097161*fr)^13.0060915993091)^0.0509040671365669

Gs	Gs -1	A _{out}	D	D/(H _{w net})	H _{snet} /H _{w net}	*Fr	V _s /H ³ _{w net}		A/(H _{w net})	A/(H _{w net})^2	**EMP
							Calculated	Measured			
1.058	0.058	0.001	0.0357	0.1811	0.3553	38.5372	0.2222	0.3760	0.0051	0.0258	0.3300
1.058	0.058	0.001	0.0357	0.1178	0.2310	50.3948	0.0622	0.1086	0.0033	0.0109	0.1083
1.058	0.058	0.001	0.0357	0.0788	0.1545	59.2880	0.0186	0.0375	0.0022	0.0049	0.0361
1.058	0.058	0.001	0.0357	0.0932	0.1828	53.3592	0.0305	0.0598	0.0026	0.0068	0.0557
1.058	0.058	0.0015	0.0437	0.2586	0.3846	35.5728	0.3571	0.6911	0.0089	0.0525	0.6905
1.058	0.058	0.0015	0.0437	0.1741	0.2590	43.4778	0.1097	0.2356	0.0060	0.0238	0.2407
1.058	0.058	0.0015	0.0437	0.1289	0.1917	51.3829	0.0449	0.1056	0.0044	0.0131	0.1091
1.058	0.058	0.0015	0.0437	0.0986	0.1467	59.2880	0.0202	0.0520	0.0034	0.0076	0.0538
1.058	0.058	0.002	0.0505	0.3077	0.3659	37.0550	0.3766	0.9547	0.0122	0.0744	0.9554
1.058	0.058	0.002	0.0505	0.1855	0.2206	47.4304	0.0831	0.2416	0.0074	0.0270	0.2466
1.058	0.058	0.002	0.0505	0.1346	0.1600	57.8058	0.0321	0.1019	0.0053	0.0142	0.1073
1.058	0.058	0.002	0.0505	0.1030	0.1224	63.7346	0.0143	0.0535	0.0041	0.0083	0.0513
1.058	0.058	0.0025	0.0564	0.3152	0.3073	37.9443	0.2634	0.9157	0.0140	0.0780	0.8553
1.058	0.058	0.0025	0.0564	0.2331	0.2273	45.0588	0.1076	0.4120	0.0103	0.0427	0.3878
1.058	0.058	0.0025	0.0564	0.1664	0.1622	53.0509	0.0393	0.1701	0.0074	0.0218	0.1572
1.058	0.058	0.0025	0.0564	0.1353	0.1319	59.5133	0.0212	0.0933	0.0060	0.0144	0.0911

Calculated V_s /H³_{w net} = 4.6 (Fr)^{0.21} (H_{snet}/H_{w net})^{2.2} (D/(H_{w net}))^{0.89}

Table 13-6 Comparison and computation of YLWM (H_s = 120mm)

Test	a ₀ , [mm]	a, [mm]	b, [mm]	H _s , [mm]	d _s , [mm]	Q, [lps]	H _w , [mm]	h _s , [mm]	H _{snet} , [m]	H _{snet} , [m]	H _{wnet} , [mm]	H _{wnet} , [m]	V _s , [m ³]	Q, [m ³ /s]	u _{out} , [m/s]
1	60	20	50	120	2	1.30	267	60	50	0.050	197	0.197	0.0015	0.0013	1.300
2	60	20	50	120	2	1.70	373	60	50	0.050	303	0.303	0.0019	0.0017	1.700
3	60	20	50	120	2	2.00	523	60	50	0.050	453	0.453	0.0023	0.002	2.000
4	60	20	50	120	2	1.80	453	60	50	0.050	383	0.383	0.0021	0.0018	1.800
5	60	30	50	120	2	1.80	244	60	45	0.045	169	0.169	0.0022	0.0018	1.200
6	60	30	50	120	2	2.20	326	60	45	0.045	251	0.251	0.0025	0.0022	1.467
7	60	30	50	120	2	2.60	414	60	45	0.045	339	0.339	0.0029	0.0026	1.733
8	60	30	50	120	2	3.00	518	60	45	0.045	443	0.443	0.0032	0.003	2.000
9	60	40	50	120	2	2.50	244	60	40	0.040	164	0.164	0.0027	0.0025	1.250
10	60	40	50	120	2	3.20	352	60	40	0.040	272	0.272	0.0032	0.0032	1.600
11	60	40	50	120	2	3.90	455	60	40	0.040	375	0.375	0.0037	0.0039	1.950
12	60	40	50	120	2	4.30	570	60	40	0.040	490	0.49	0.0043	0.0043	2.150
13	60	50	50	120	2	3.20	264	60	35	0.035	179	0.179	0.0035	0.0032	1.280
14	60	50	50	120	2	3.80	327	60	35	0.035	242	0.242	0.0040	0.0038	1.520
15	60	50	50	120	2	4.47	424	60	35	0.035	339	0.339	0.0046	0.004474	1.790
16	60	50	50	120	2	5.02	502	60	35	0.035	417	0.417	0.0048	0.005019	2.008

Fr = u_{out} / (sqrt(g(G_s-1)d₅₀)))

**EMP = (A/(H_{wnet})^2) * (H_s/H_{wnet}) * ((5.82207907097161*fr)^13.0060915993091)^0.0509040671365669

Gs	Gs-1	A _{out}	D	D/(H _w _{net})	H _{snet} /H _{wnet}	*Fr	V _s /H ³ _{wnet}		A/(H _w _{net})	A/(H _w _{net})^2	**EMP
							Calculated	Measured			
1.058	0.058	0.001	0.0357	0.1811	0.2538	38.5372	0.1060	0.2022	0.0051	0.0258	0.0979
1.058	0.058	0.001	0.0357	0.1178	0.1650	50.3948	0.0296	0.0674	0.0033	0.0109	0.0393
1.058	0.058	0.001	0.0357	0.0788	0.1104	59.2880	0.0089	0.0246	0.0022	0.0049	0.0123
1.058	0.058	0.001	0.0357	0.0932	0.1305	53.3592	0.0145	0.0378	0.0026	0.0068	0.0195
1.058	0.058	0.0015	0.0437	0.2586	0.2663	35.5728	0.1590	0.4541	0.0089	0.0525	0.2676
1.058	0.058	0.0015	0.0437	0.1741	0.1793	43.4778	0.0489	0.1577	0.0060	0.0238	0.0874
1.058	0.058	0.0015	0.0437	0.1289	0.1327	51.3829	0.0200	0.0753	0.0044	0.0131	0.0377
1.058	0.058	0.0015	0.0437	0.0986	0.1016	59.2880	0.0090	0.0371	0.0034	0.0076	0.0178
1.058	0.058	0.002	0.0505	0.3077	0.2439	37.0550	0.1544	0.6094	0.0122	0.0744	0.3583
1.058	0.058	0.002	0.0505	0.1855	0.1471	47.4304	0.0340	0.1582	0.0074	0.0270	0.0851
1.058	0.058	0.002	0.0505	0.1346	0.1067	57.8058	0.0132	0.0708	0.0053	0.0142	0.0351
1.058	0.058	0.002	0.0505	0.1030	0.0816	63.7346	0.0059	0.0361	0.0041	0.0083	0.0160
1.058	0.058	0.0025	0.0564	0.3152	0.1955	37.9443	0.0974	0.6076	0.0140	0.0780	0.3018
1.058	0.058	0.0025	0.0564	0.2331	0.1446	45.0588	0.0398	0.2790	0.0103	0.0427	0.1302
1.058	0.058	0.0025	0.0564	0.1664	0.1032	53.0509	0.0145	0.1173	0.0074	0.0218	0.0499
1.058	0.058	0.0025	0.0564	0.1353	0.0839	59.5133	0.0079	0.0658	0.0060	0.0144	0.0280
Calculated V _s /H ³ _{wnet} = 4.6 (Fr) ^{0.21} (H _{snet} /H _{wnet}) ^{2.2} (D/(H _w _{net})) ^{0.89}											

